NASA

Technical Memorandum 83855

Compensation for Use of Monthly-Averaged Winds in Numerical Modeling

Claire L. Parkinson

NOVEMBER 1981

National Aeronautics and
Space Administration

Goddard Space Flight Center
Greenbelt, Maryland 20771

COMPENSATION FOR USE OF MONTHLY-AVERAGED WINDS IN NUMERICAL MODELING

Claire L. Parkinson
Goddard/Laboratory for Atmospheric Sciences
NASA/Goddard Space Flight Center
Greenbelt, MD 20771

November 1981

GODDARD SPACE FLIGHT CENTER

Greenbelt, Maryland 20771

COMPENSATION FOR USE OF MONTHLY-AVERAGED WINDS IN NUMERICAL MODELING

Claire L. Parkinson
Goddard/Laboratory for Atmospheric Sciences
NASA/Goddard Space Flight Center
Greenbelt, MD 20771

ABSTRACT

The use of monthly-averaged wind vectors in numerical modeling experiments causes difficulties when averaged wind speeds are required as well as wind velocities. This occurs, for instance, in bulk-aerodynamic formulae for sensible and latent heat transfers and in equations for wind stress. In this note, ratios R of the monthly-averaged wind speeds to the magnitudes of the monthly-averaged wind vectors are presented for each month of 1974 and 1975 over a 41 x 41 grid covering the Southern Ocean and the Antarctic continent. The ratio is found to vary from 1 to over 1000, with an average value of 1.86. These ratios R are relevant for converting from sensible and latent heats calculated with mean monthly data to those calculated with 12-hourly data. The corresponding ratios α for wind stress, along with the angle deviations involved, are also presented for each of the 24 months over the same 41 x 41 grid. The values for α generally exceed those for R and average 2.66 over the 2 years. Regions in zones of variable wind directions have larger R and α ratios, with the two-year averages over the ice-covered portions of the Southern Ocean averaging 2.74 and 4.35 for R and α respectively. Thus adjustments to compensate for the use of mean monthly wind velocities should be stronger for wind stress than for turbulent heats and stronger over ice-covered regions than over regions with more persistent wind directions, e.g., those in the belt of mid-latitude westerlies.

CONTENTS

COMPENSATION FOR USE OF MONTHLY-AVERAGED WINDS IN NUMERICAL MODELING

I. INTRODUCTION

The use of mean monthly averages in various modeling studies requires certain adjustments, especially for vector quantities whose magnitudes are used in addition to their vector components. For instance, in the modeling of oceans and sea ice, wind speeds are employed for calculations of sensible and latent heats and for determining the wind stress term in the calculation of surface currents and ice drift. Since the average wind speed does not, except under rare conditions, equal the speed of the average wind vector, some care is called for in using average vectors for calculations dependent upon average speeds.

Ocean and sea ice modeling studies which do not involve coupled atmospheric calculations often employ atmospheric variables averaged over various time periods. This is true, for instance, in the ocean studies of Bryan and Lewis (1979), Meehl et al. (1982), Schopf (1980), and Semtner (1976b), and in the sea ice studies of Hibler (1979), Maykut and Untersteiner (1971), Parkinson and Washington (1979), Pease (1975), Semtner (1976a), and Washington et al. (1976). Not untypically, Parkinson and Washington (1979) employ climatological monthly averages for temperatures, pressures, dew points, and the u and v components of the geostrophic wind. Temperature, pressure and dew point being scalar quantities, those are not considered below. Instead the emphasis centers on wind velocity, a vector whose magnitude, as well as its individual components, is employed in the sensible heat, latent heat, and wind stress calculations.

The magnitude of the average of any 2 vectors $\vec{V}_1 = (a,b)$ and $\vec{V}_2 = (c,d)$ is necessarily less than or equal to the average of the magnitudes, a result immediate from the following algebraic inequality:

$$\sqrt{1/4\ (a+c)^2 + 1/4\ (b+d)^2} \leq 1/2\ [\ \sqrt{a^2+b^2} + \sqrt{c^2+d^2}\ ]. \quad (1)$$

Thus usage of averaged wind vectors and determination of wind speeds from them necessarily underestimates (or, in the unlikely event that the wind direction remains constant, equals) the averaged wind speeds. Recognizing this, Parkinson and Washington (1979) inserted a factor α set equal to 3.0 in the equation of wind stress [$\vec{\tau}_a = \alpha\ C_D\ \rho_a V^2\ (\cos\beta\vec{i} + \sin\beta\vec{j})$] to compensate for the use of mean monthly climatological inputs. This value of 3.0 was recommended by A. Semtner (personal communication) and was not varied either spatially or through time. In this note, 12-hourly wind data for each month of 1974 and 1975 are used to calculate appropriate adjustment factors both for the sensible and latent heat calculations, which treat the wind velocity in a linear fashion, and for the more-complicated wind stress calculations, where the wind speed and direction are both relevant. Displaying the data on a 2-dimensional grid for each month of the 2-year period allows both the spatial and temporal variations to be illustrated, including interannual as well as interseasonal contrasts.

II. WIND USAGE IN FLUX AND STRESS FORMULATIONS

Sensible and latent heats, H and LE, are typically calculated from bulk aerodynamic formulae:

$$H = \rho_a\ c_p\ C_H\ W(T_a - T_{sfc}) \quad (2)$$

$$LE = \rho_a L C_E W(q_{10m} - q_s), \quad (3)$$

where ρ_a is air density, c_p is the specific heat of air, L is the latent heat of vaporization (for a water surface) or of sublimation (for an ice surface), C_H and C_E are the transfer coefficients for sensible and latent heats respectively, W is the wind speed, T_a and T_{sfc} are the air and surface temperatures, and q_{10m} and q_s are the specific humidities at heights of 10 m and the surface. The appropriate wind speed is the instantaneous value. Over a time interval in which the other terms remain essentially constant, the average sensible and latent heats will be:

$$\overline{H} = \rho_a c_p C_H \overline{W}(T_a - T_{sfc}) \quad (4)$$

$$\overline{LE} = \rho_a L C_E \overline{W}(q_{10m} - q_s), \quad (5)$$

so that the average wind speed is appropriate in the calculations. Thus in a case where average wind speeds are not available but average wind vectors are, the magnitude of the average vector should be multiplied by a conversion factor deemed reasonable for the ratio

$$R = \frac{\overline{W}}{W_m} \quad (6)$$

where $\overline{W}$ is the average wind speed and $W_m = |\vec{V}_m|$ is the magnitude of the average wind vector $\vec{V}_m = \overline{\vec{V}} = (\overline{u_i}, \overline{v_i})$. Hence, for the sensible and latent heat calculations, with a time period of one month the appropriate conversion factor is simply the ratio of monthly-averaged wind speed $\overline{W}$ to the speed W_m of the monthly-averaged vector. Such ratios will be presented below over a 41 x 41 grid for each month of 1974 and 1975. The grid is centered at the South Pole and extends northward to mid latitudes.

In the case of wind stress, the wind enters the calculations in a non-linear fashion, making the appropriate conversion somewhat more complicated. Wind stress $\vec{\tau}_a$ can be calculated as

$$\vec{\tau}_a = \rho_a C_D W \vec{V} , \tag{7}$$

where C_D is the appropriate drag coefficent, $\vec{V}$ is the wind velocity, and $W = |\vec{V}|$ is, as before, the wind speed. Hence, for constant ρ_a and C_D, the average stress over a given time interval will be

$$\bar{\vec{\tau}}_a = \rho_a C_D \overline{W \vec{V}} \tag{8}$$

with a wind stress magnitude of

$$\left|\bar{\vec{\tau}}_a\right| = \rho_a C_D \left|\overline{W \vec{V}}\right| . \tag{9}$$

When only monthly average vectors are available and wind stress is calculated as

$$\bar{\vec{\tau}}_a = \alpha \rho_a C_D W_m \vec{V}_m \tag{10}$$

with magnitude

$$\left|\bar{\vec{\tau}}_a\right| = \alpha \rho_a C_D (W_m)^2 , \tag{11}$$

then the appropriate ratio α to convert to the proper wind stress magnitude is, as presented also in Semtner (1976b),

$$\alpha = \frac{\left|\overline{W \vec{V}}\right|}{W_m^2} . \tag{12}$$

Monthly values for α are tabulated below for data from 1974 and 1975. It is relevant, in addition, to consider the turning angle A between the 2 wind stress calculations (Equations 8 and 10), i.e., between the vectors $\overline{W \vec{V}}$ and $\vec{V}_m$. Values for these angles also are tabulated for the 24 months

of 1974 and 1975. It should be noted that the above formulations assume surface wind values, without incorporating additional adjustments for conversion from surface geostrophic winds to actual surface winds. A first-order conversion would reduce the magnitudes of the geostrophic wind by a constant factor and insert a constant turning angle. Such a first-order adjustment would not affect the values of the ratios or angle differences tabulated below.

To summarize, monthly averaged sensible and latent heats depend on monthly averaged wind speeds $\overline{W}$, and monthly-averaged wind stresses depend on monthly-averaged products of wind speed by wind velocity, $\overline{W\,\vec{V}}$. However, often the quantities available are instead the monthly averaged vectors $\vec{V}_m$ and their magnitudes W_m. The ratios R and α provide the adjustments necessary when using W_m in place of $\overline{W}$ and W_m^2 in place of $\left|\overline{W\,\vec{V}}\right|$.

III. DATA SOURCE AND GRID

The data employed for these calculations are 12-hourly surface geostrophic wind vectors from the Australian Bureau of Meteorology. These data were obtained in digitized form, on a 47 x 47 Southern Hemisphere grid, through the courtesy of G. Walters of the Data Support Section, National Center for Atmospheric Research, Boulder, Colorado, and were interpolated to the 41 x 41 Parkinson and Washington (1979) grid of the south polar region (Figure 1) and averaged over each month of 1974 and 1975. The arrays of monthly averaged u and v components determined the monthly averaged vectors $\vec{V}_m$ and enabled calculation of the magnitudes $W_m = |\vec{V}_m|$. Additionally, for each 12-hour period the 41 x 41 array of wind speeds was calculated, and these arrays were averaged over each month to obtain the monthly averaged wind speeds, $\overline{W}$. Monthly averages of both components of $W\,\vec{V}$ were also calculated, thereby enabling determination of ratios R

and α and of the turning angle A between $\overline{W}\,\overline{V}$ and $\overline{V}_m$.

IV. RESULTS

a. Ratios R for sensible and latent heat.

Figures 2-25 present for each month of 1974 and 1975 the 41 x 41 array of ratios R of the average wind magnitude $\overline{W}$ to the magnitude W_m of the average wind vector. The larger this ratio R, the more significant is the speed underestimation in calculations which replace $\overline{W}$ by W_m, for instance in determining sensible and latent heat fluxes. In Figures 2-25 the continental boundaries of Antarctica and the southern tip of South America are outlined, as is the boundary of the maximum extent of sea ice coverage during the given month, the latter being determined from the Electrically Scanning Microwave Radiometer (ESMR) data set from the Nimbus 5 satellite (Zwally et al., 1982).

As can be seen from Figures 2-25, the ratio R exhibits, over the southern hemisphere for this 2-year period, significant spatial variations and lesser temporal variations. Of particular relevance, R tends to be noticeably larger over sea-ice regions than over continental and open-ocean regions. Hence Tables 1 and 2, which summarize the data from Figures 2-25, present spatially-averaged values of R for each of four geophysical subsets as well as for the full 41 x 41 grid. The four subsets are as follows: (1) the continent of Antarctica, covering a constant 328 grid squares; (2) the southern tip of South America, covering 6 grid squares; (3) the region covering all grid squares with a sea ice coverage sometime during the given month; i.e., the region determined from the ESMR data set and outlined in Figures 2-25; and (4) the region of ice-free ocean.

For each month the ice-laden grid squares have a higher average value of R than either the open ocean or the Antarctic or South American grid

Table 1. Spatially-Averaged Wind Ratios R, 1974.

	Number of Grid Squares With Ice	Number of Days Missing Ice Data	Average Wind Ratio R				
			Overall	Over Ice	Over Ice-Free Ocean	Over Antarctica	Over S. America
January	213	0	2.16	3.43	2.00	1.91	1.48
February	136	0	1.70	3.89	1.42	1.86	1.10
March	158	0	1.58	3.34	1.31	1.73	1.14
April	258	6	1.95	2.76	1.84	1.68	1.11
May	361	9	1.64	2.45	1.39	1.50	1.43
June	449	0	2.21	3.55	1.81	1.47	1.75
July	510	0	2.02	3.02	1.60	1.55	1.14
August	550	12	2.17	3.37	1.68	1.39	1.21
September	577	0	1.69	2.32	1.23	1.68	1.14
October	547	6	1.59	2.26	1.24	1.31	1.15
November	509	0	1.83	2.77	1.45	1.34	1.38
December	392	0	1.67	2.17	1.63	1.21	1.23
Yearly Average	---	---	1.85	2.94	1.55	1.55	1.27

Table 2. Spatially-Averaged Wind Ratios R, 1975.

	Number of Grid Squares With Ice	Number of Days Missing Ice Data	Averaged Wind Ratio R				
			Overall	Over Ice	Over Ice-Free Ocean	Over Antarctica	Over S. America
January	203	3	1.86	2.44	1.95	1.21	1.24
February	124	0	1.73	2.26	1.82	1.23	1.20
March	167	0	1.55	2.92	1.44	1.25	1.07
April	198	18	1.75	2.89	1.65	1.41	1.46
May	327	6	1.79	2.14	1.86	1.22	1.32
June	327	27	1.87	2.62	1.74	1.37	1.48
July	---	31	3.17	----	----	1.68	1.95
August	517	24	1.88	2.93	1.35	1.54	1.26
September	565	6	1.72	2.43	1.21	1.71	1.22
October	562	0	1.54	1.96	1.28	1.48	1.12
November	506	0	1.80	2.86	1.31	1.42	1.23
December	369	0	1.77	2.56	1.63	1.29	1.21
Yearly Average	---	---	1.87	2.55	1.57	1.40	1.31

squares. This results basically from the broad features of atmospheric circulation rather than from the presence of the ice. Many of the ocean grid squares without an ice cover are in the region of persistent westerly winds, whereas the grid squares with ice are in the 60-78°S latitude belt in which migrating storms dominate the wind field.

The ratio tends to be about 50% larger over the ice-covered regions than over the grid as a whole. Hence, due to the geographic placement of sea ice in a zone of highly-variable winds, sea-ice calculations warrant a higher value of R than calculations for some of the other regions of the world ocean.

Interannually, over the ice-laden grid squares the average ratio R is greater in 1975 than in 1974 for April, September, November, and December and greater in 1974 than in 1975 for each of the remaining seven months having ESMR ice data in both years. The year-to-year differences exceed the seasonal ones; and hence, in modeling experiments inserting wind ratios appropriate for the entire ice-covered region it is not useful to vary the ratio through the year unless interannual differences are accounted for also. The yearly averages would suggest a factor R of 2.5-3.0 for adjusting from average wind vector magnitudes to average wind speeds over ice-laden grid squares and a factor of 1.8 - 1.9 over the full 41 x 41 grid (extending from 40°S to 90°S).

b. Ratios α and turning angles A for wind stress.

Full 41 x 41 arrays of the ratio α (Equation 12) are presented in Figures 26-49 for each month of 1974 and 1975; and corresponding arrays of the turning angle from the wind stress as calculated from 12-hourly data to the wind stress as calculated from monthly averages (positive clockwise) are presented in Figures 50-73. As in Figures 2-25, the

continental and sea ice boundaries have been outlined on these additional 48 figures. Also, Tables 3 and 4 summarize the data for α (Figures 26-49) in the same manner that Tables 1 and 2 summarize the data for R (Figures 2-25); and Tables 5 and 6 present an alternate summary for the turning angle A, which assumes negative as well as positive values.

Like the ratio R, the ratio α shows significant spatial and temporal variations, with average values over the sea ice region generally exceeding average values over other regions. This, as before, is due to the variable wind directions in the sea ice latitudes. Since high values of α signify significant underestimation of the wind stress when monthly average wind vectors are used without the α correction, the higher values in the sea ice region indicate that it is even more important to insert a correction term in this region than in the others. The monthly values of α range from 2.7 to 6.3 over the ice and from 2.0 to 4.3 over the entire 41 x 41 grid. Over the two years, the values average 4.3 over the ice and 2.7 over the full grid. These values exceed the corresponding values for the ratio R by about 50%.

The turning angle A between the wind stress vector calculated from 12-hourly winds and the wind stress vector calculated from monthly average winds does not present as major a problem as the contrast--reflected in the α ratio--between the two wind-stress magnitudes. The turning angles (Figures 50-73) generally have absolute values under 5°. Tables 5 and 6 present the averages of these angles over the 41 x 41 grid and the averages of their absolute values. In addition, Tables 5 and 6 include the percentages of grid squares with turning angles falling in each of 6 binning ranges. These percentages are presented both for the full grid and, in parentheses, for the ice-laden portion of the grid. In 1975, at least 80% of the

Table 3. Spatially-Averaged Ratios α, 1974.

	Overall	Over Ice	Over Ice-Free Ocean	Over Antarctica	Over S. America
January	3.23	5.39	2.86	3.14	1.95
February	2.34	6.25	1.81	2.71	1.27
March	2.11	5.43	1.59	2.41	1.38
April	3.16	3.96	3.27	2.21	1.25
May	2.19	3.75	1.68	2.01	1.89
June	3.24	5.76	2.47	1.92	2.38
July	3.00	5.00	2.15	2.11	1.34
August	3.18	5.40	2.21	1.94	1.44
September	2.42	3.87	1.40	2.25	1.26
October	2.07	3.20	1.46	1.69	1.31
November	2.62	4.52	1.81	1.77	1.72
December	2.20	2.94	2.12	1.53	1.42
Yearly Average	2.65	4.62	2.07	2.13	1.55

Table 4. Spatially-Averaged Ratios α, 1975.

	Overall	Over Ice	Over Ice-Free Ocean	Over Antarctica	Over S. America
January	2.94	4.23	3.14	1.47	1.41
February	2.60	3.66	2.81	1.47	1.36
March	2.12	5.55	1.80	1.53	1.17
April	3.11	4.91	3.14	1.93	1.86
May	2.48	2.92	2.66	1.50	1.60
June	2.60	3.83	2.45	1.84	1.93
July	4.28*	----	----	2.26	2.83
August	2.72	4.69	1.68	2.26	1.51
September	2.36	3.73	1.42	2.24	1.53
October	2.00	2.73	1.50	1.94	1.29
November	2.52	4.54	1.58	1.85	1.48
December	2.47	4.02	2.14	1.73	1.51
Yearly Average	2.68	4.07	2.21	1.84	1.62

* The ratio for point (28,9) was omitted from the overall average for July because the variability of the winds at this location resulted in a value of 109,356 for α. Including this point would produce a July average of 69.33.

Table 5. Turning angles A over the 41 x 41 grid, 1974.

	$\bar{A}$	$\overline{\lvert A \rvert}$	Percentages falling within binned categories						Number of grid squares with ice
			A<-10°	-10°--5°	-5°-0°	0°-5°	5°-10°	A>10°	
January	0.2° (3.2°)*	4.7° (8.3°)	3 (4)	7 (10)	47 (18)	29 (31)	7 (21)	6 (15)	213
February	-0.3° (-2.0°)	3.2° (9.5°)	2 (13)	6 (20)	49 (31)	35 (18)	6 (7)	3 (10)	136
March	0.0° (-0.4°)	2.8° (6.7°)	2 (13)	2 (11)	51 (25)	37 (29)	6 (14)	2 (8)	158
April	0.9° (1.5°)	4.4° (6.9°)	3 (8)	6 (13)	39 (31)	39 (28)	6 (10)	6 (10)	258
May	-0.6° (-1.2°)	2.8° (5.4°)	2 (7)	6 (15)	46 (34)	41 (35)	3 (5)	1 (5)	361
June	-1.3° (0.3°)	4.8° (7.4°)	7 (11)	12 (11)	37 (29)	35 (27)	5 (11)	4 (12)	449
July	0.1° (0.2°)	3.9° (6.8°)	2 (6)	9 (16)	37 (26)	39 (30)	7 (11)	5 (11)	510
August	1.1° (2.7°)	5.3° (10.3°)	4 (12)	8 (11)	32 (17)	37 (25)	11 (17)	7 (19)	550
September	0.0° (-0.3°)	2.7° (4.0°)	2 (5)	3 (5)	41 (34)	49 (48)	3 (5)	2 (3)	577
October	-0.2° (-0.1°)	2.8° (5.3°)	2 (5)	4 (9)	49 (41)	41 (35)	2 (4)	2 (6)	547
November	0.0° (0.1°)	3.1° (5.4°)	2 (7)	6 (11)	41 (27)	43 (40)	5 (9)	2 (6)	509
December	1.1° (2.1°)	3.2° (5.3°)	2 (4)	3 (5)	36 (25)	46 (40)	10 (16)	4 (10)	392

Table 6. Turning angles A over the 41 x 41 grid, 1975.

	$\bar{A}$	$\overline{\lvert A \rvert}$	Percentages falling within binned categories						Number of grid squares with ice
			A<-10°	-10°--5°	-5°-0°	0°-5°	5°-10°	A>10°	
January	0.0° (0.5°)*	4.0° (4.2°)	4 (4)	7 (10)	40 (22)	40 (52)	6 (9)	2 (3)	203
February	-0.6° (-0.0°)	3.4° (5.0°)	4 (11)	6 (5)	41 (26)	43 (46)	4 (9)	3 (3)	124
March	0.2° (1.7°)	3.3° (9.0°)	3 (11)	2 (8)	44 (23)	43 (32)	5 (8)	4 (17)	167
April	-0.4° (-0.0°)	3.2° (7.0°)	2 (6)	6 (5)	44 (32)	40 (37)	5 (13)	2 (8)	198
May	0.0° (1.4°)	3.0° (3.9°)	1 (2)	7 (8)	39 (21)	45 (54)	6 (9)	2 (6)	327
June	0.3° (1.2°)	3.6° (5.8°)	1 (3)	9 (9)	36 (40)	44 (29)	7 (11)	2 (7)	327
July	1.1° (--)	4.9° (--)	4 (--)	7 (--)	33 (--)	34 (--)	16 (--)	6 (--)	---
August	0.0° (0.1°)	3.5° (5.9°)	2 (7)	5 (9)	48 (38)	35 (26)	5 (8)	4 (10)	517
September	0.6° (2.3°)	3.4° (5.6°)	2 (4)	4 (4)	51 (35)	33 (37)	6 (10)	4 (10)	565
October	0.0° (0.0°)	2.6° (3.8°)	1 (2)	5 (8)	48 (48)	39 (30)	5 (9)	1 (3)	562
November	0.1° (-0.8°)	3.7° (7.0°)	3 (10)	6 (14)	36 (25)	45 (34)	6 (10)	3 (8)	506
December	-0.2° (0.1°)	3.3° (6.1°)	3 (8)	7 (15)	42 (22)	39 (33)	7 (14)	2 (8)	369

*Parentheses enclose values for the ice-covered portion of the grid.

grid squares had turning angles within the range 0° ± 5° in every month except July, when the percentage was 67%. In 1974, five months had less than 80% of the grid squares within the 0° ± 5° range, but still there was no month with fewer than 67% in this range. Over sea ice-laden regions the average turning angles tended to exceed those over the grid as a whole, though still most of the turning angles fell within the 0° ± 10° range. Of the 24 months, five had more than 20% of the grid squares outside of the 0° ± 10° range.

ACKNOWLEDGEMENTS. The author thanks Gregg Walters of the National Center for Atmospheric Research for providing in digitized form the Southern Hemisphere data from the Australian Bureau of Meteorology; Ian Wang of Computer Sciences Corporation for assistance in the compilation of the data; Frank Carsey, Don Cavalieri, and Paul Schopf of Goddard Space Flight Center for helpful discussions regarding the work; and Tracy Pepin for typing and retyping the manuscript.

REFERENCES

Bryan, K. and L. Lewis, 1979: A water mass model of the world oceans. J. Geophys. Res., 84, 2503-2517.

Hibler, W. D. III, 1979: A dynamic thermodynamic sea ice model. J. Phys. Oceanography, 9, 815-846.

Maykut, G. A. and N. Untersteiner, 1971: Some results from a time-dependent thermodynamic model of sea ice. J. Geophys. Res., 76, 1550-1575.

Meehl, G. A., W. M. Washington, and A. J. Semtner, 1982: Experiments with a global ocean model driven by observed atmospheric forcing. J. Phys. Oceanography, accepted for publication.

Parkinson, C. L. and W. M. Washington, 1979: A large-scale numerical model of sea ice. J. Geophys. Res., 84, 311-337.

Pease, C. H., 1975: A model for the seasonal ablation and accretion of Antarctic sea ice. AIDJEX Bulletin No. 29, 151-172.

Schopf, P. S., 1980: The role of Ekman flow and planetary waves in the oceanic cross-equatorial heat transport. J. Phys. Oceanography, 10, 330-341.

Semtner, A. J., Jr., 1976a: A model for the thermodynamic growth of sea ice in numerical investigations of climate. J. Phys. Oceanography, 6, 379-389.

Semtner, A. J., Jr., 1976b: Numerical simulation of the Arctic Ocean circulation. J. Phys. Oceanography, 6, 409-425.

Washington, W. M., A. J. Semtner, Jr., C. L. Parkinson and L. Morrison, 1976: On the development of a seasonal change sea-ice model. J. Phys. Oceanography, 6, 679-685.

Zwally, H. J., J. C. Comiso, C. L. Parkinson, W. J. Campbell, F. D. Carsey, and P. Gloersen, 1982: Antarctic Sea Ice Cover 1973-76 From Satellite Passive Microwave Observations, NASA SP, in preparation.

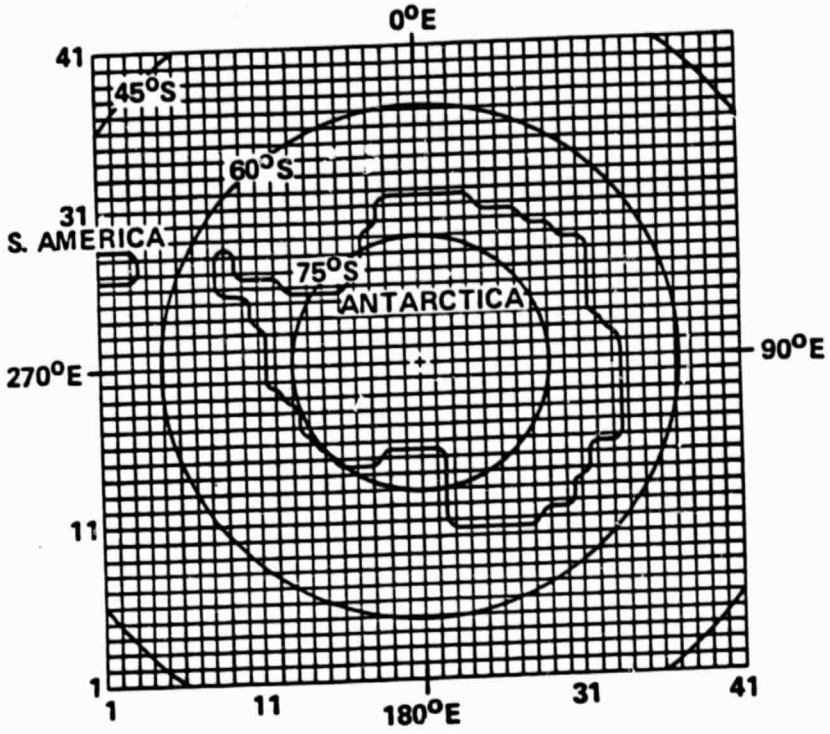

Figure 1. Grid structure.

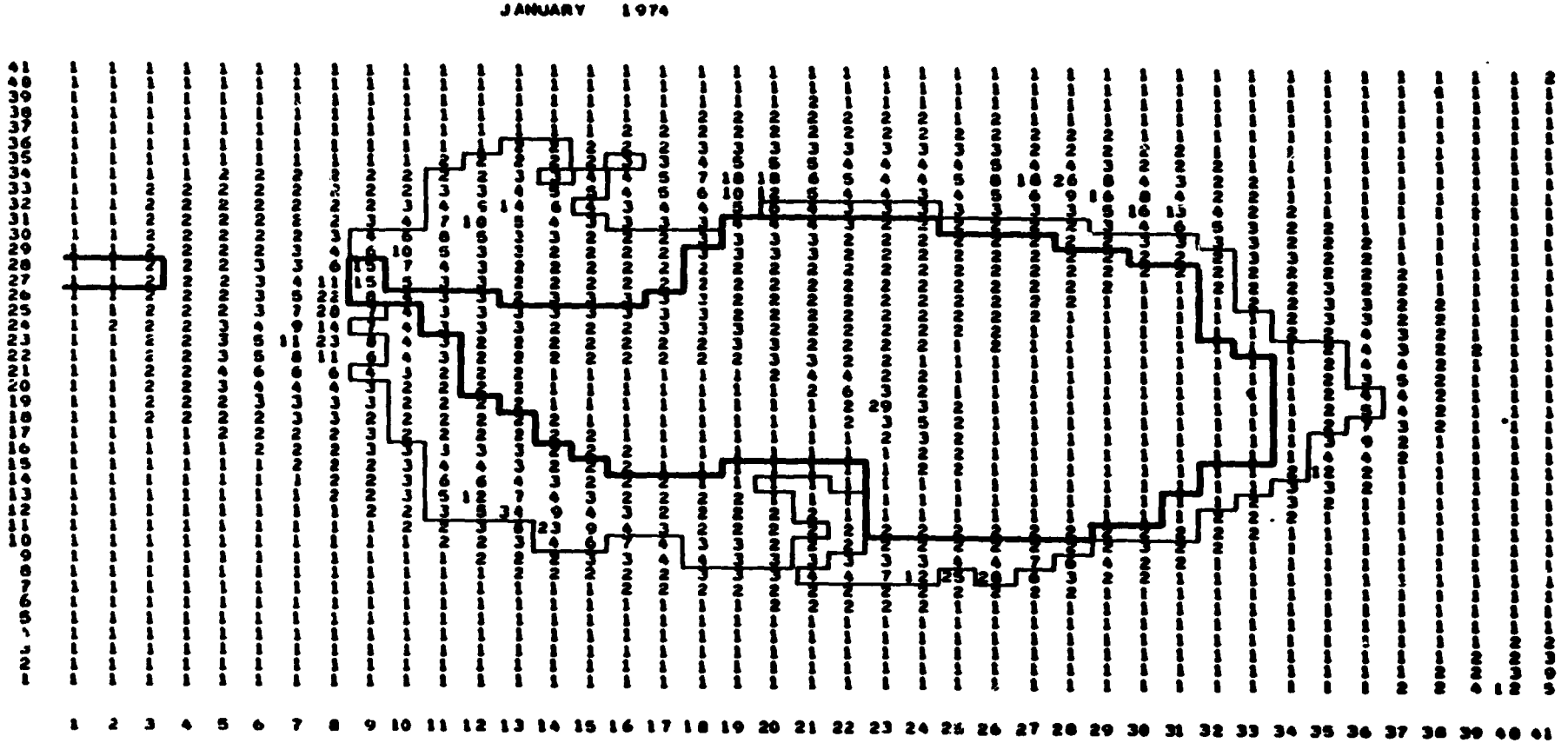

Figure 2. Ratio R over the 41 x 41 south polar grid for January 1974. Here and in Figures 3-73, the dark black lines are continental boundaries and the light black lines identify the border between sea ice and open water.

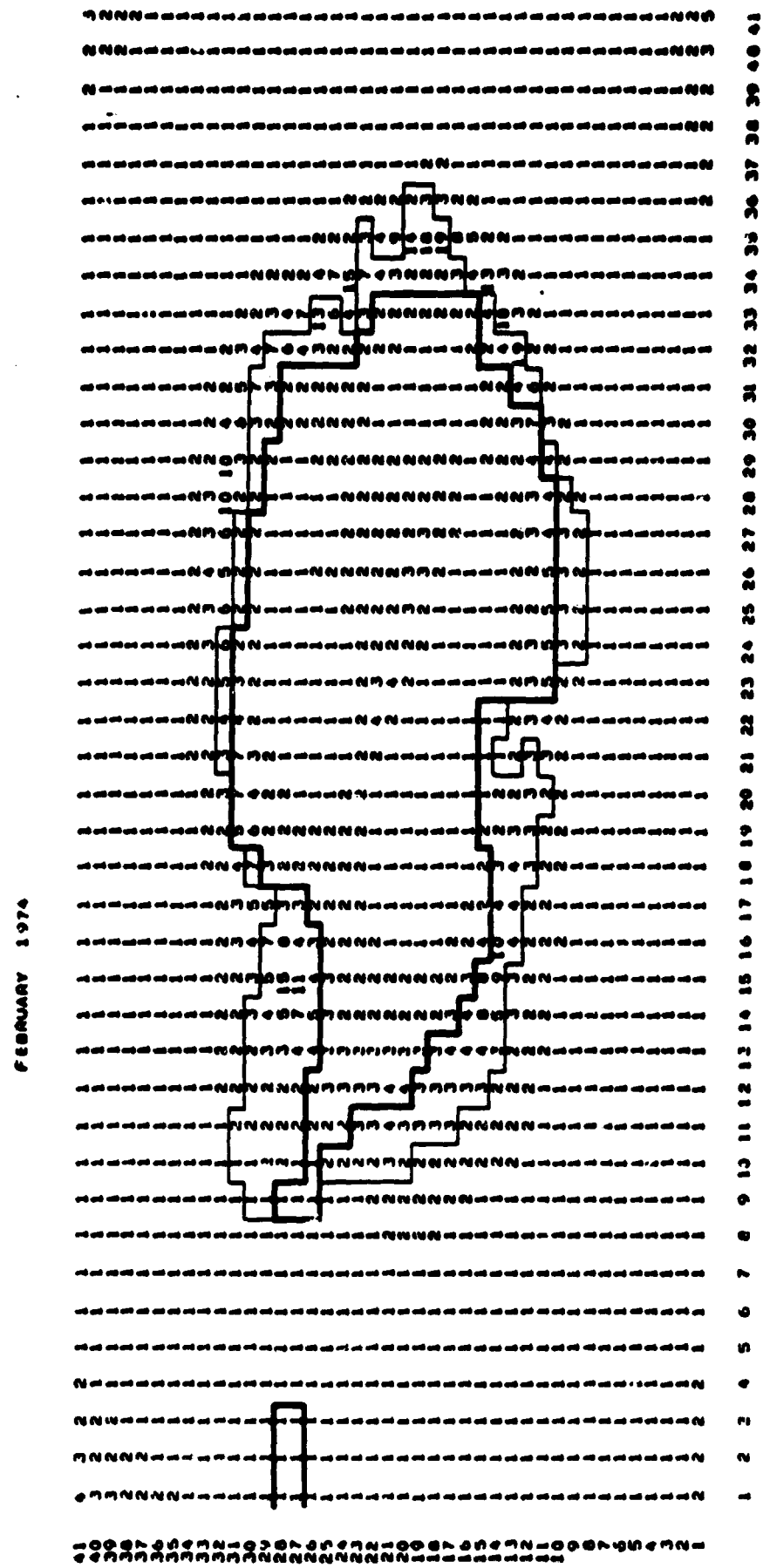

Figure 3. Ratio R over the south polar grid for February 1974.

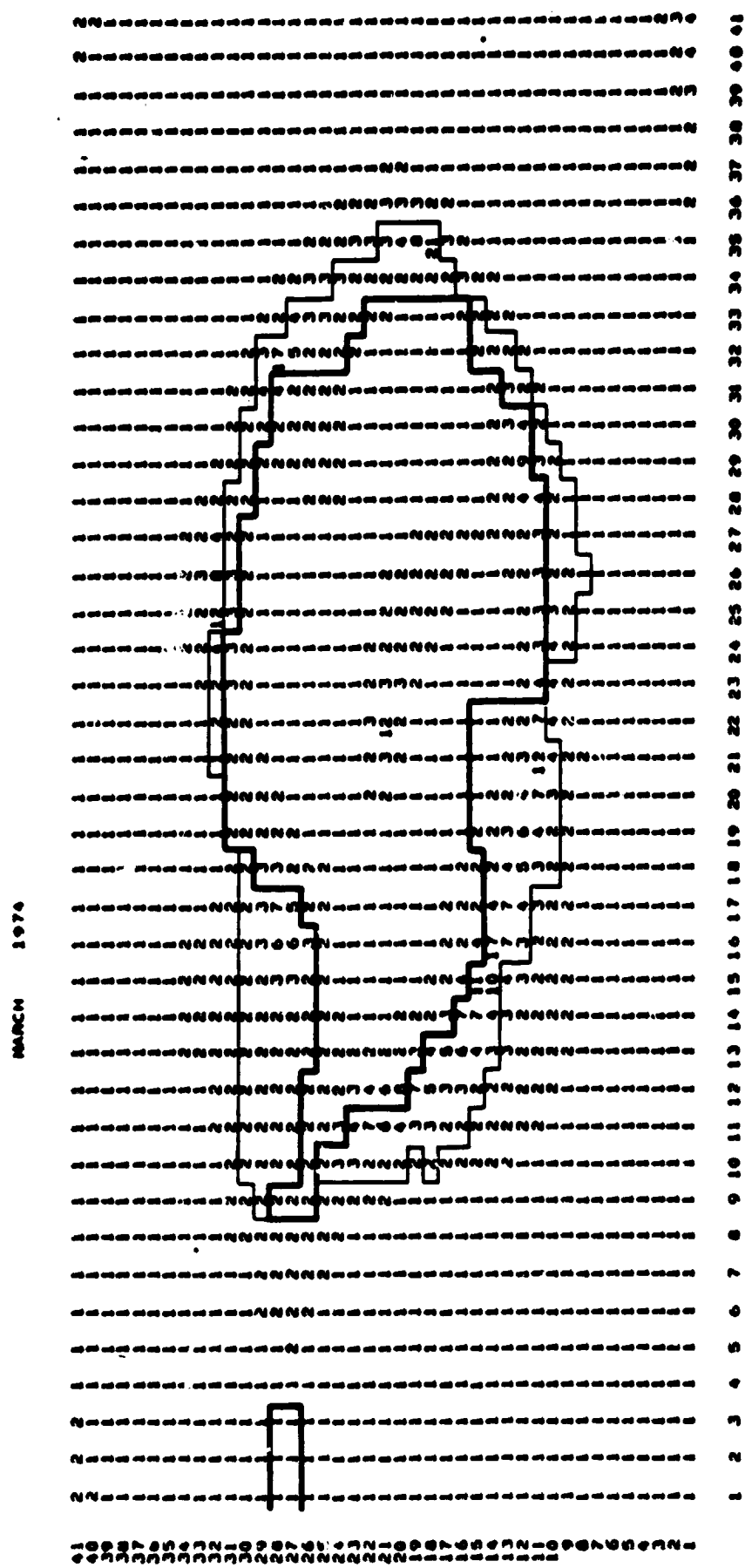

Figure 4. Ratio R over the south polar grid for March 1974.

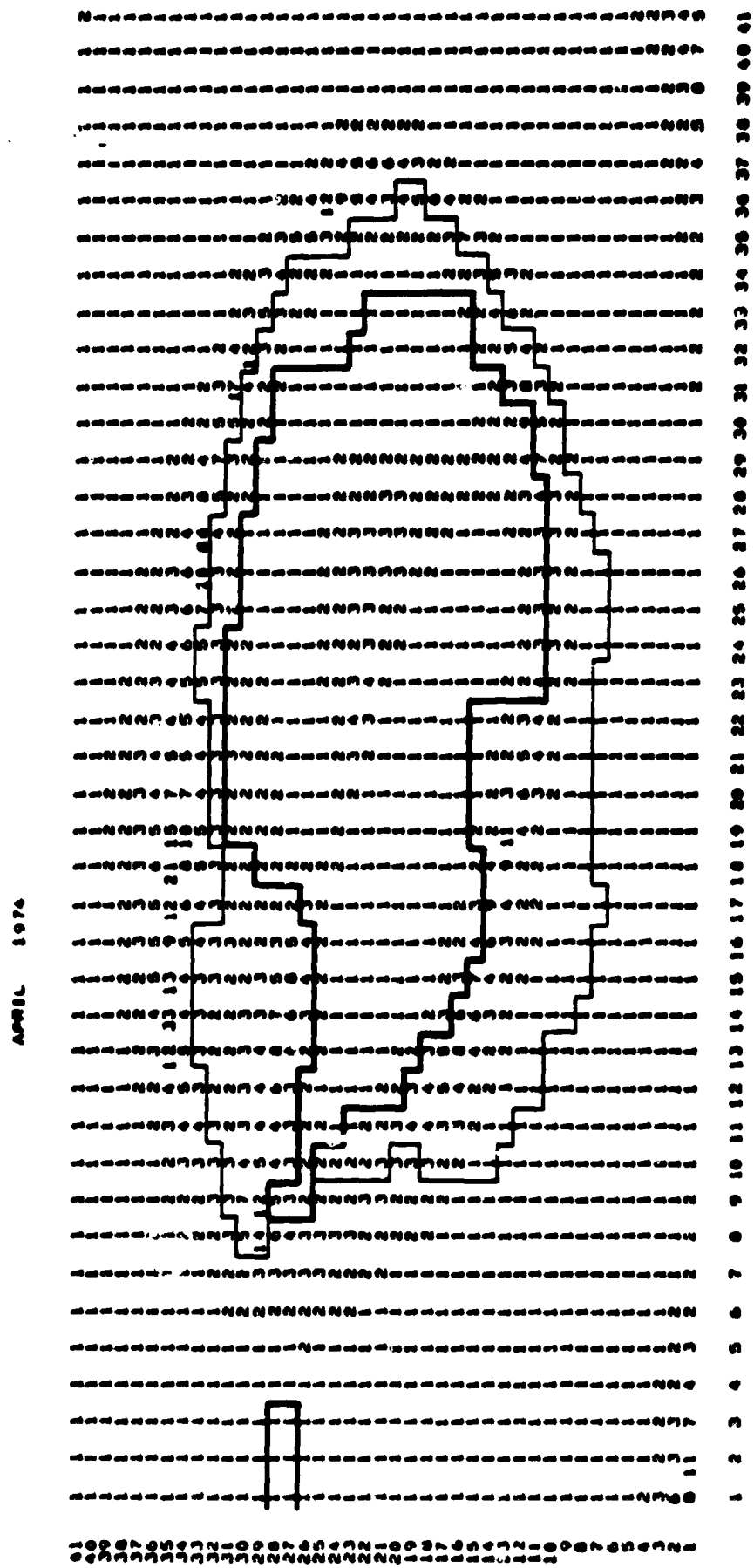

Figure 5. Ratio R over the south polar grid for April 1974.

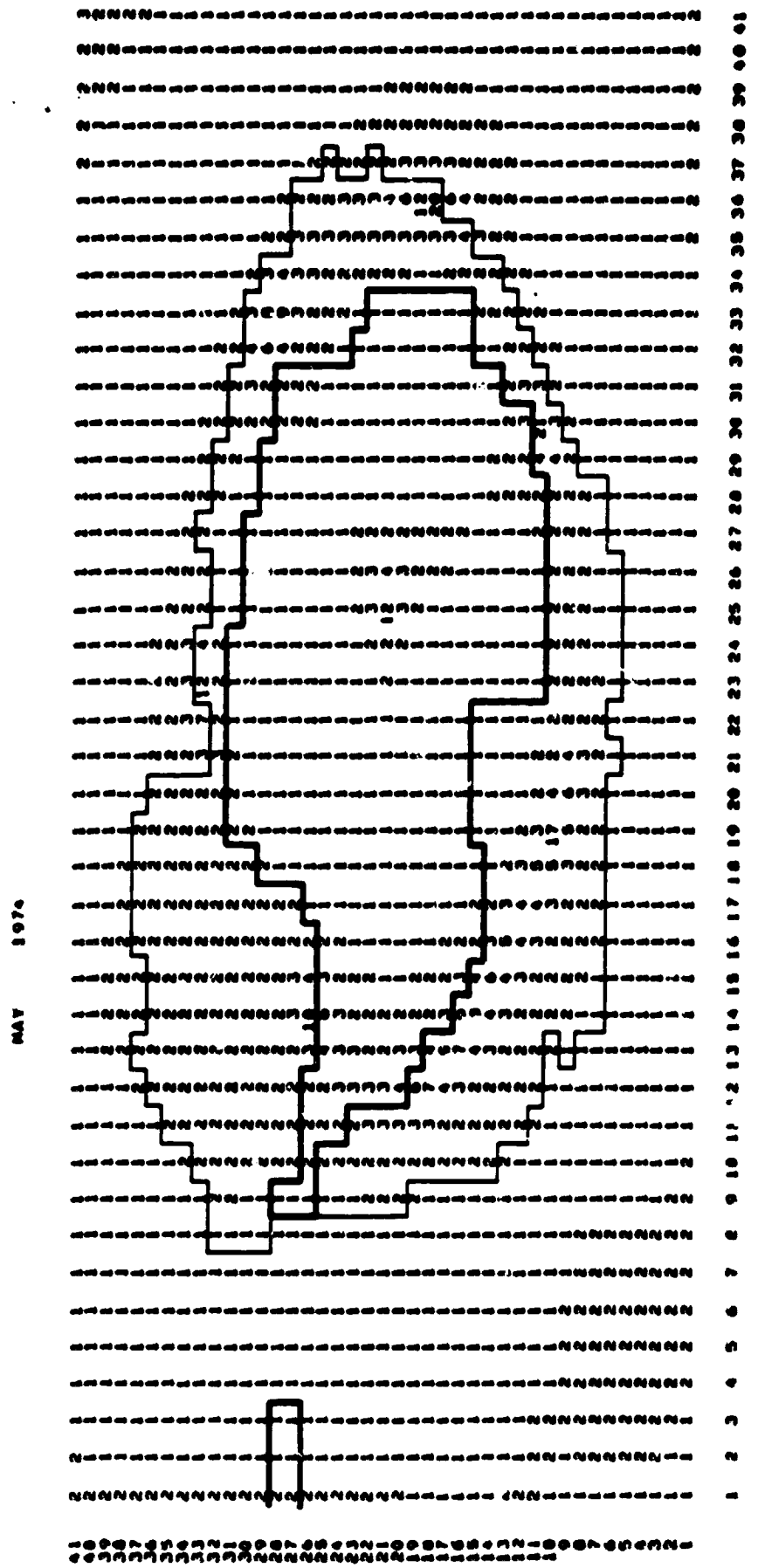

Figure 6. Ratio R over the south polar grid for May 1974.

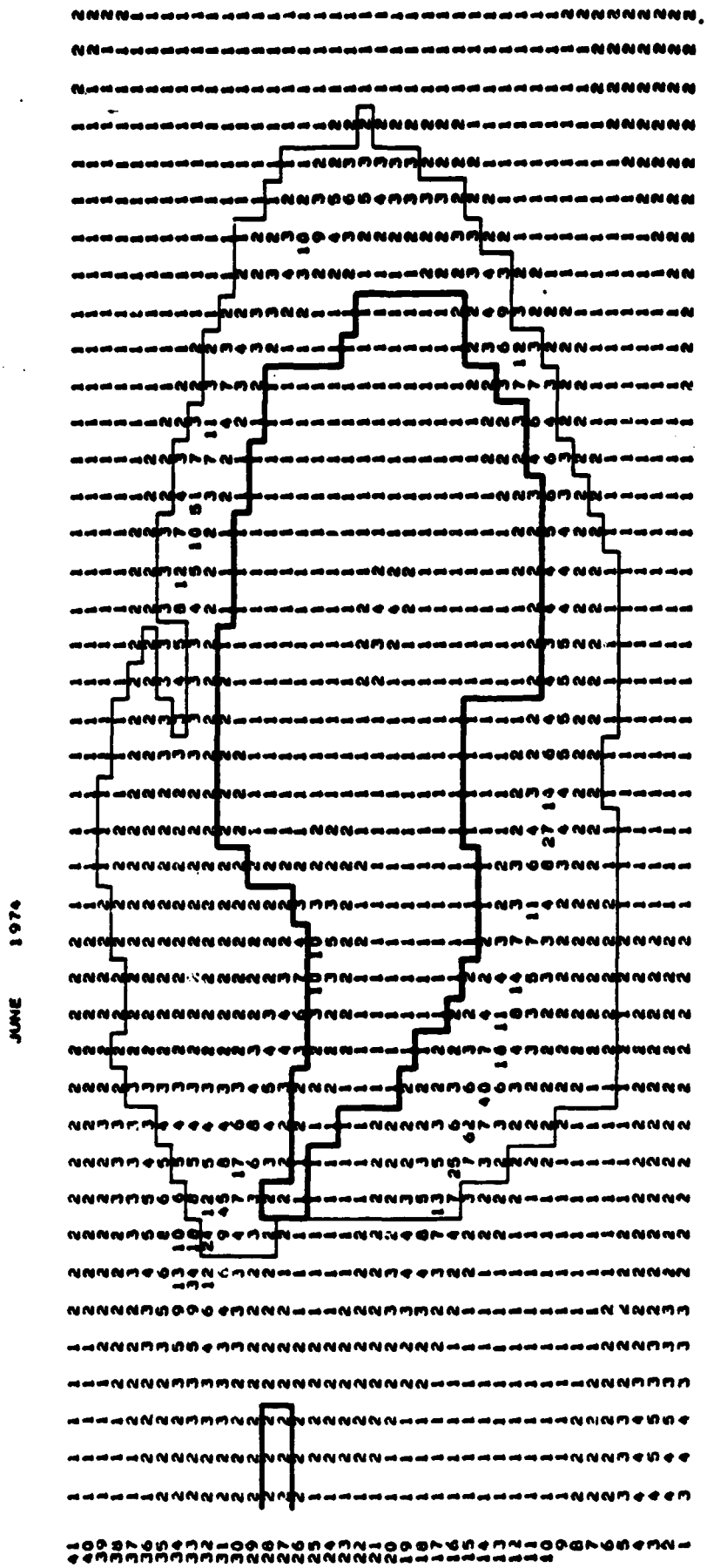

Figure 7. Ratio R over the south polar grid for June 1974.

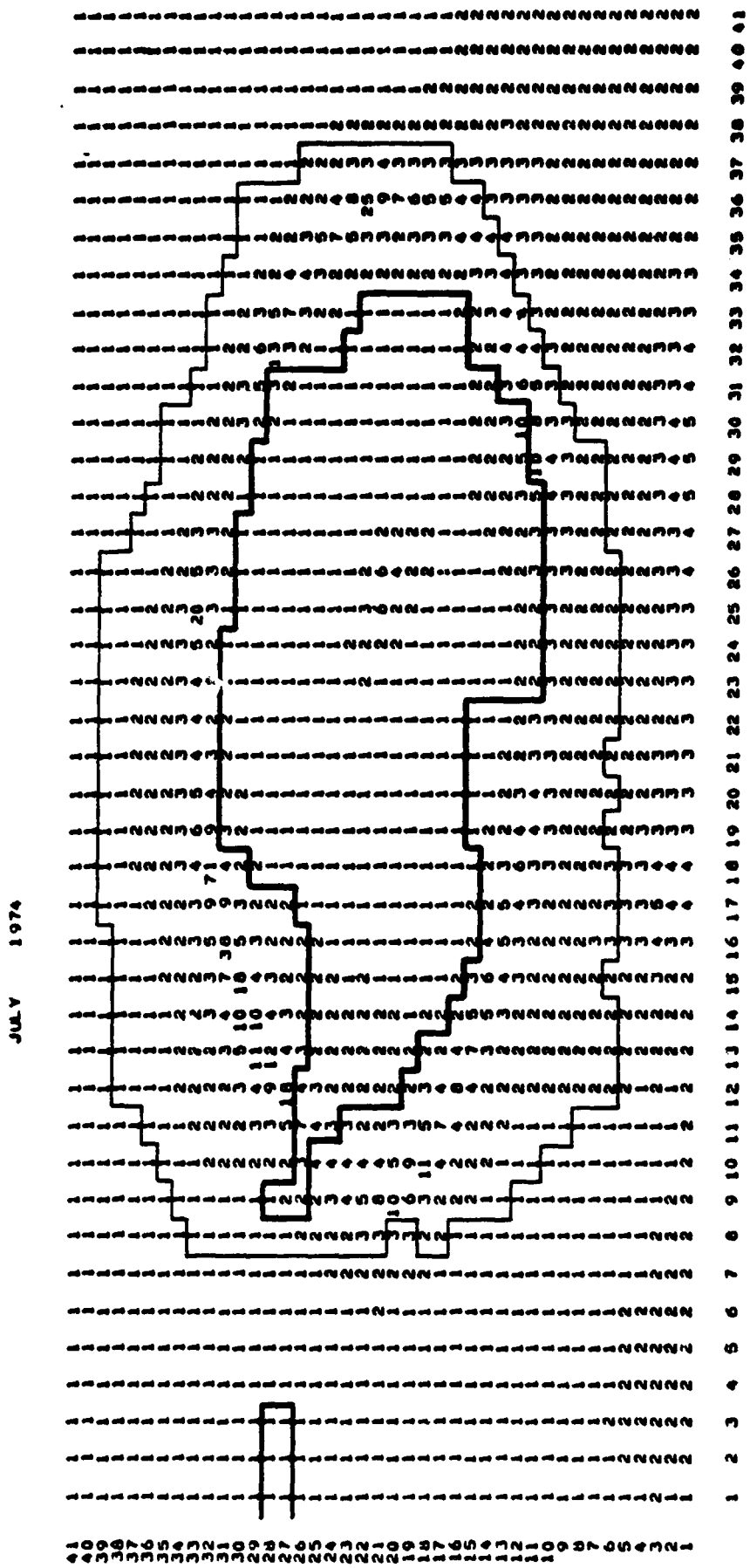

Figure 8. Ratio R over the south polar grid for July 1974.

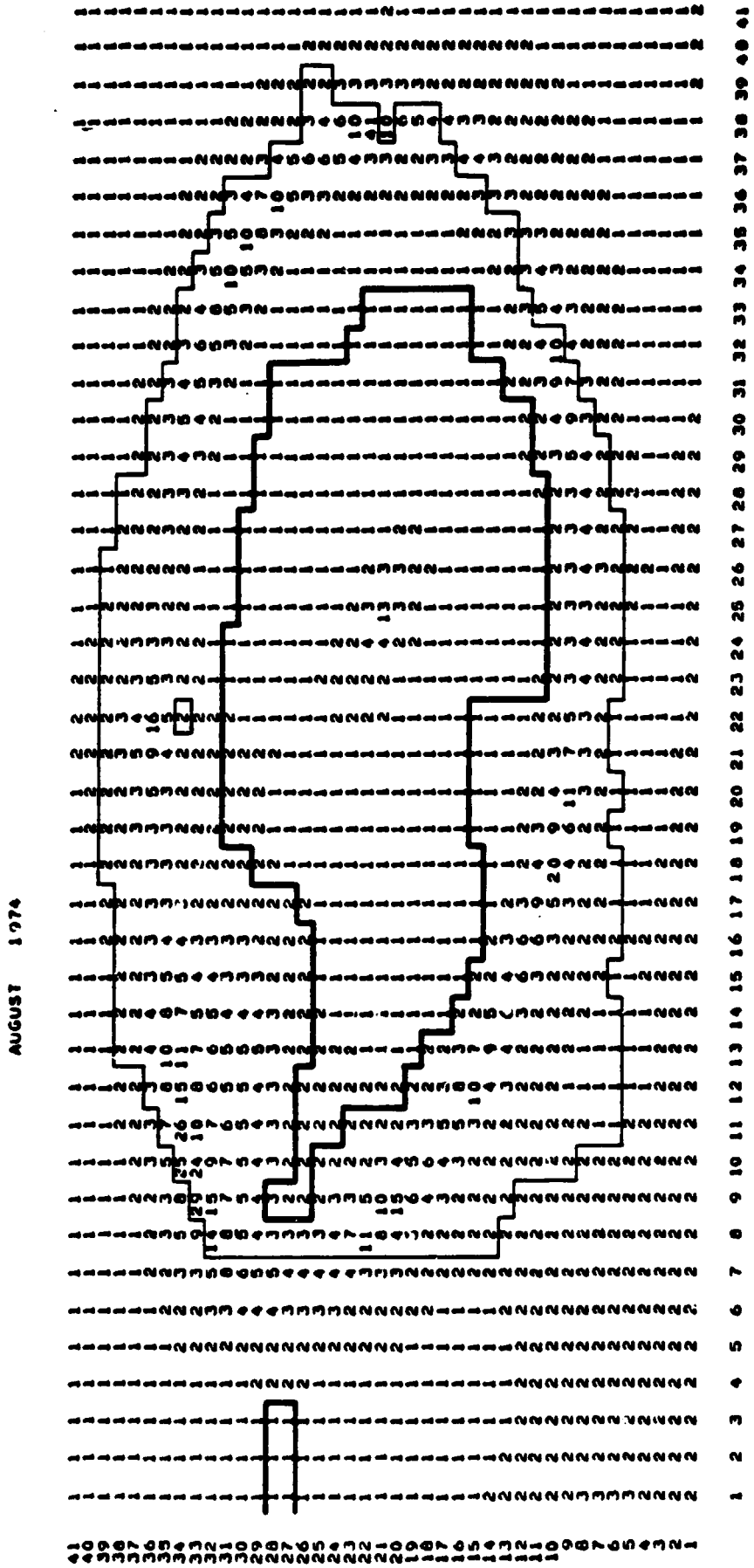

Figure 9. Ratio R over the south polar grid for August 1974.

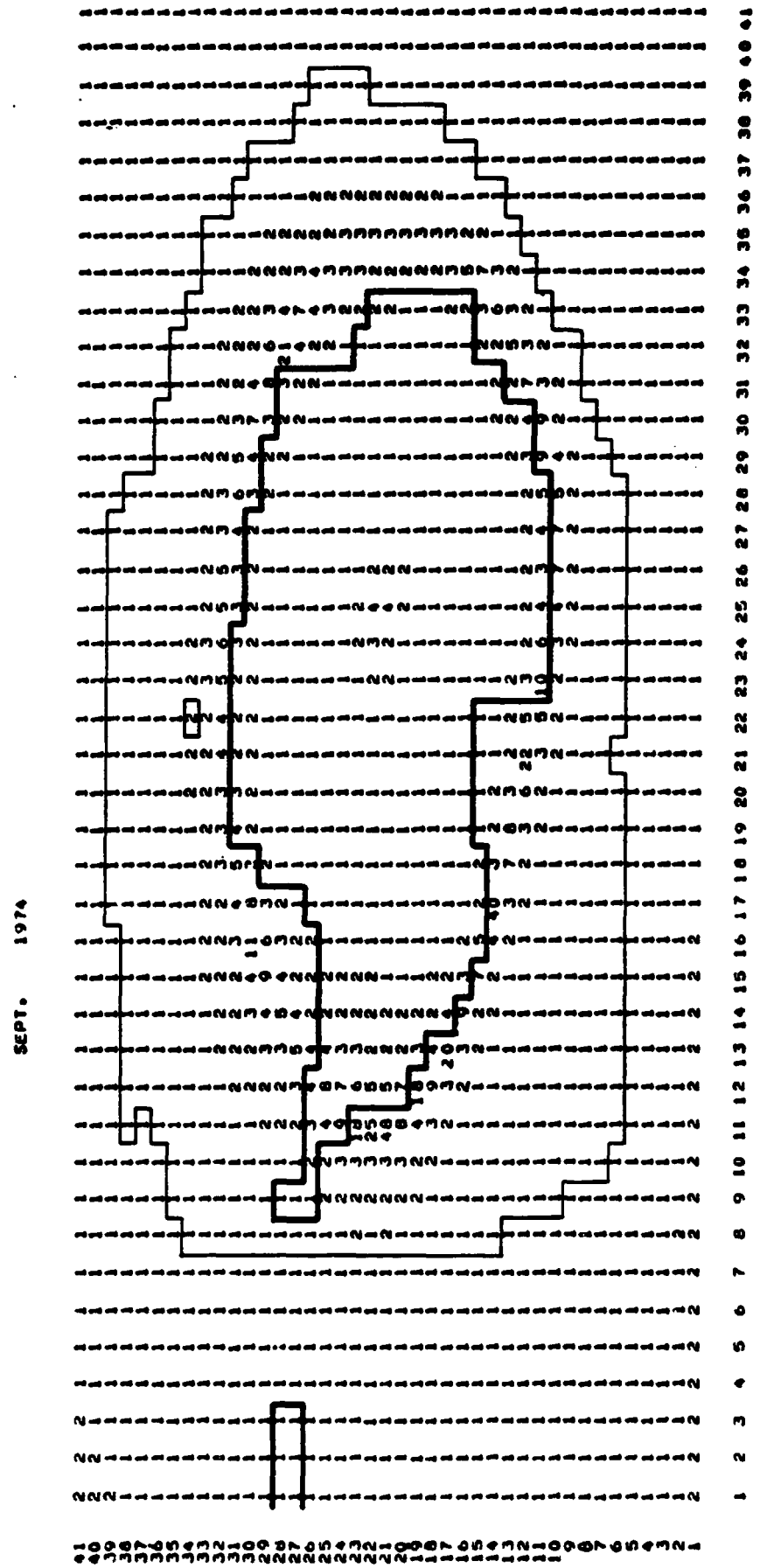

Figure 10. Ratio R over the south polar grid for September 1974.

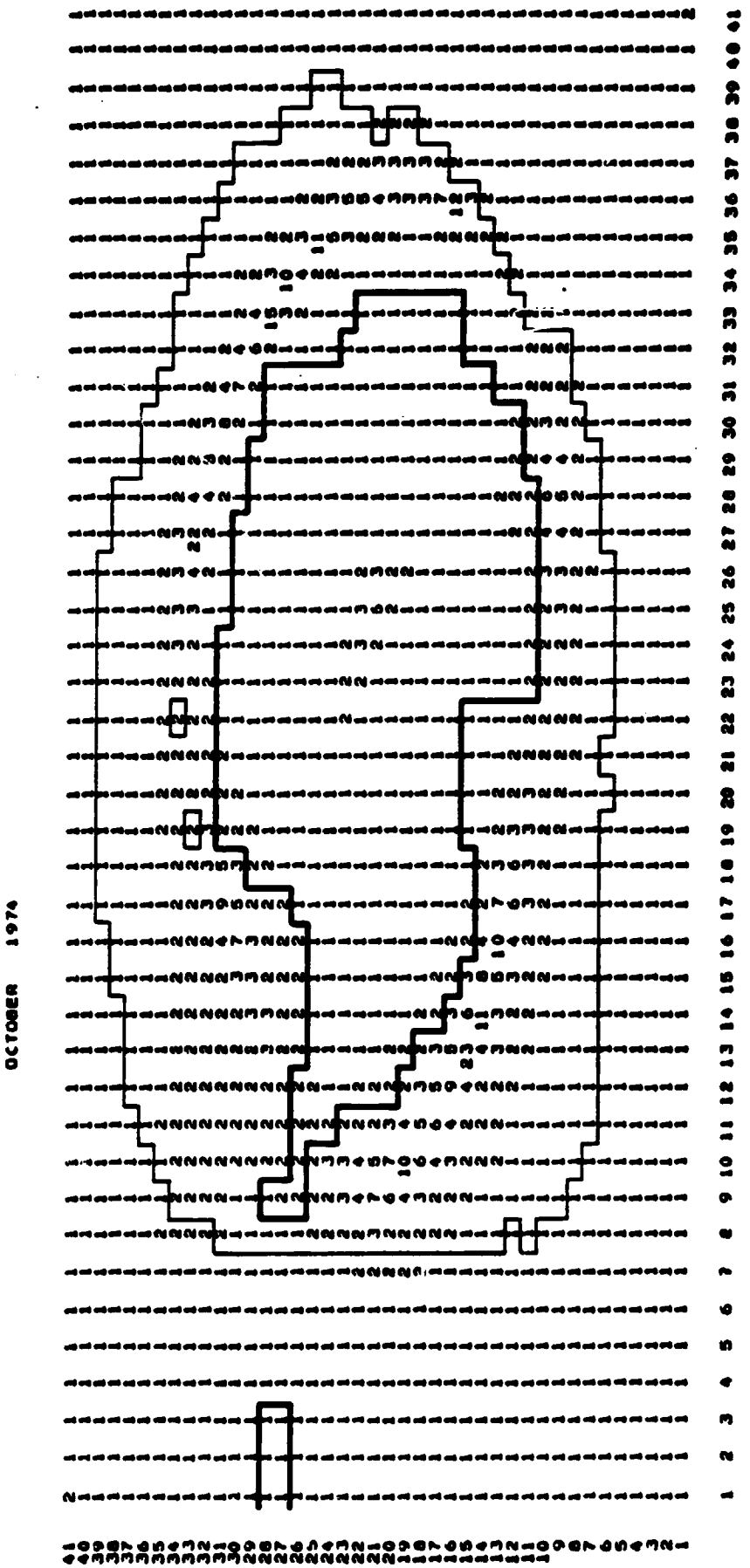

Figure 11. Ratio R over the south polar grid for October 1974.

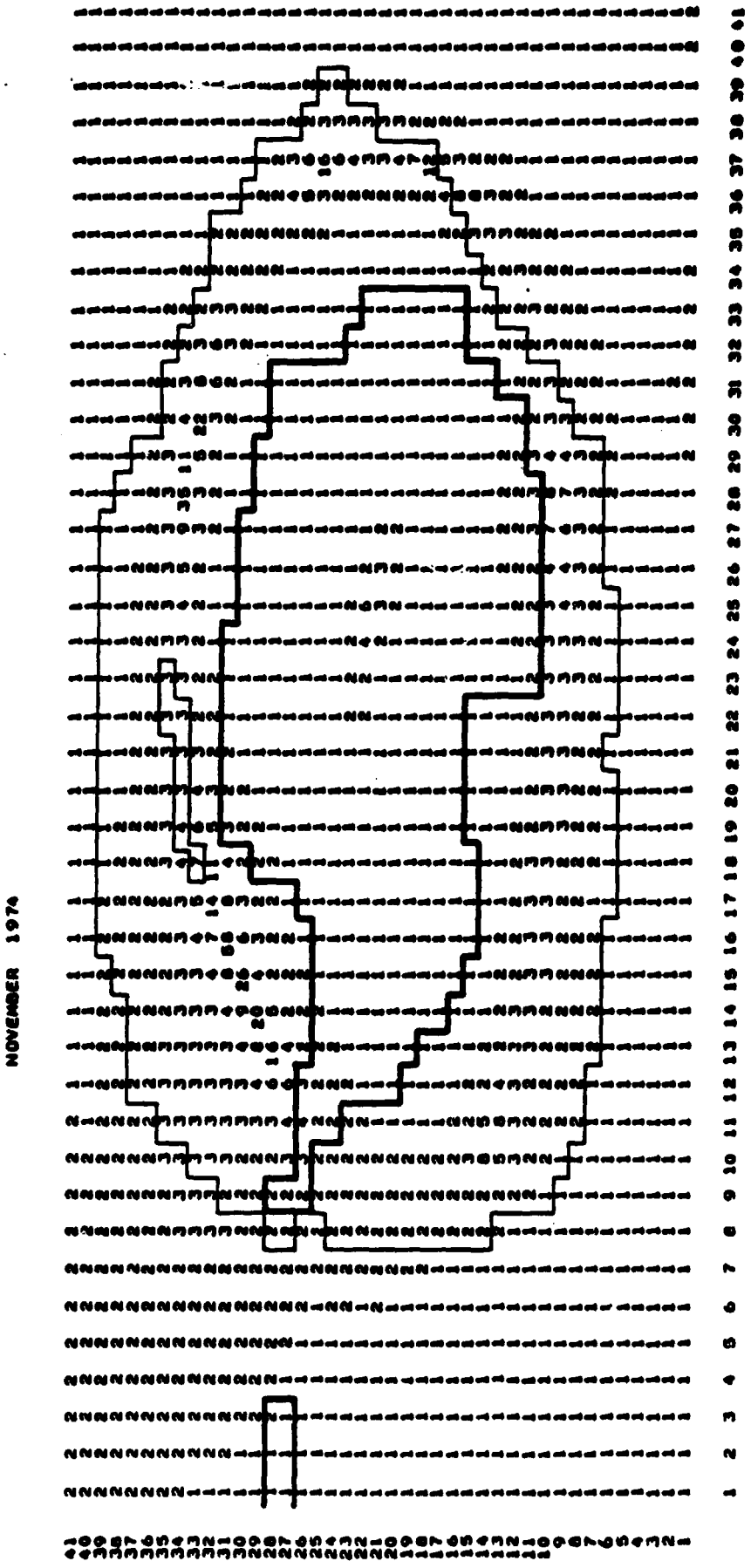

Figure 12. Ratio R over the south polar grid for November 1974.

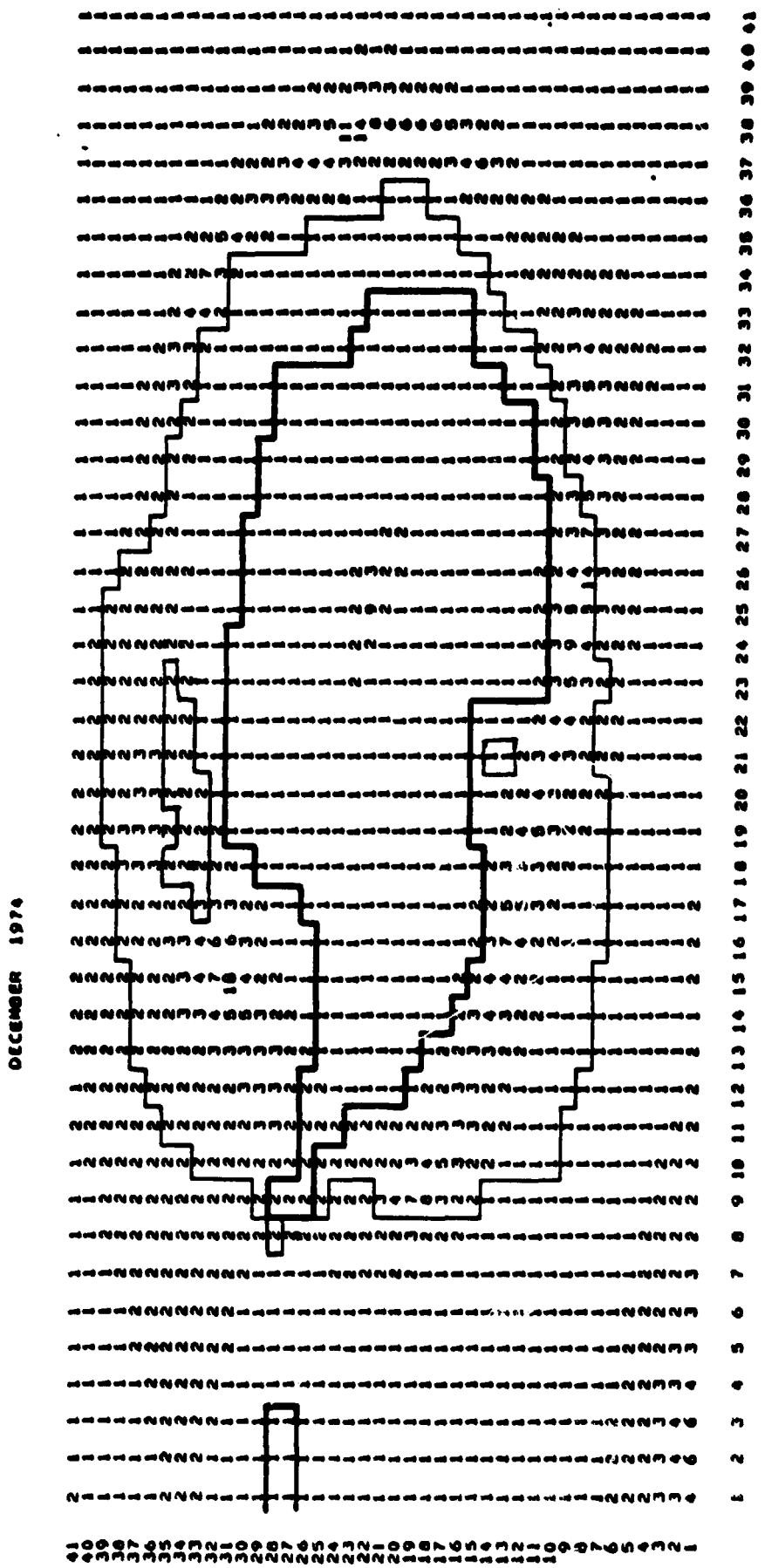

Figure 13. Ratio R over the south polar grid for December 1974.

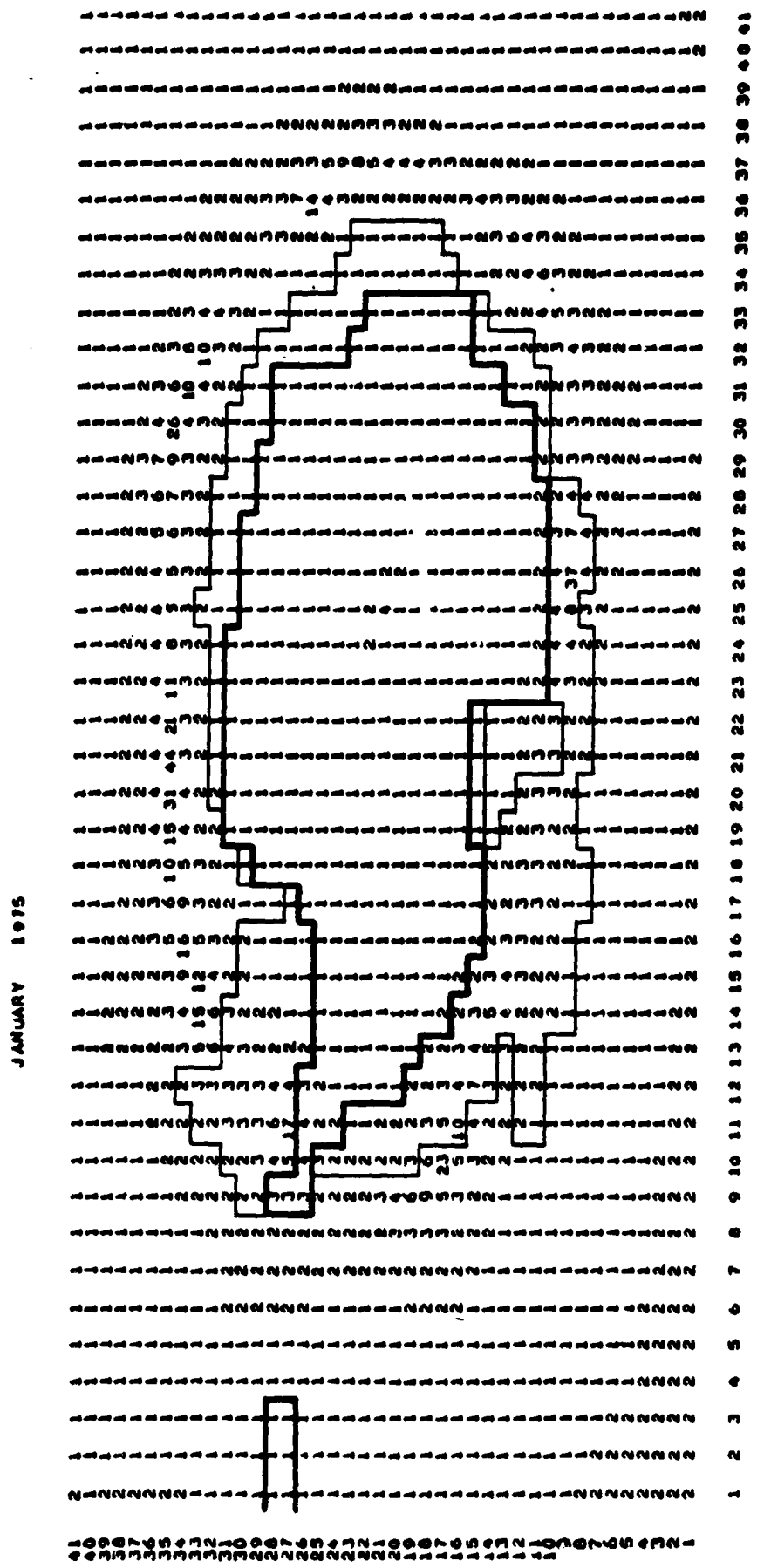

Figure 14. Ratio R over the south polar grid for January 1975.

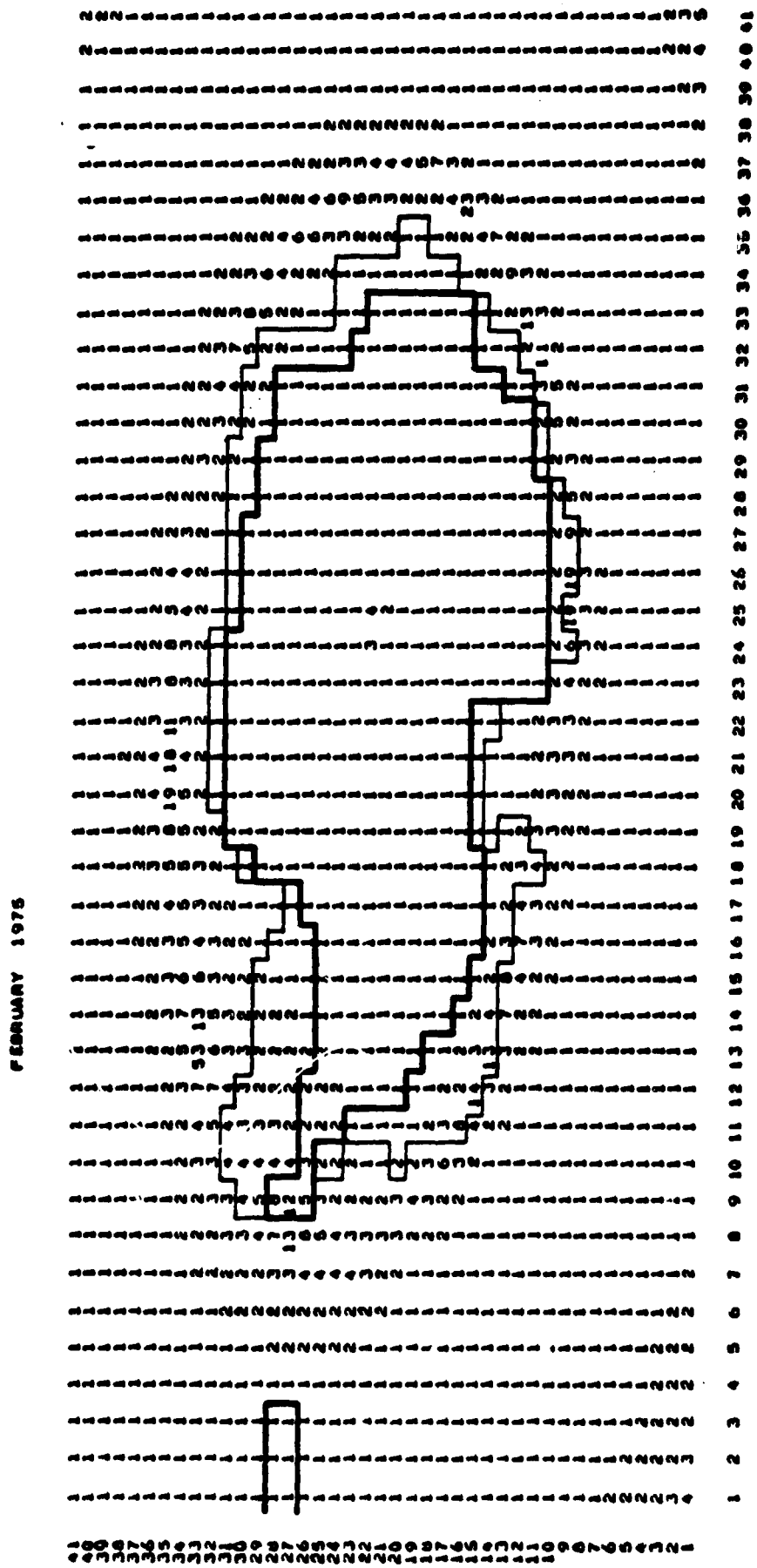

Figure 15. Ratio R over the south polar grid for February 1975.

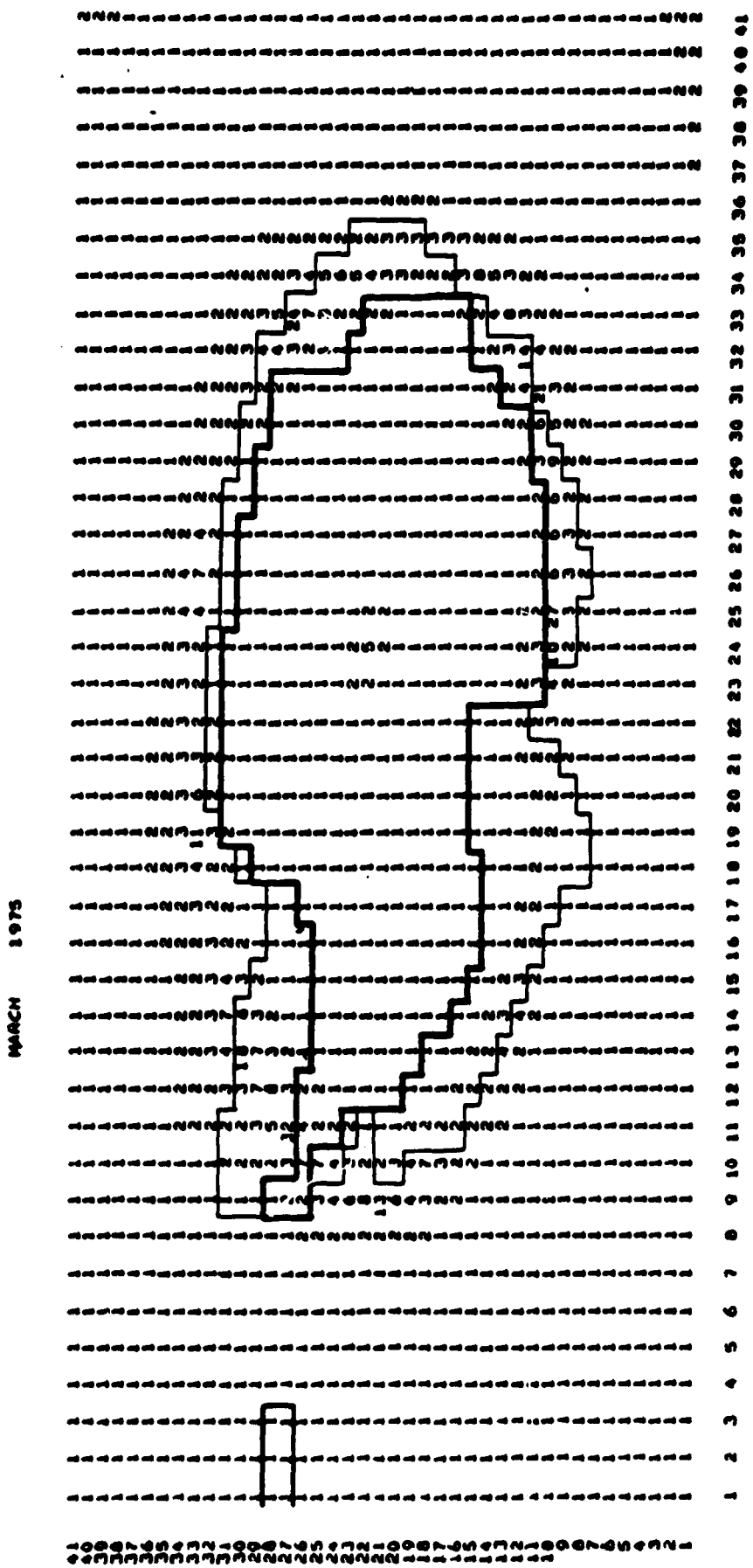

Figure 16. Ratio R over the south polar grid for March 1975.

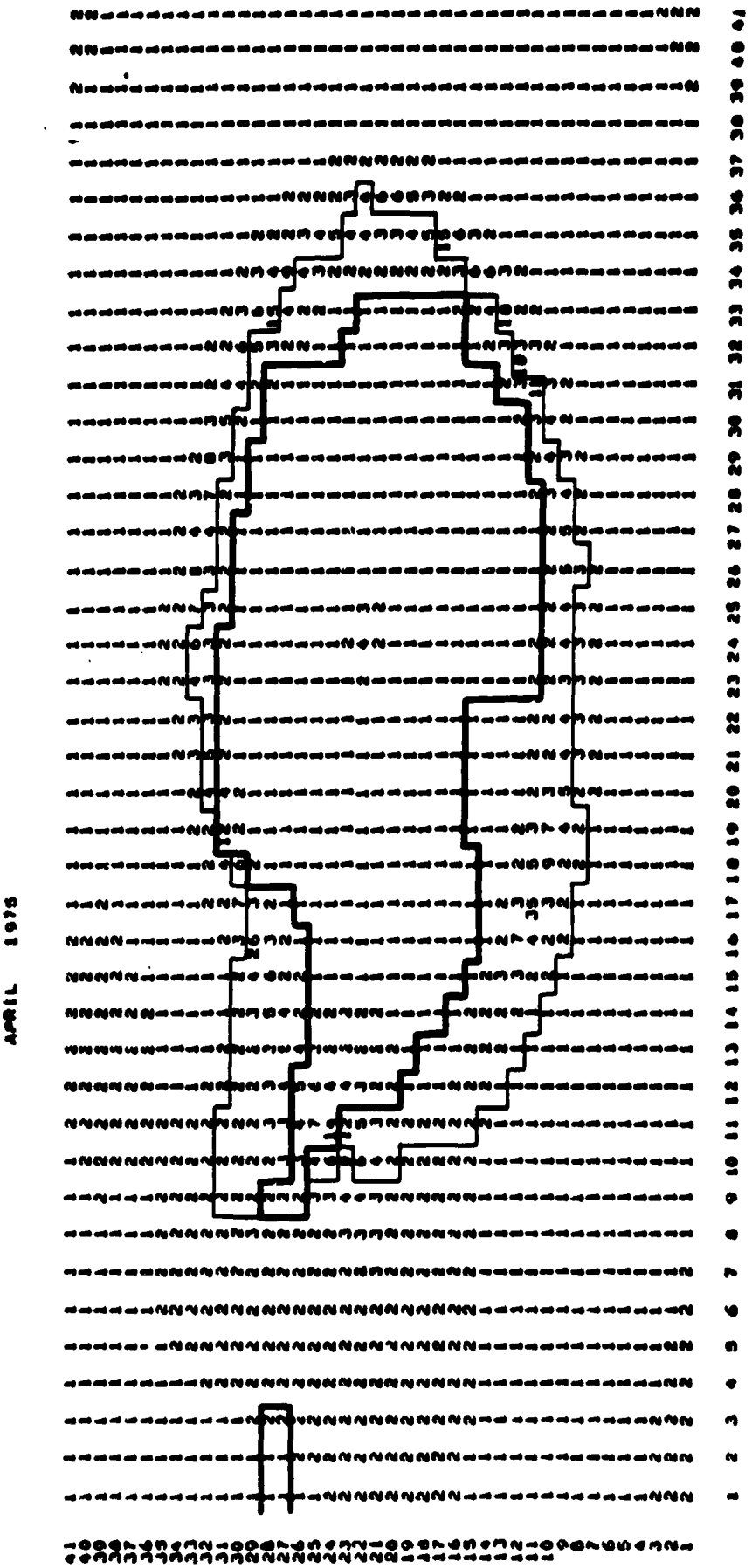

Figure 17. Ratio R over the south polar grid for April 1975.

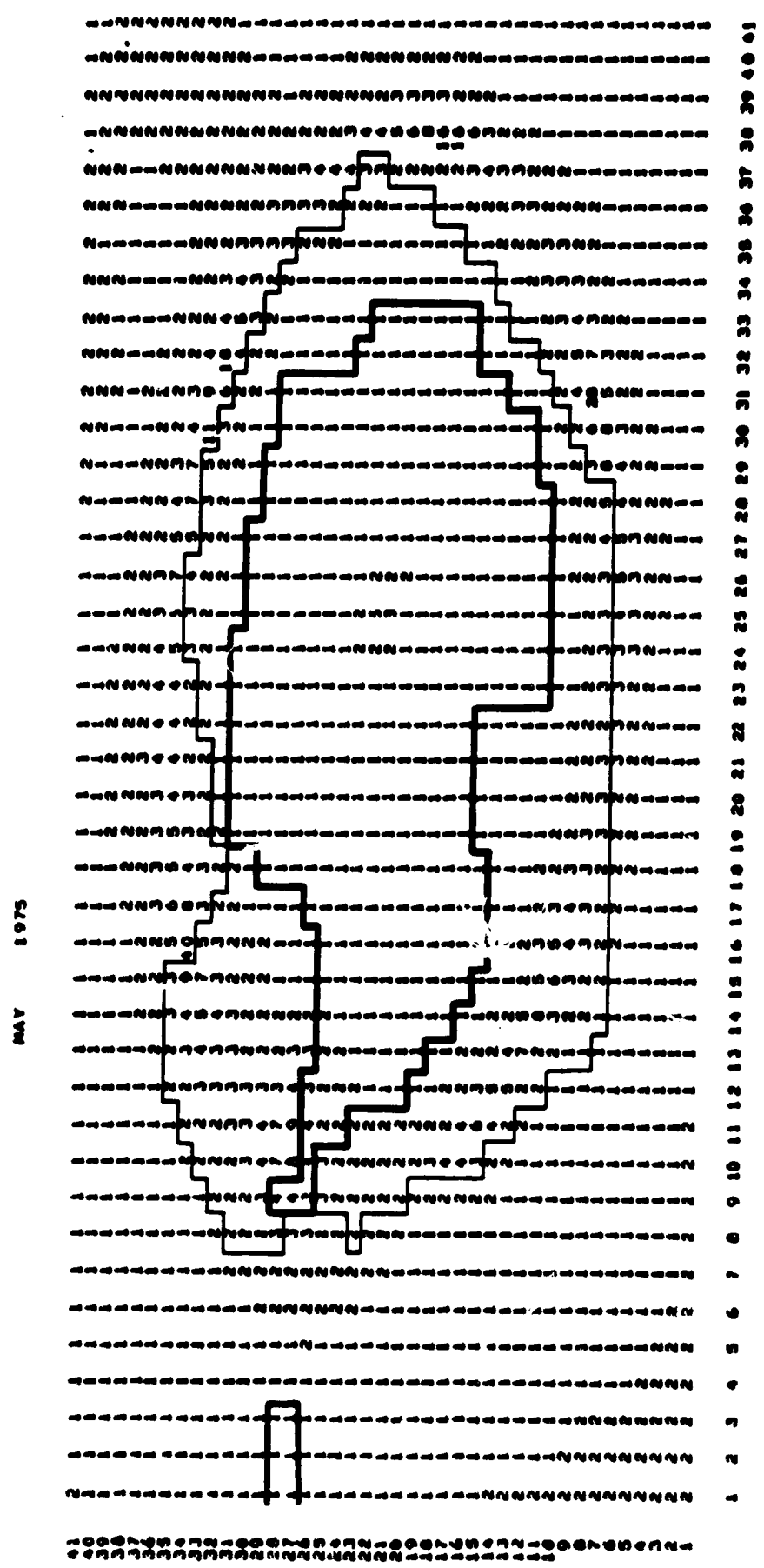

Figure 18. Ratio R over the south polar grid for May 1975.

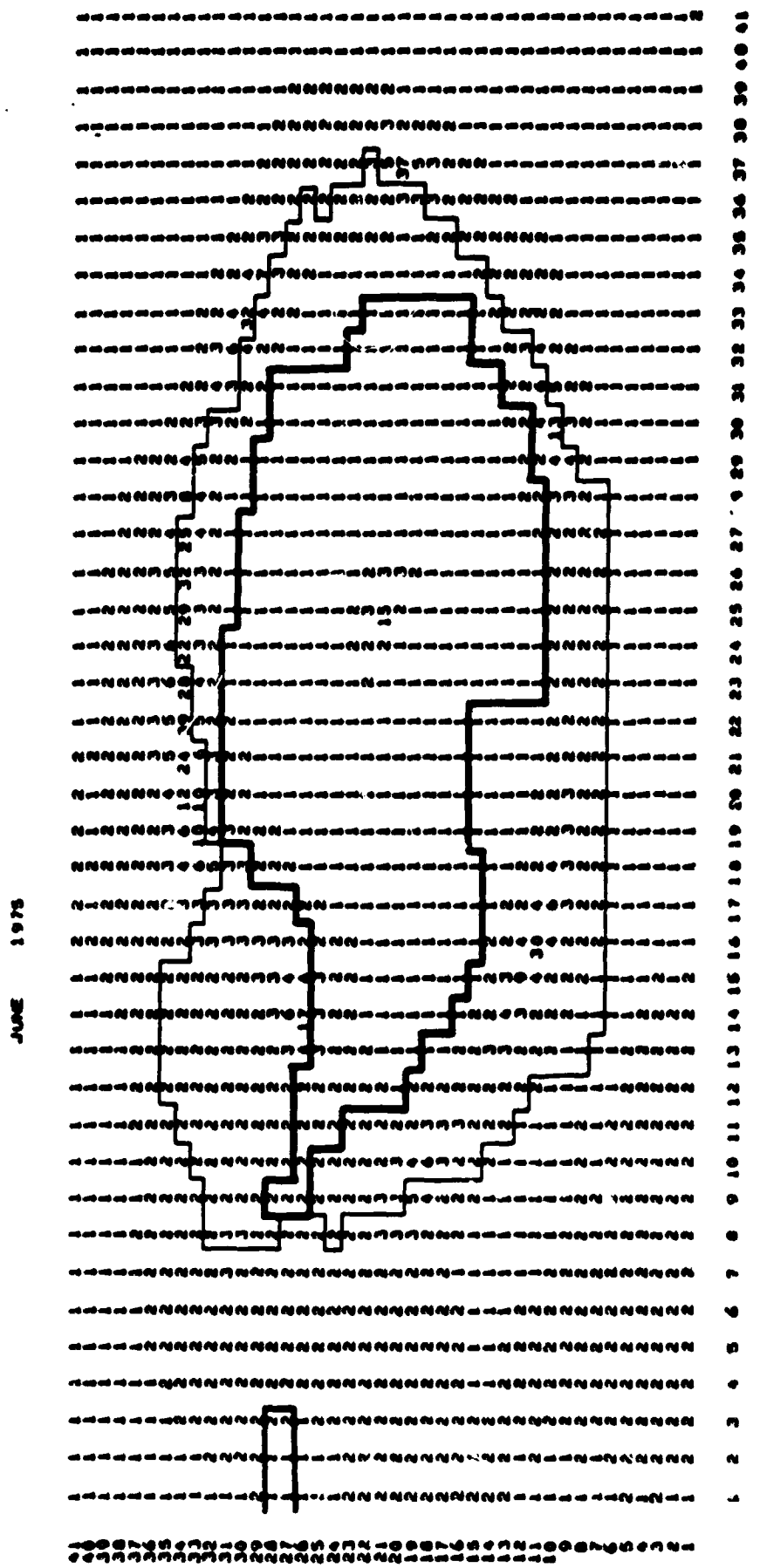

Figure 19. Ratio R over the south polar grid for June 1975.

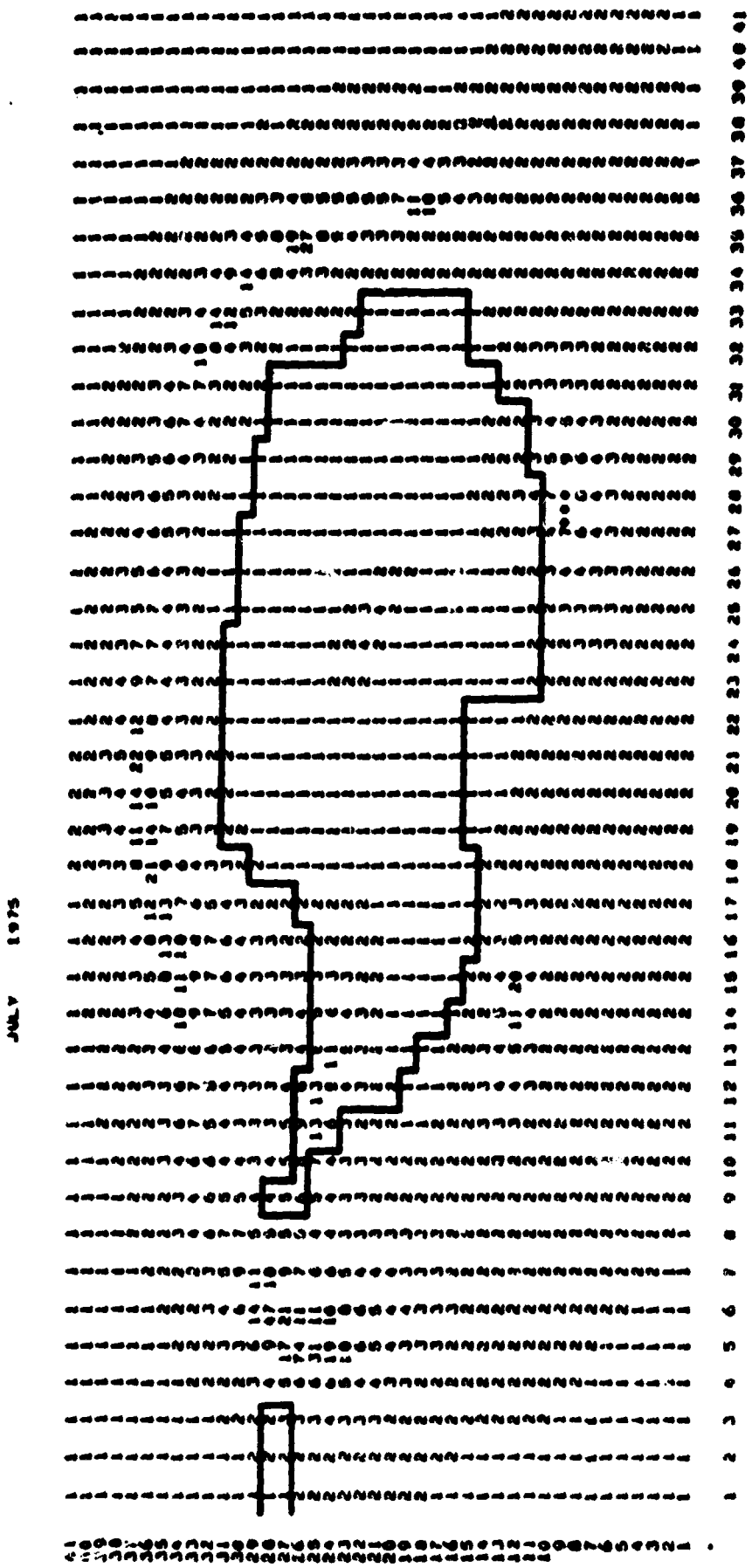

Figure 20. Ratio R over the south polar grid for July 1975.

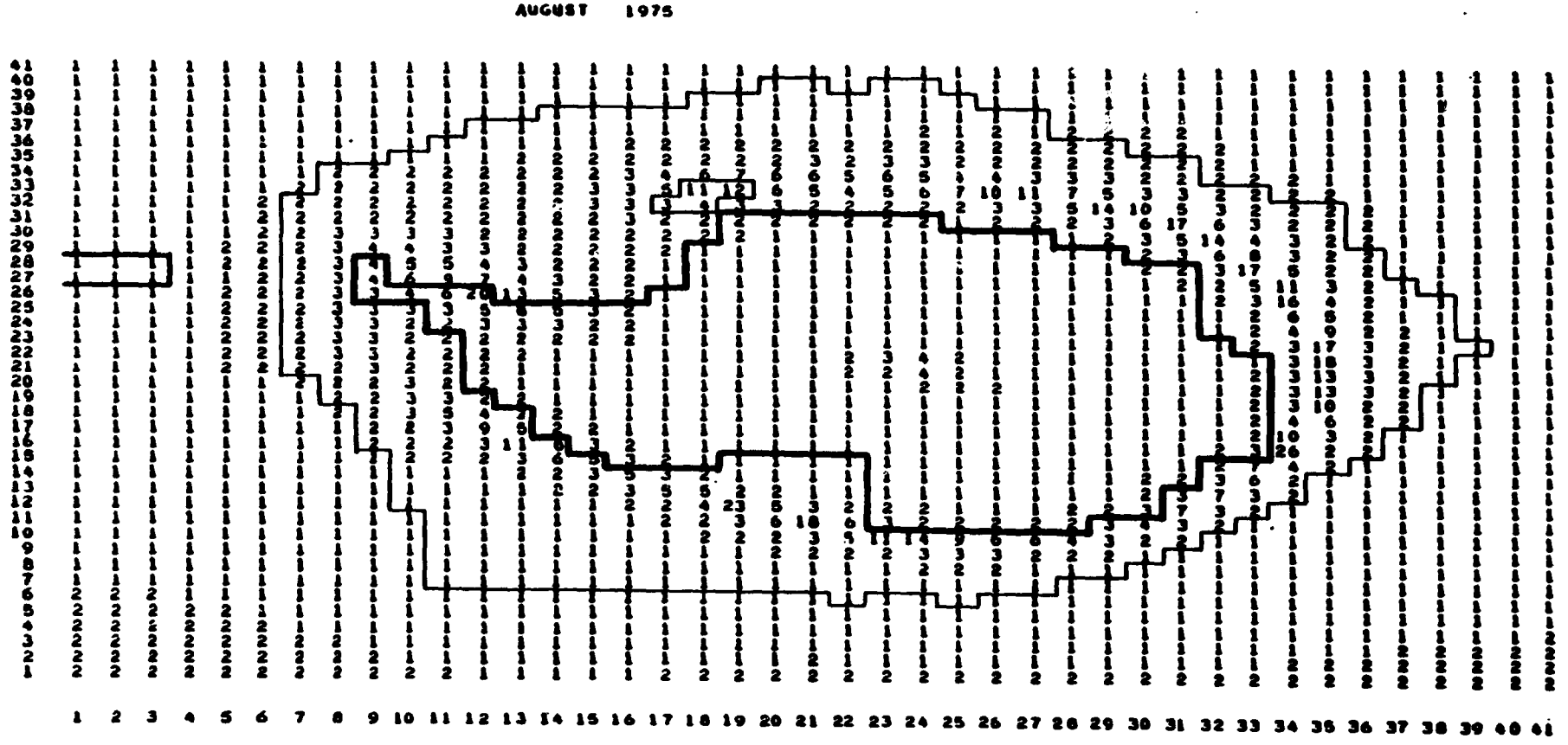

Figure 21. Ratio R over the south polar grid for August 1975.

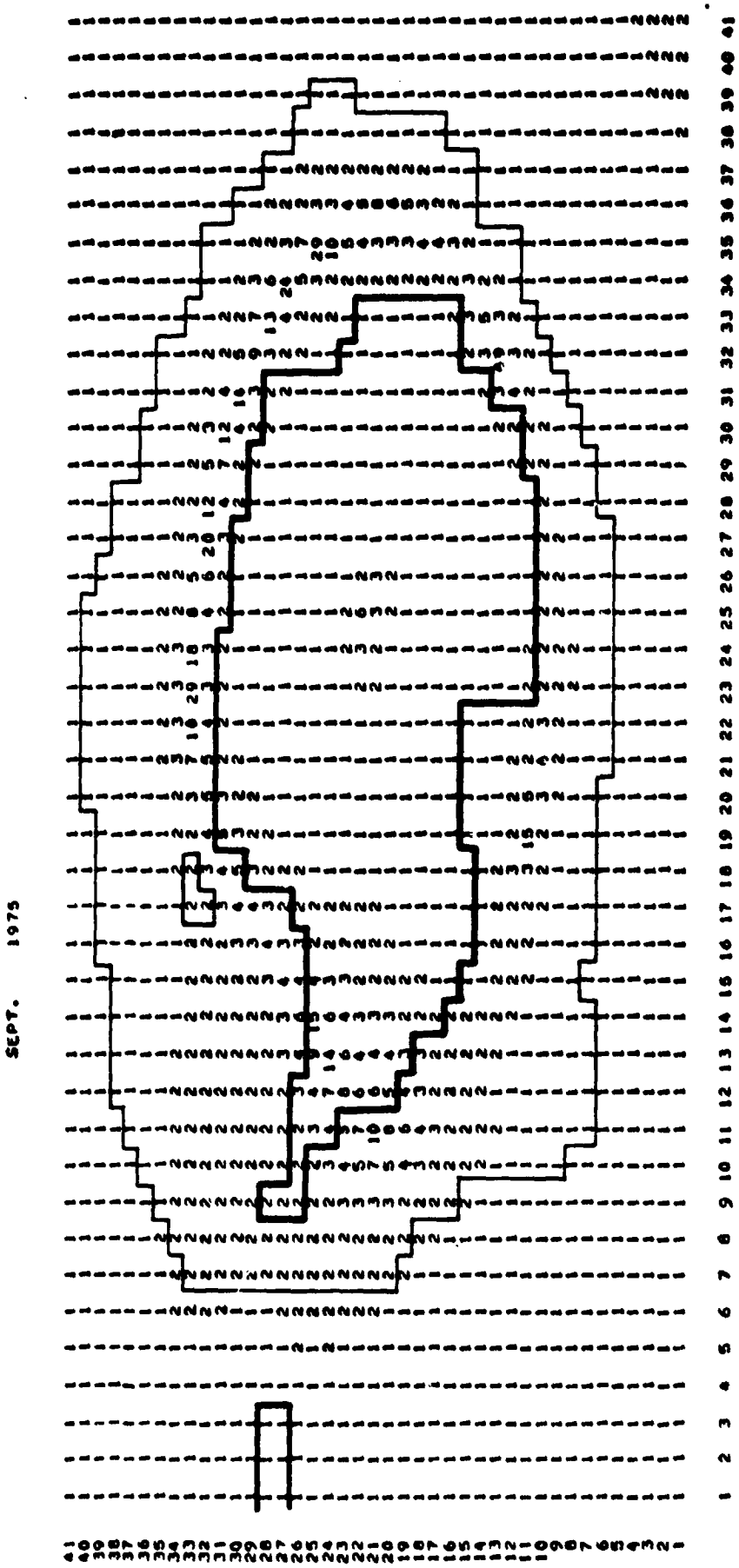

Figure 22. Ratio R over the south polar grid for September 1975.

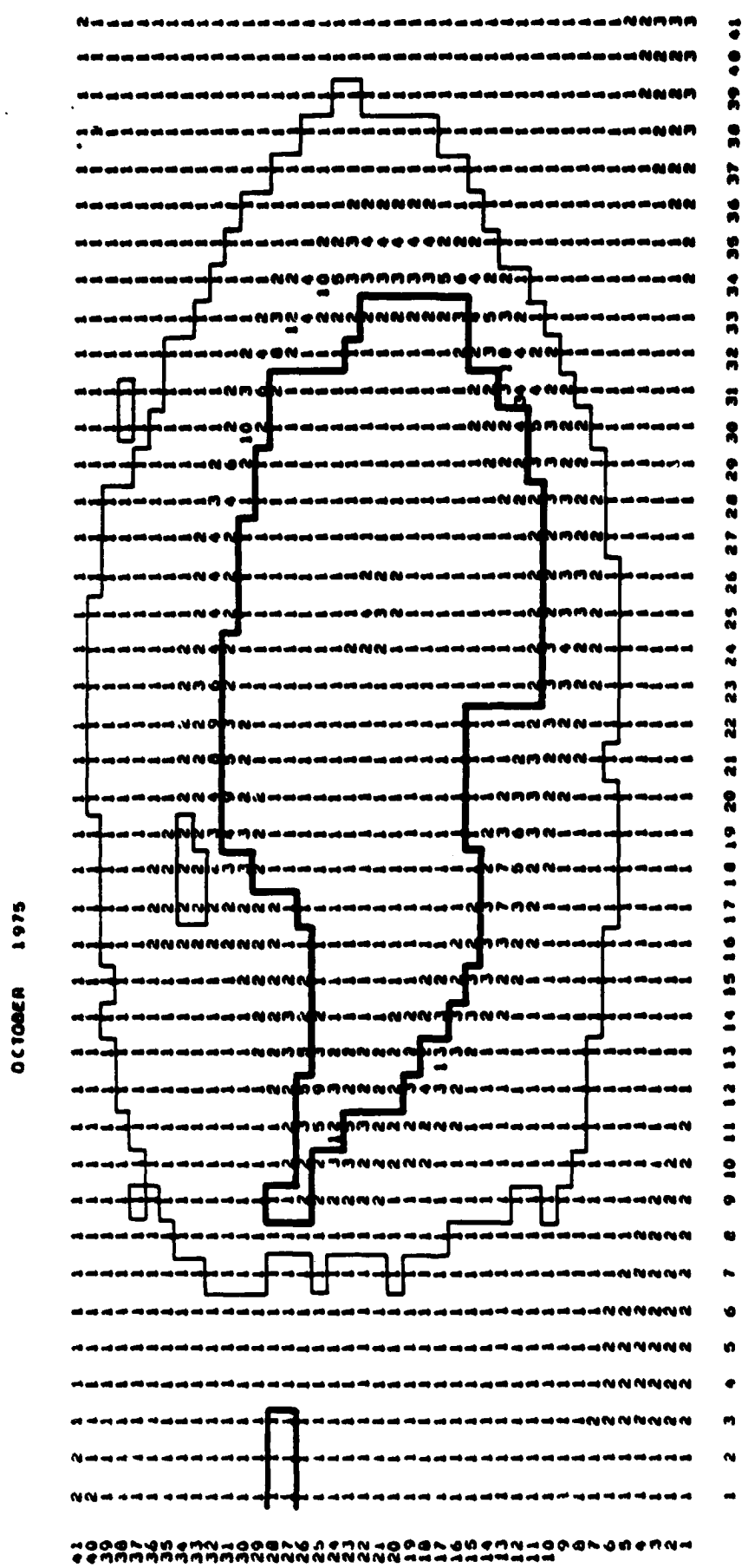

Figure 23. Ratio R over the south polar grid for October 1975.

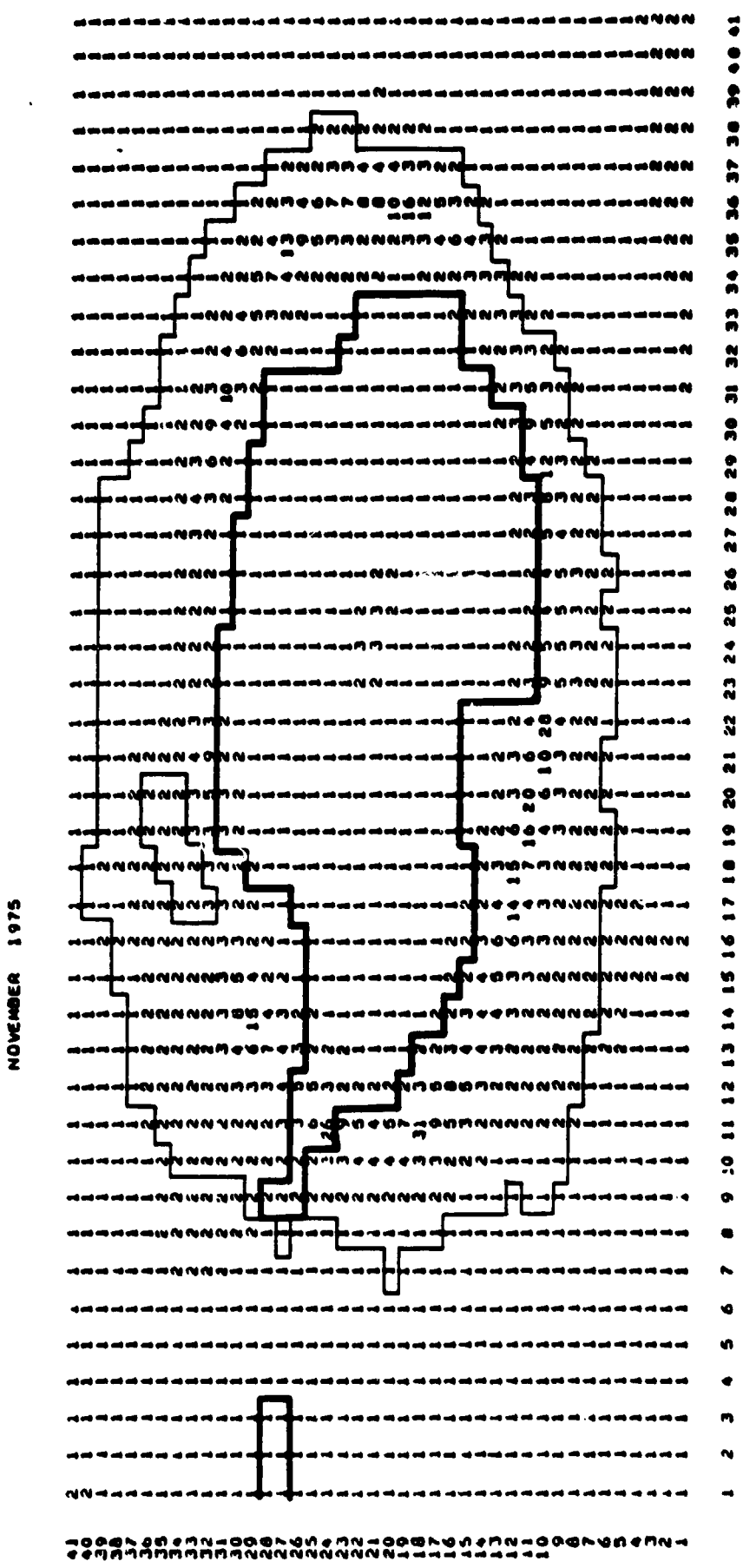

Figure 24. Ratio R over the south polar grid for November 1975.

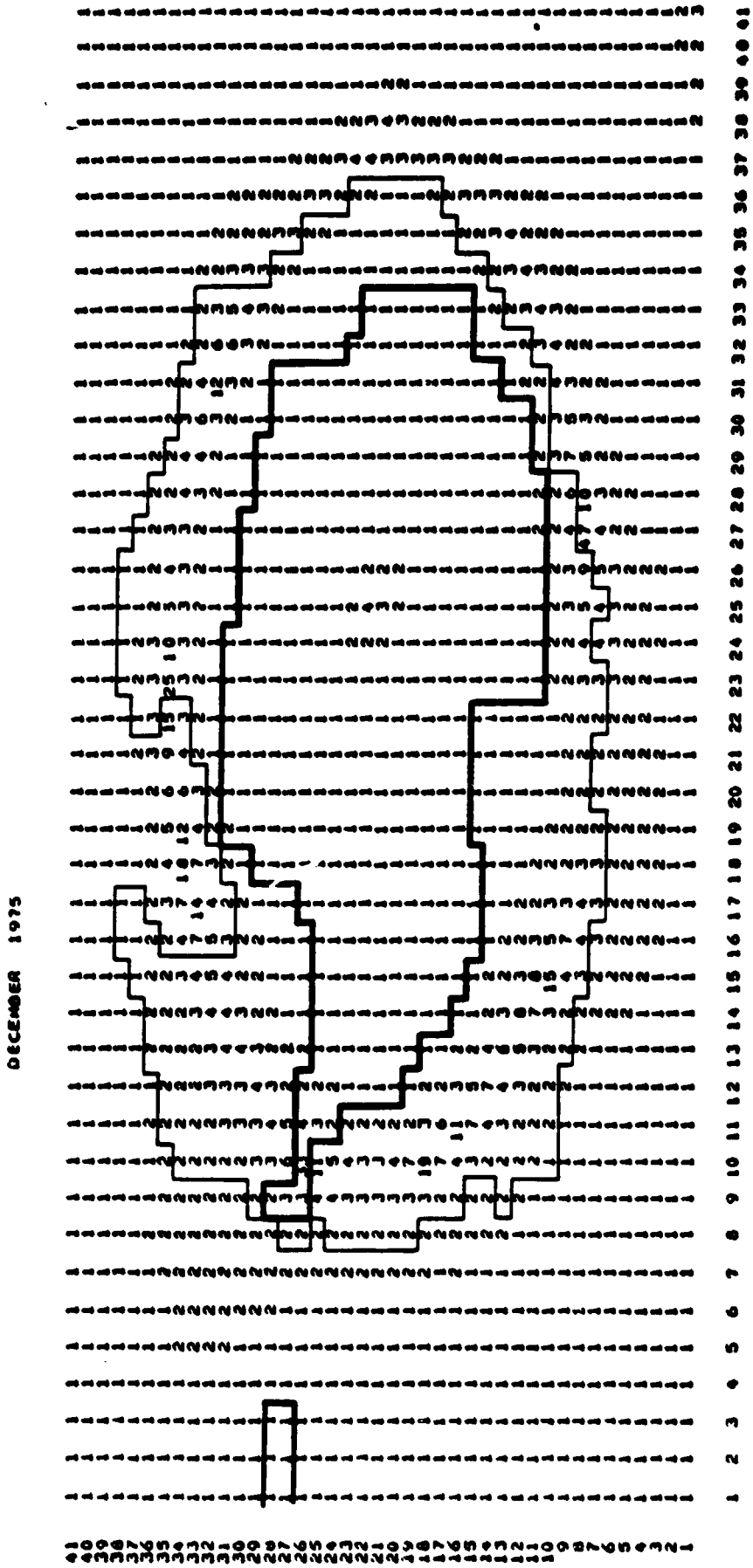

Figure 25. Ratio R over the south polar grid for December 1975.

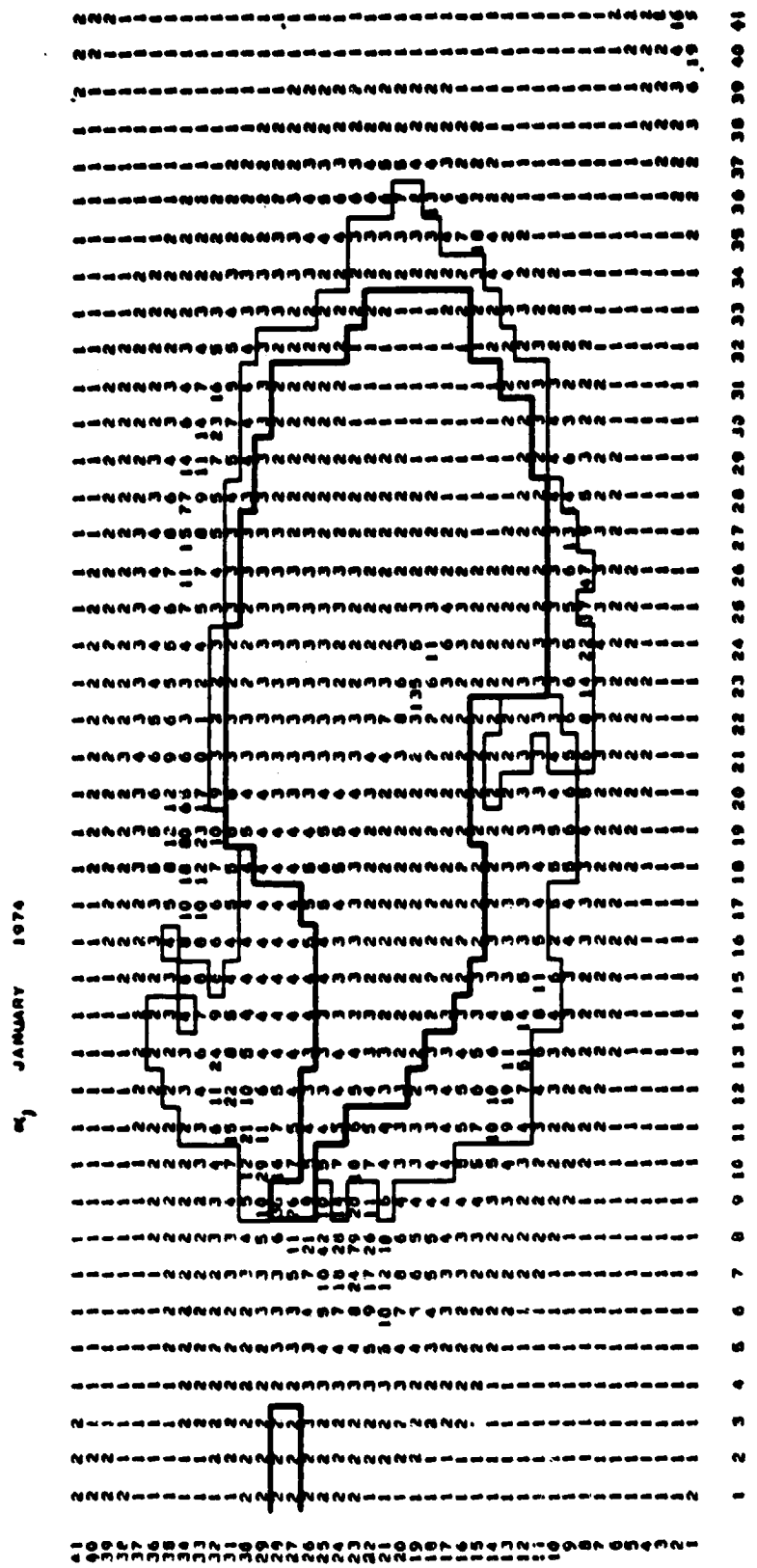

Figure 26. Ratio α over the south polar grid for January 1974.

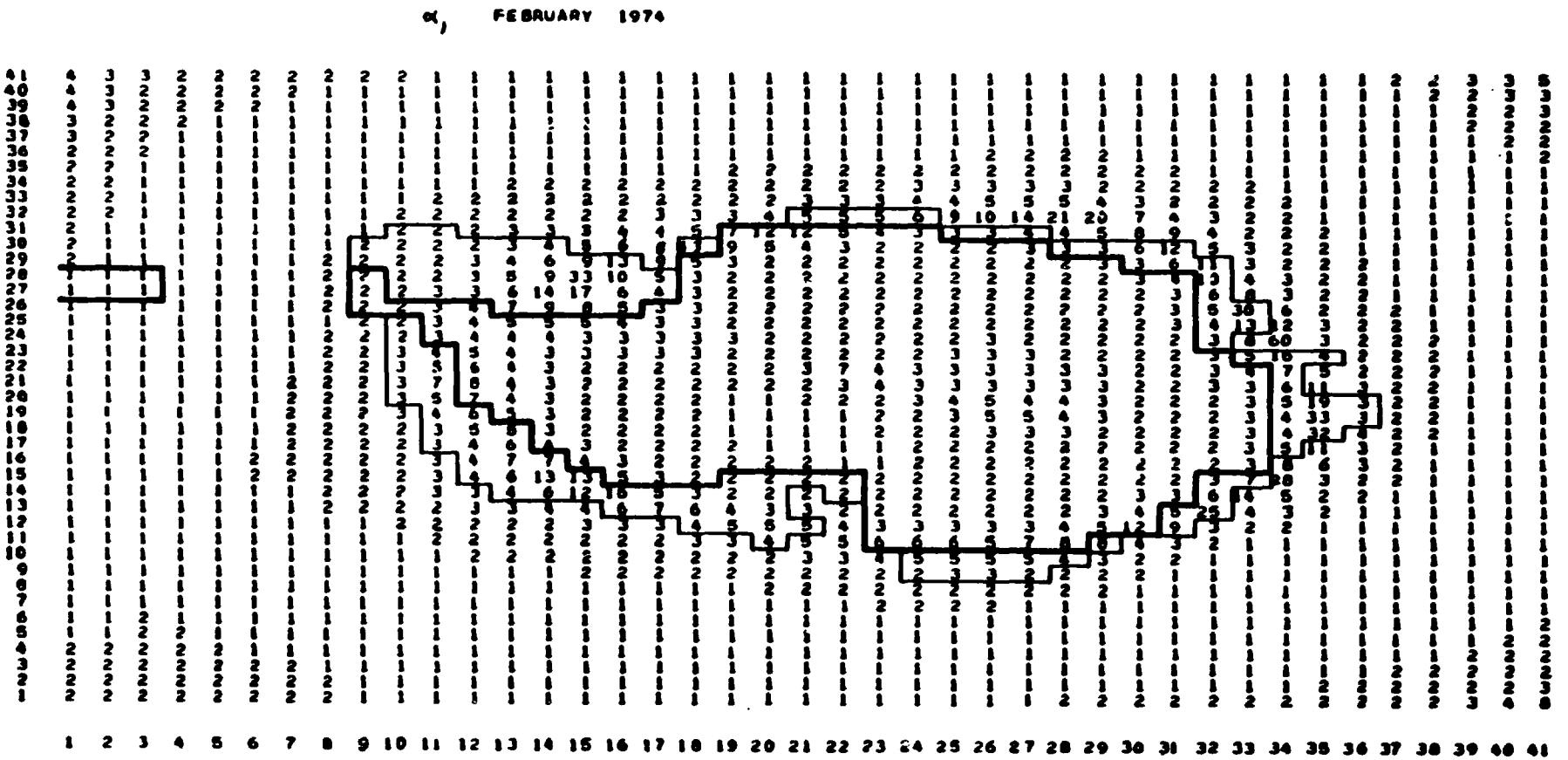

Figure 27. Ratio α over the south polar grid for February 1974.

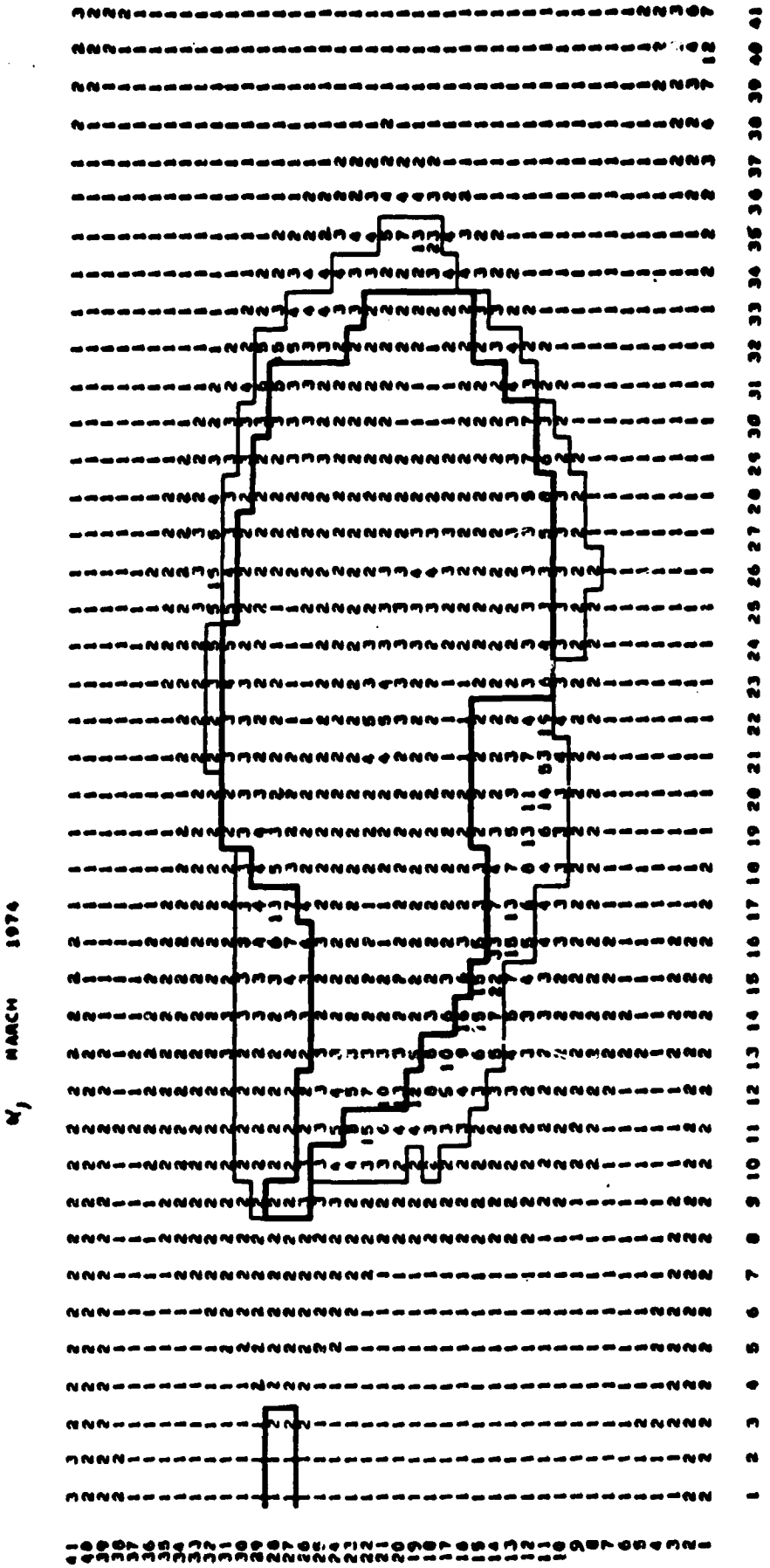

Figure 28. Ratio α over the south polar grid for March 1974.

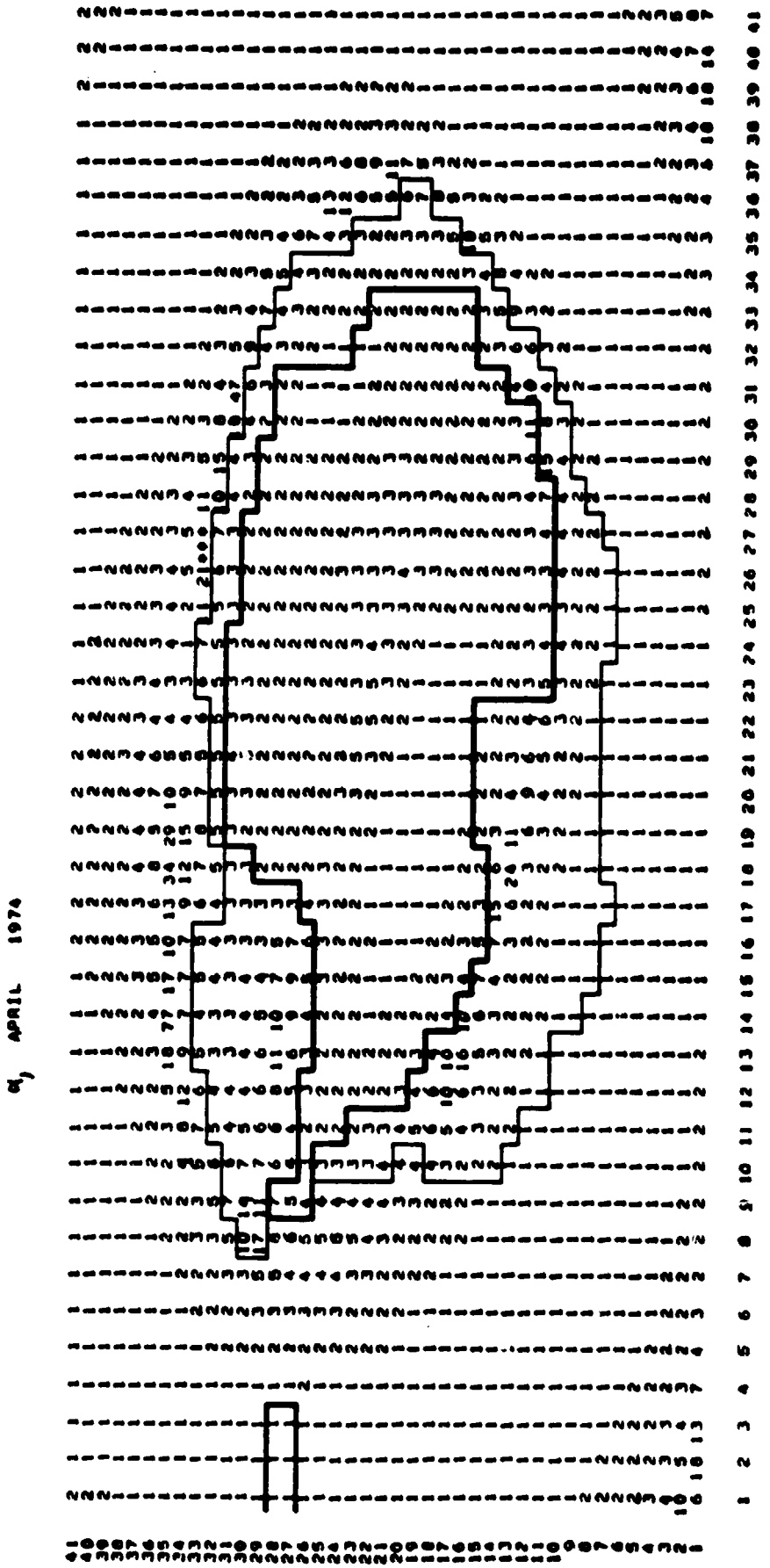

Figure 29. Ratio α over the south polar grid for April 1974.

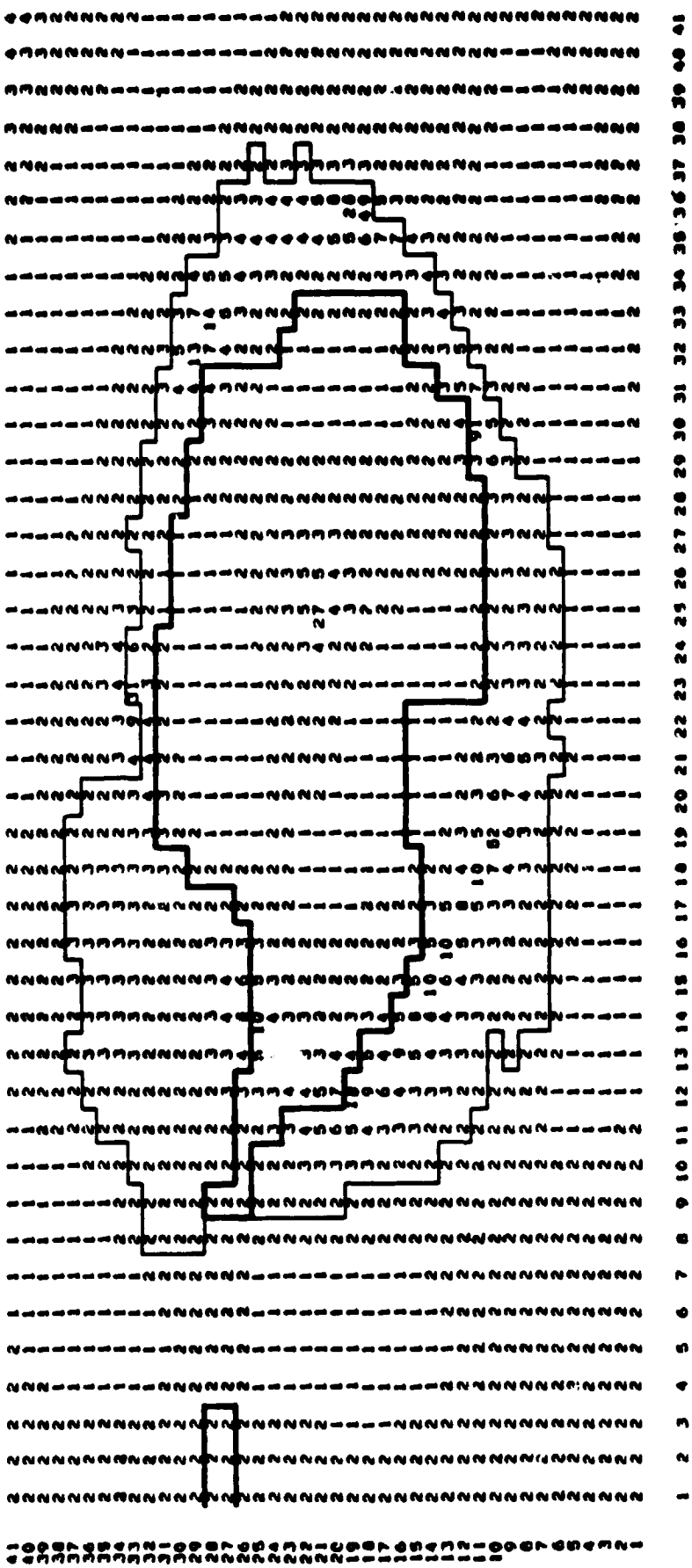

Figure 30. Ratio α over the south polar grid for May 1974.

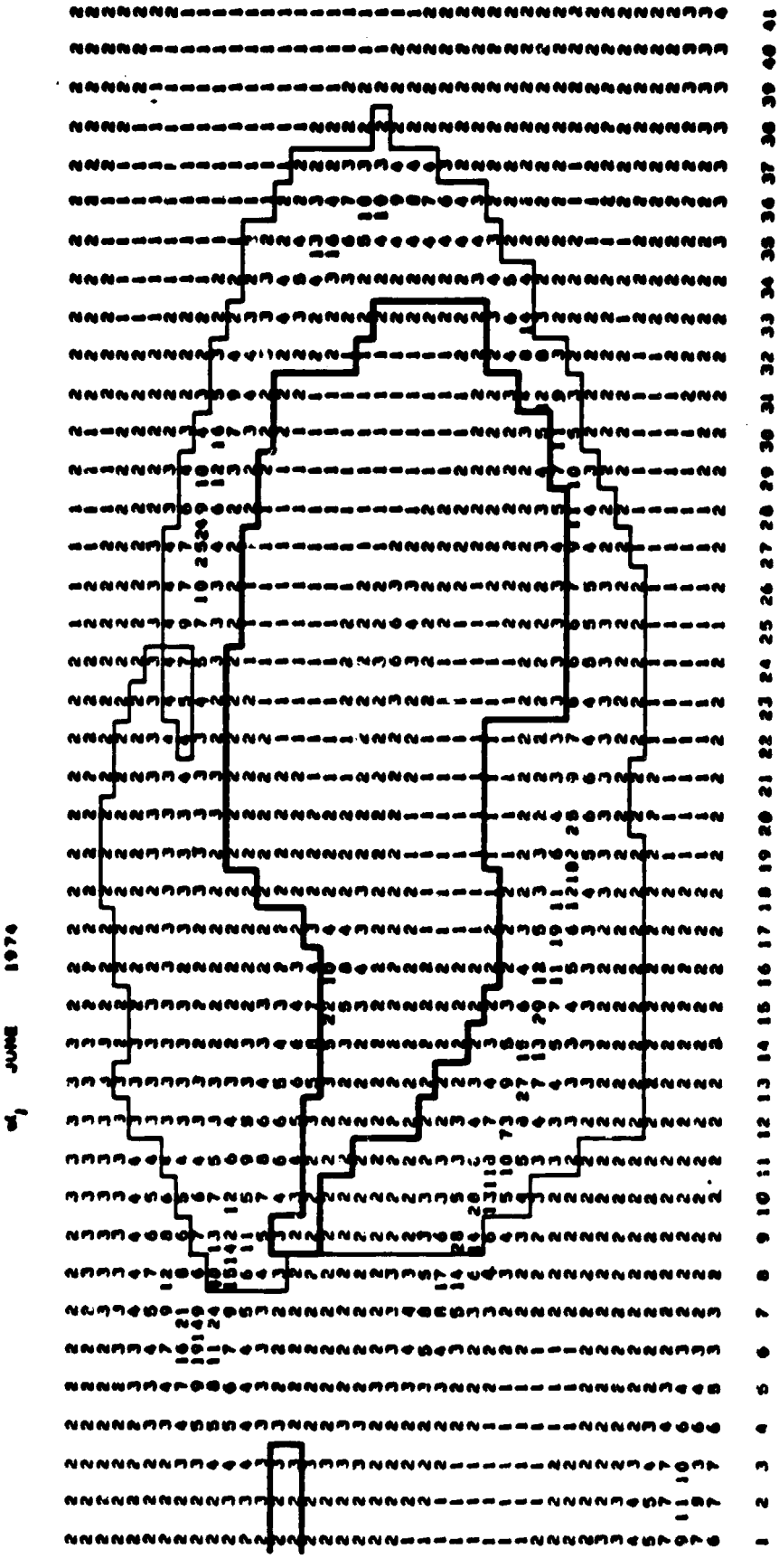

Figure 31. Ratio α over the south polar grid for June 1974.

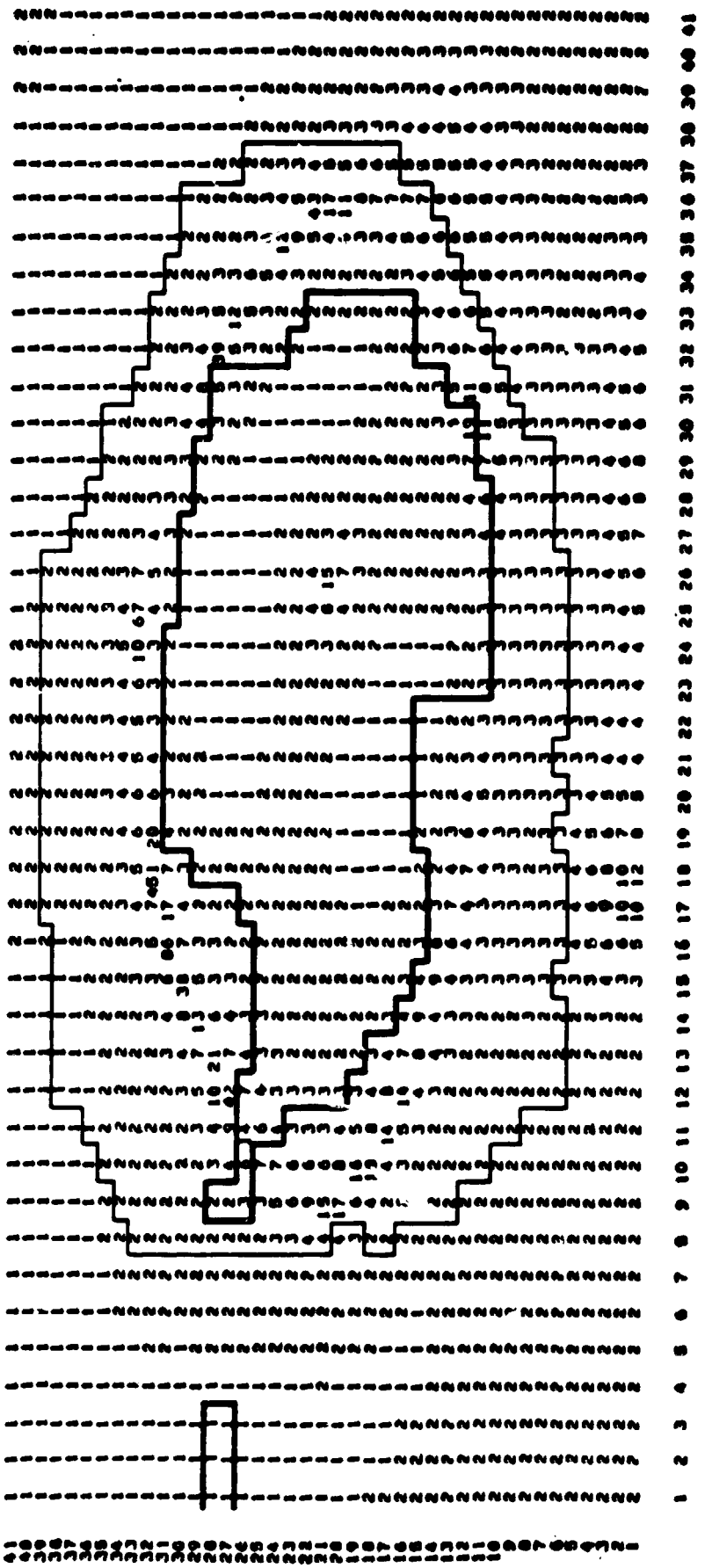

Figure 32. Ratio α over the south polar grid for July 1974.

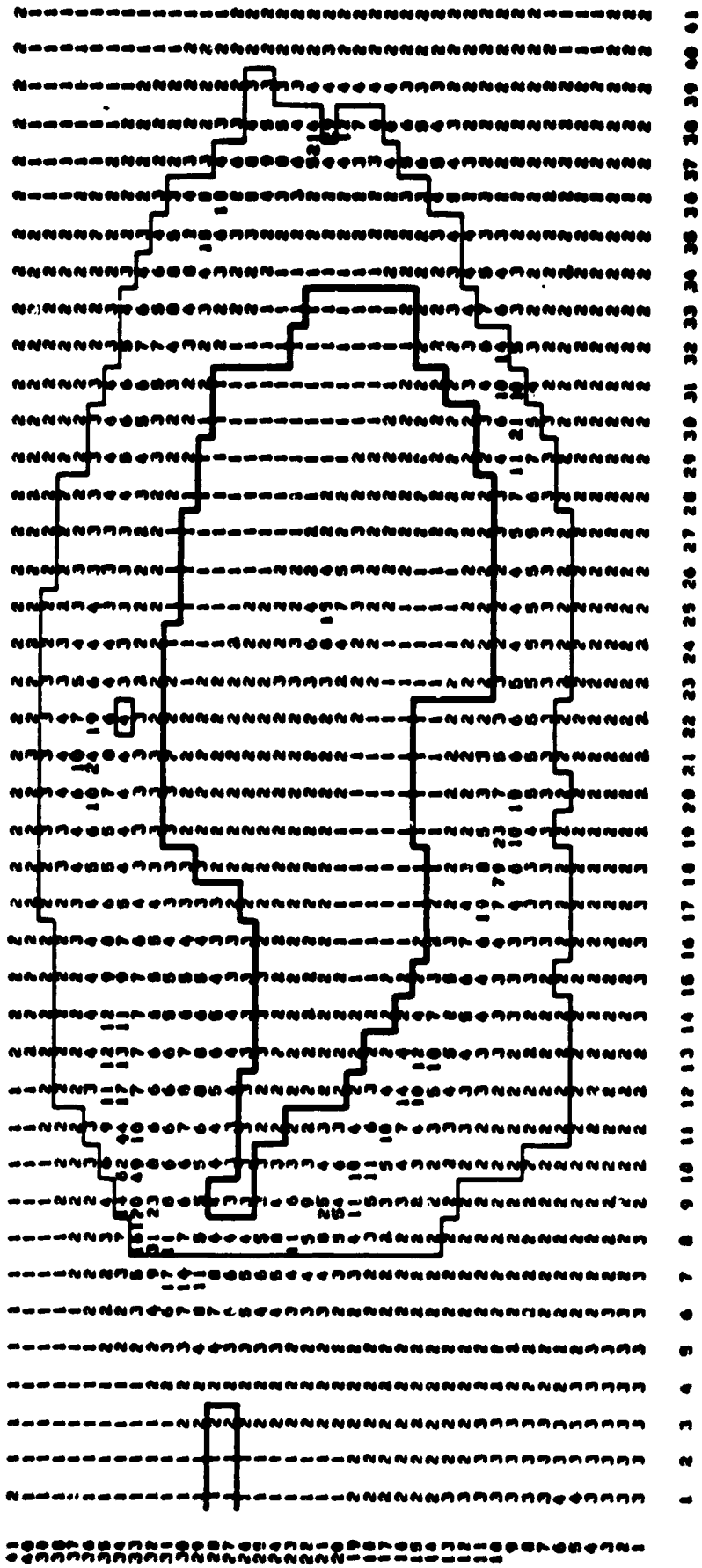

Figure 33. Ratio α over the south polar grid for August 1974.

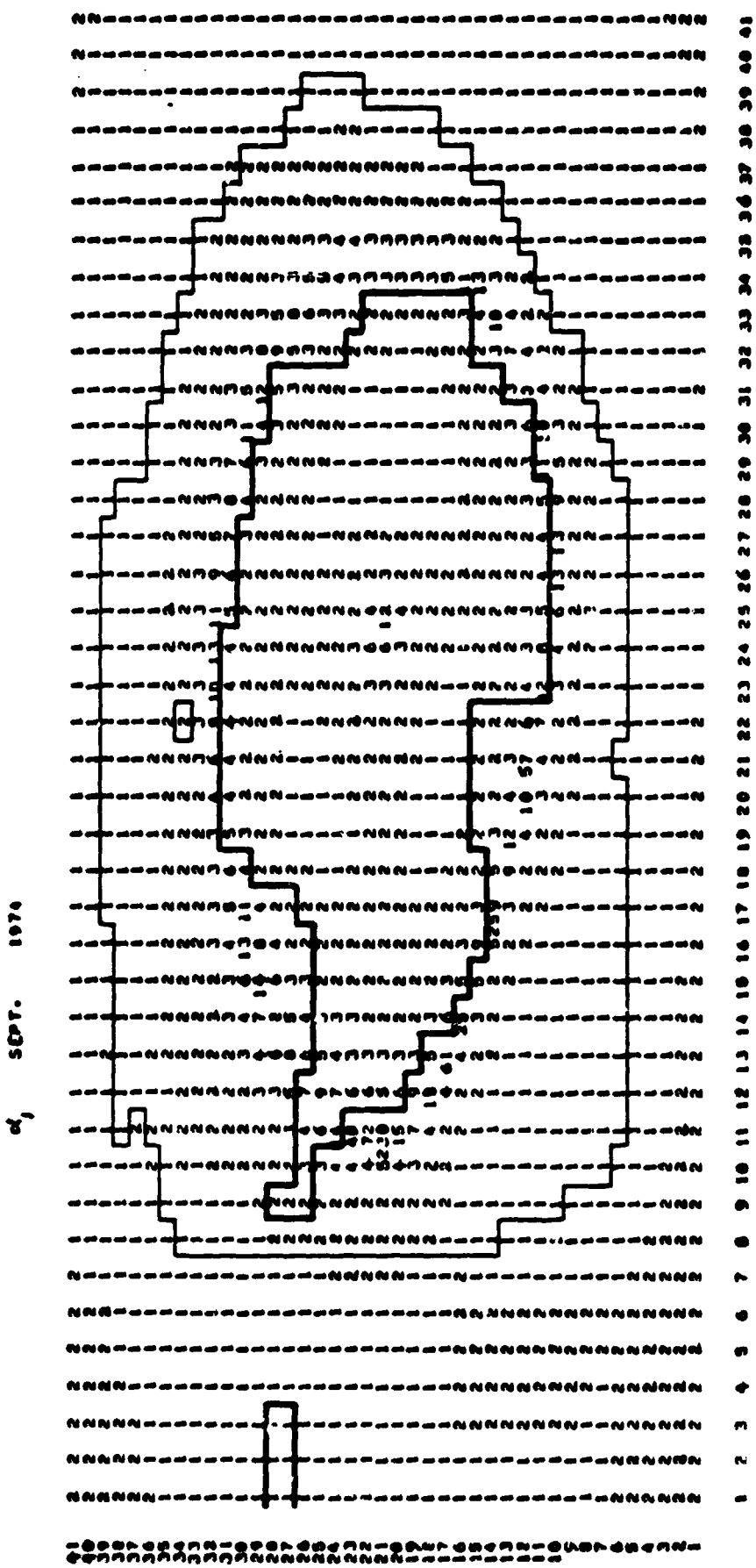

Figure 34. Ratio α over the south polar grid for September 1974.

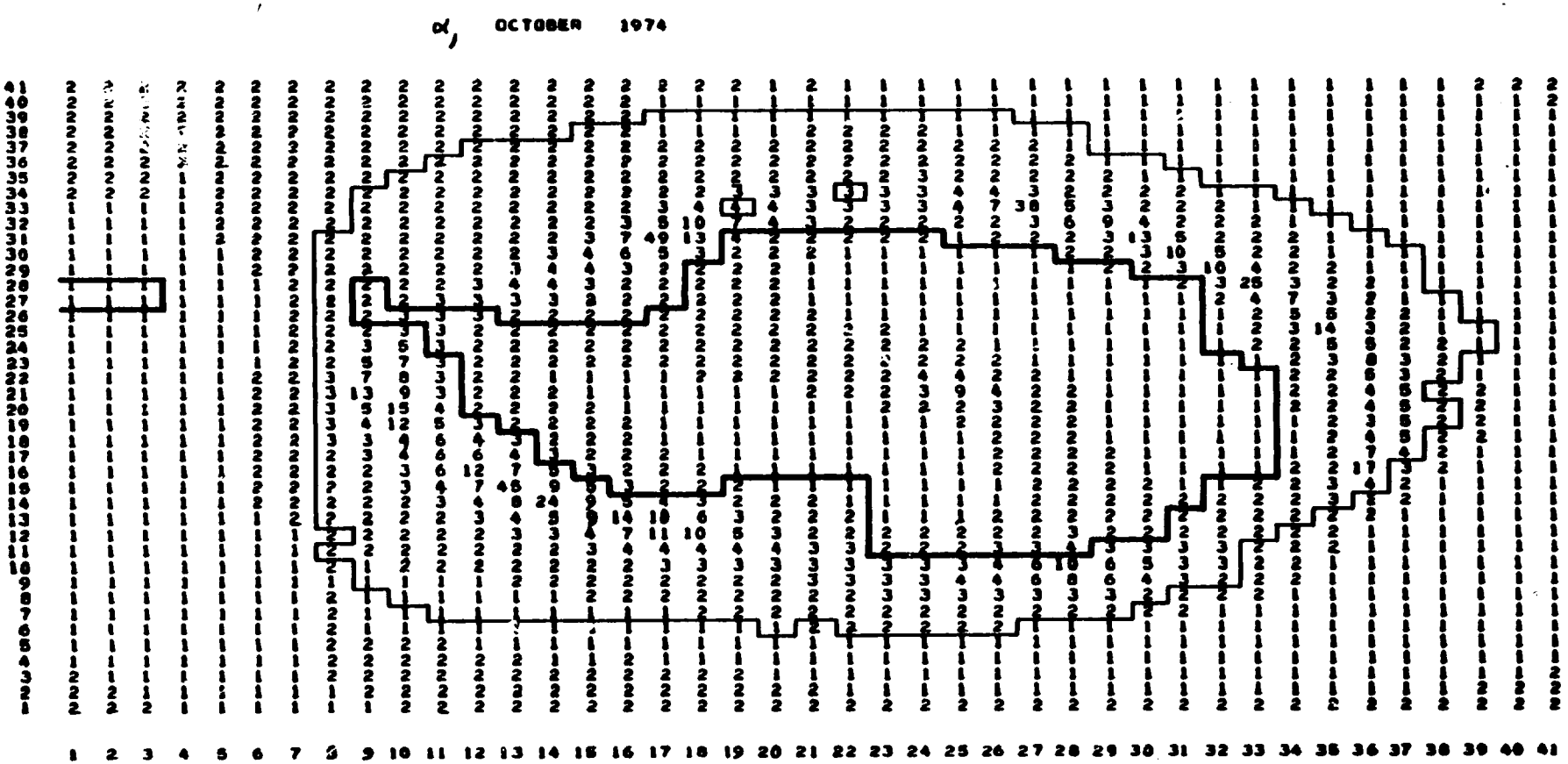

Figure 35. Ratio α over the south polar grid for October 1974.

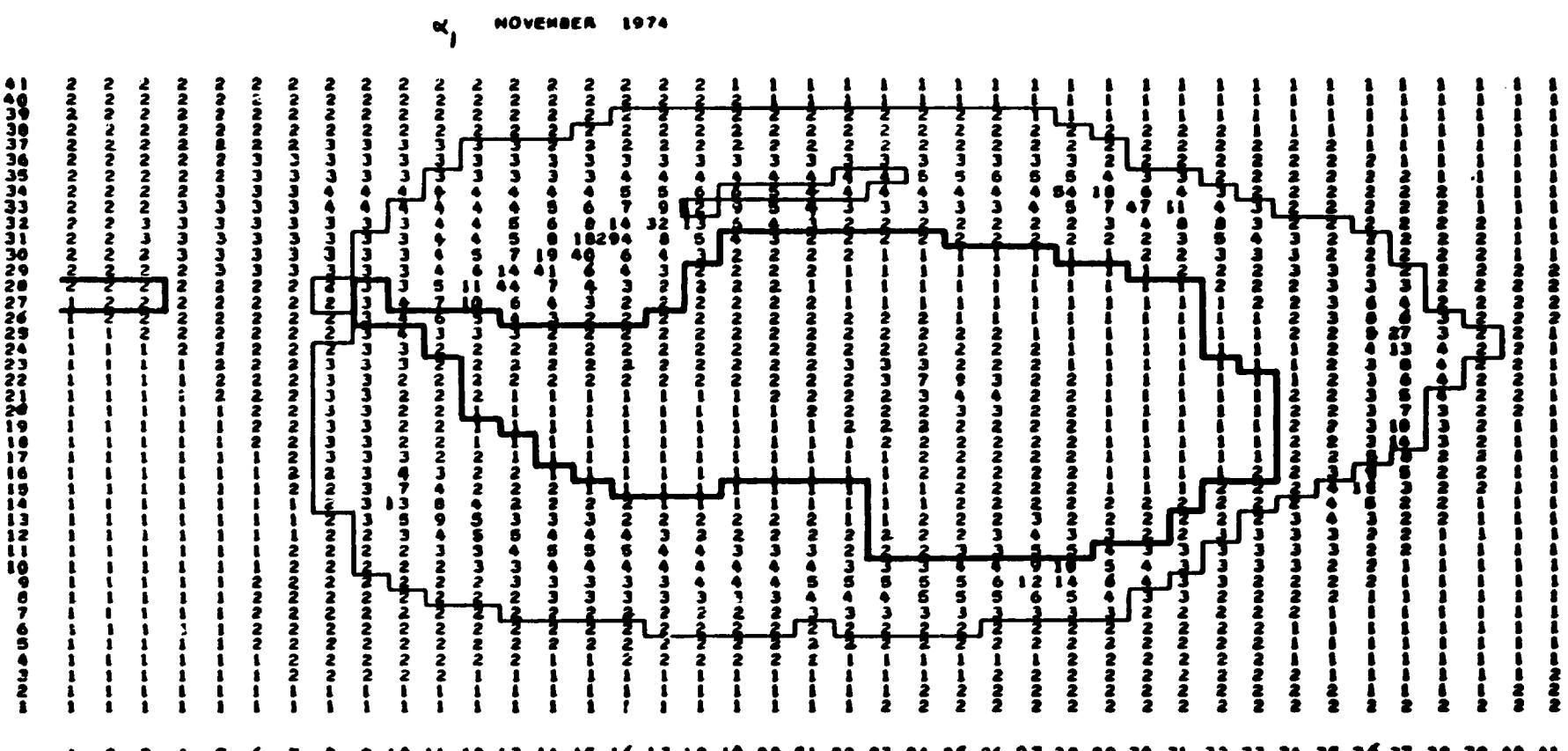

Figure 36. Ratio α over the south polar grid for November 1974.

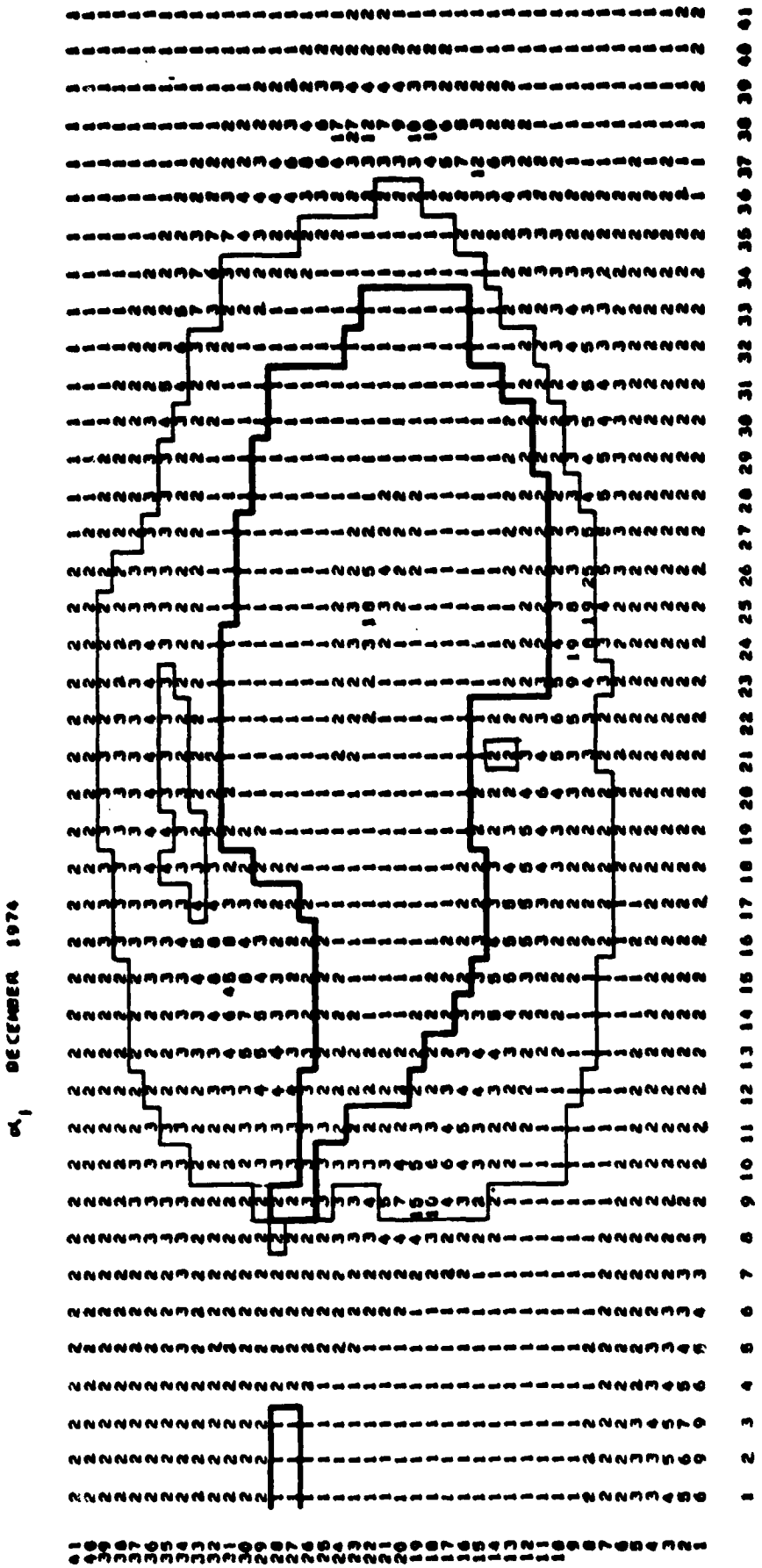

Figure 37. Ratio α over the south polar grid for December 1974.

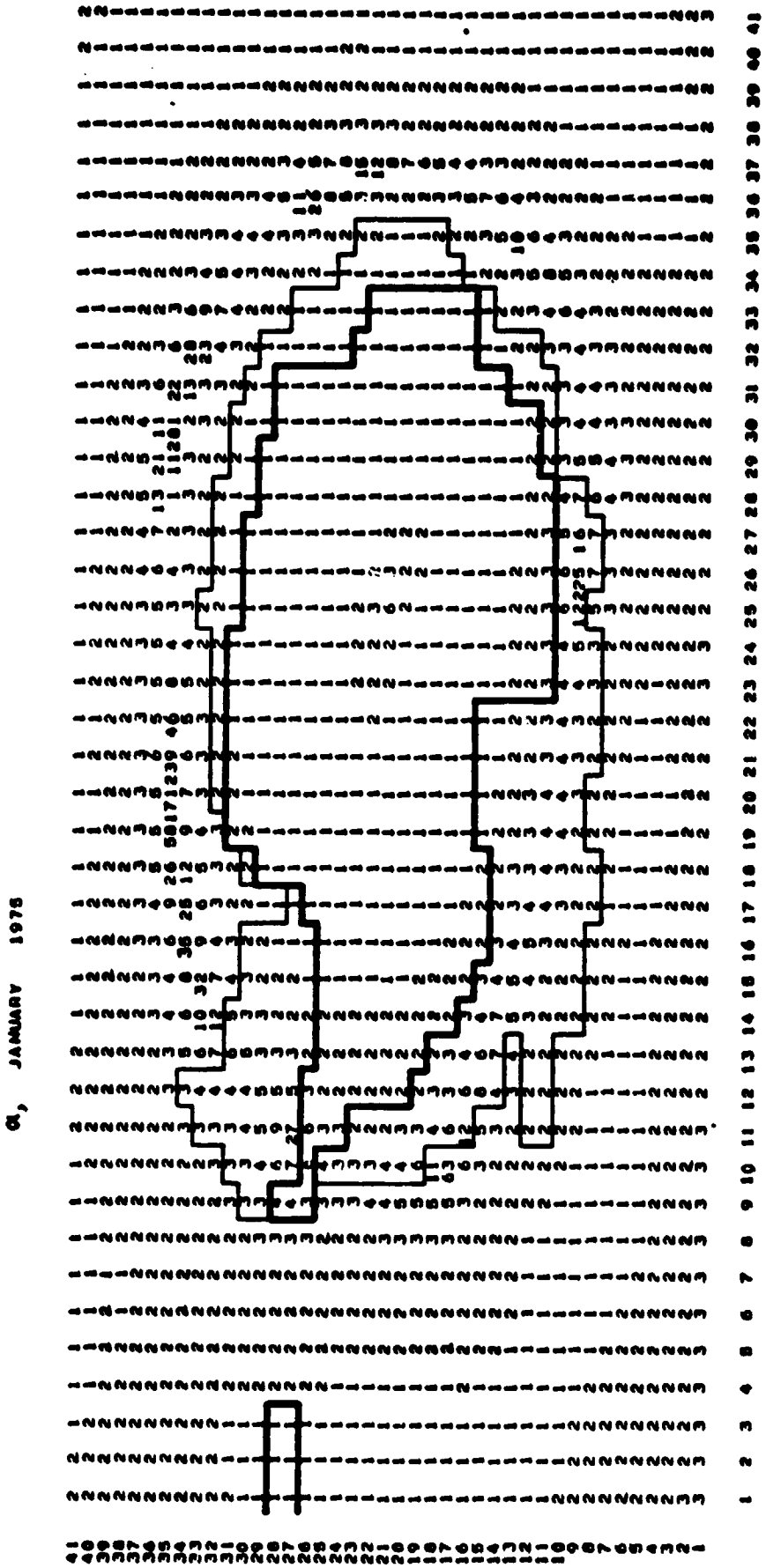

Figure 38. Ratio α over the south polar grid for January 1975.

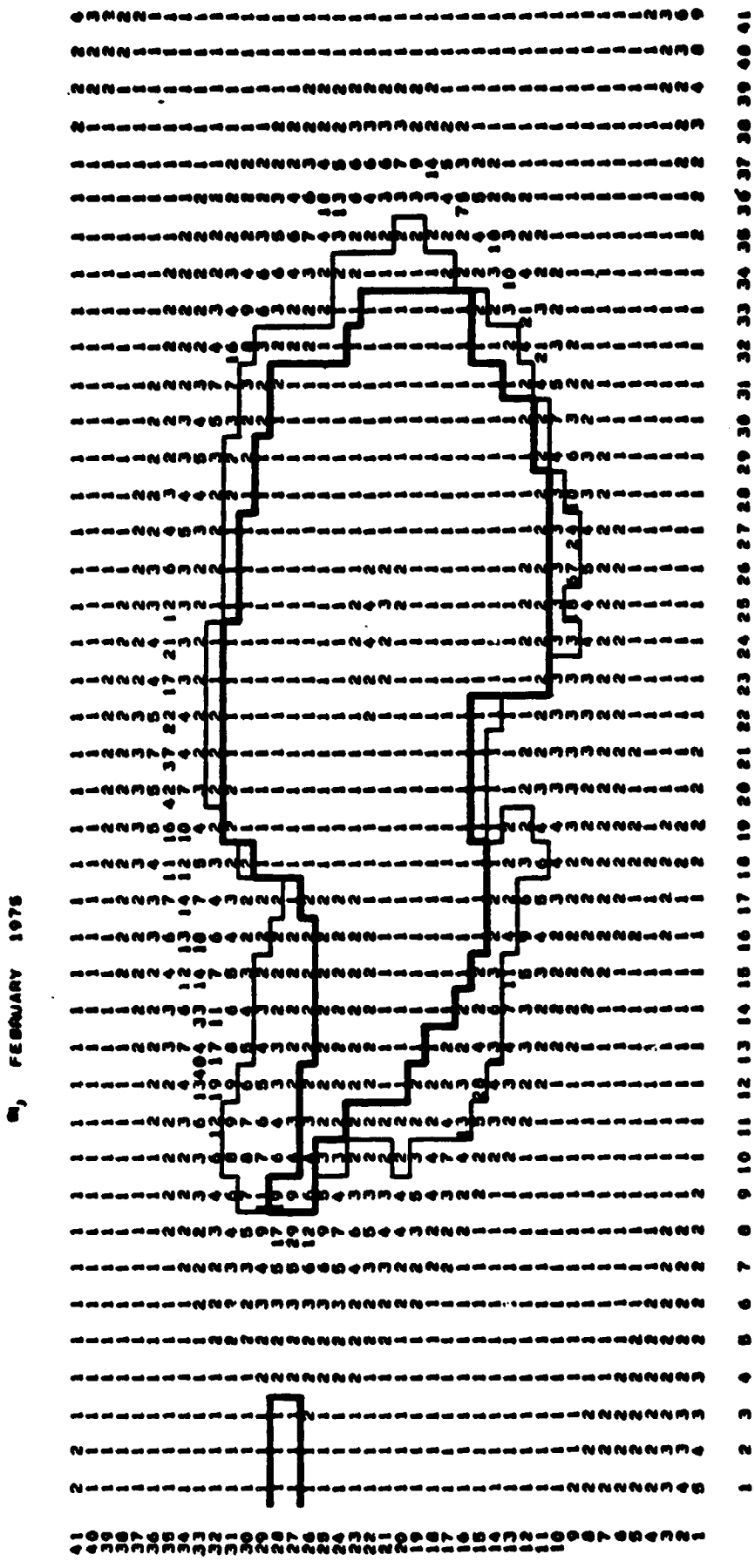

Figure 39. Ratio α over the south polar grid for February 1975.

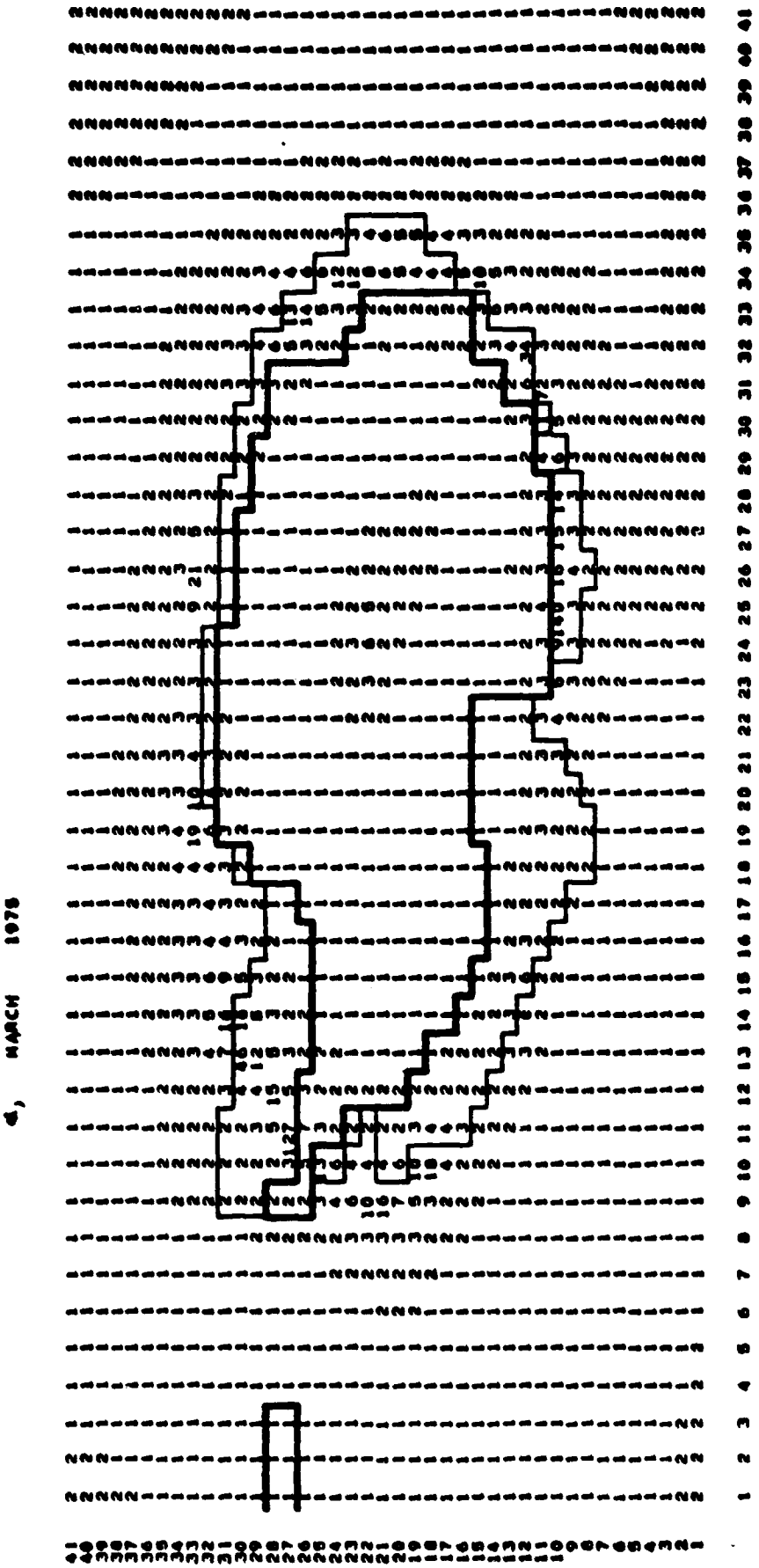

Figure 40. Ratio α over the south polar grid for March 1975.

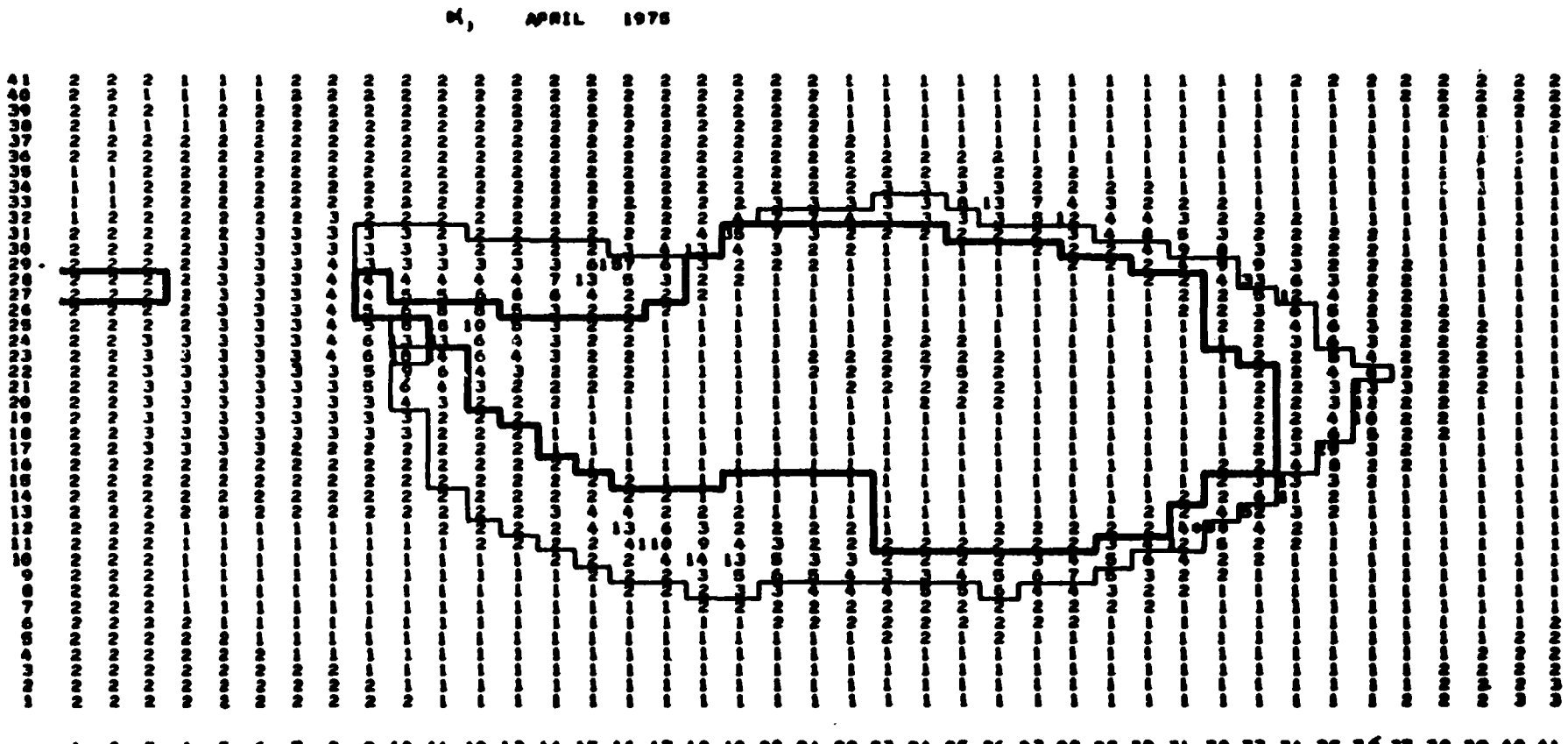

Figure 41. Ratio α over the south polar grid for April 1975.

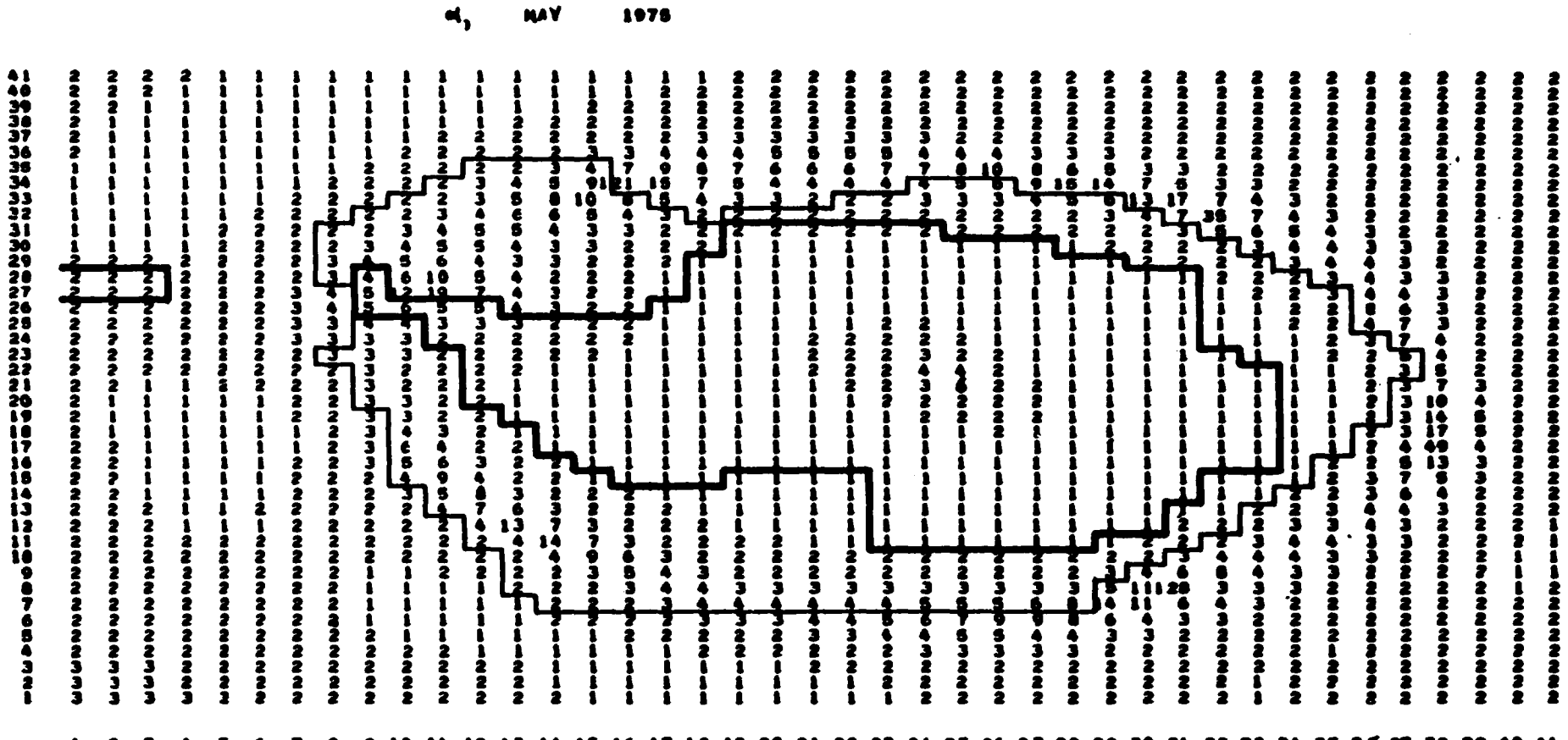

Figure 42. Ratio α over the south polar grid for May 1975.

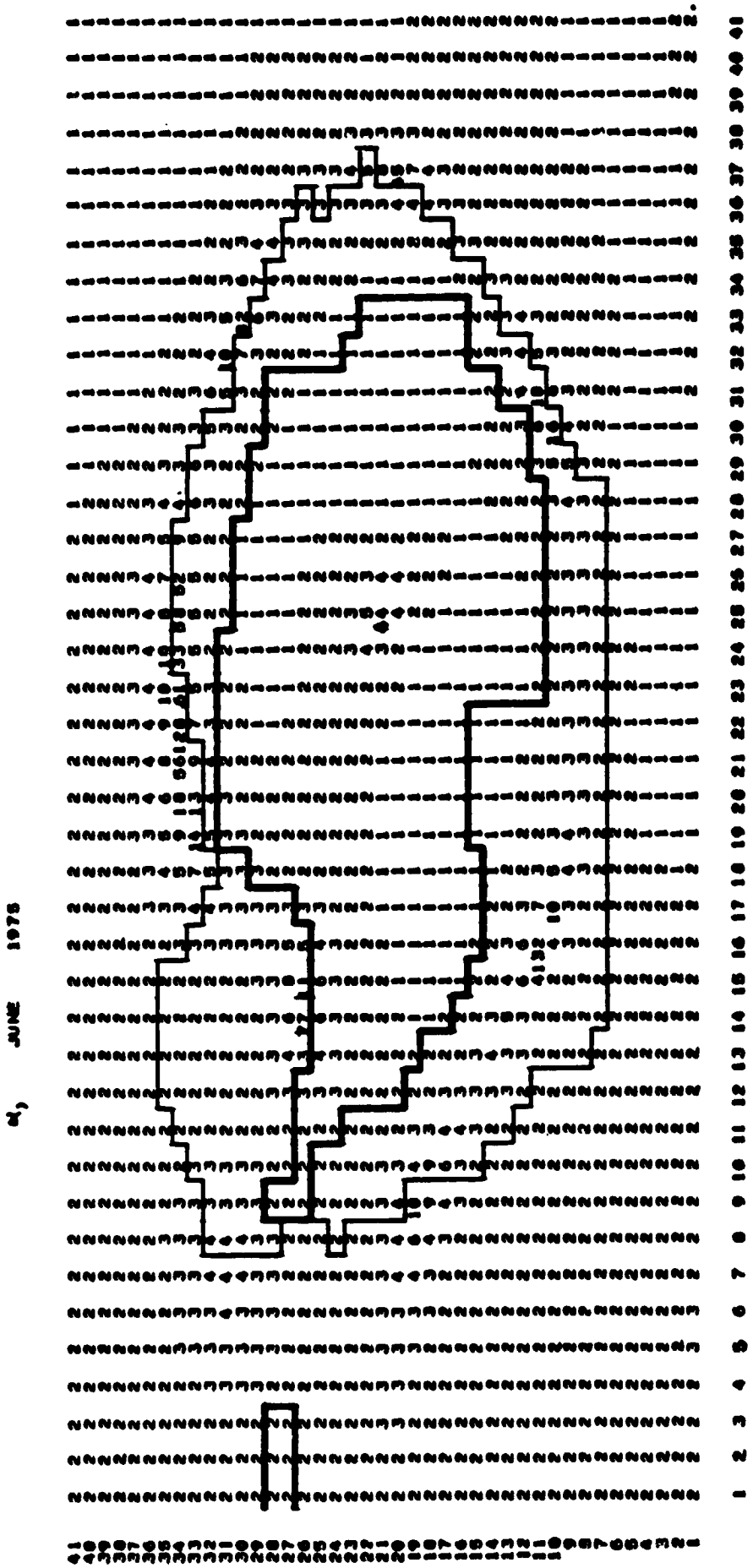

Figure 43. Ratio α over the south polar grid for June 1975.

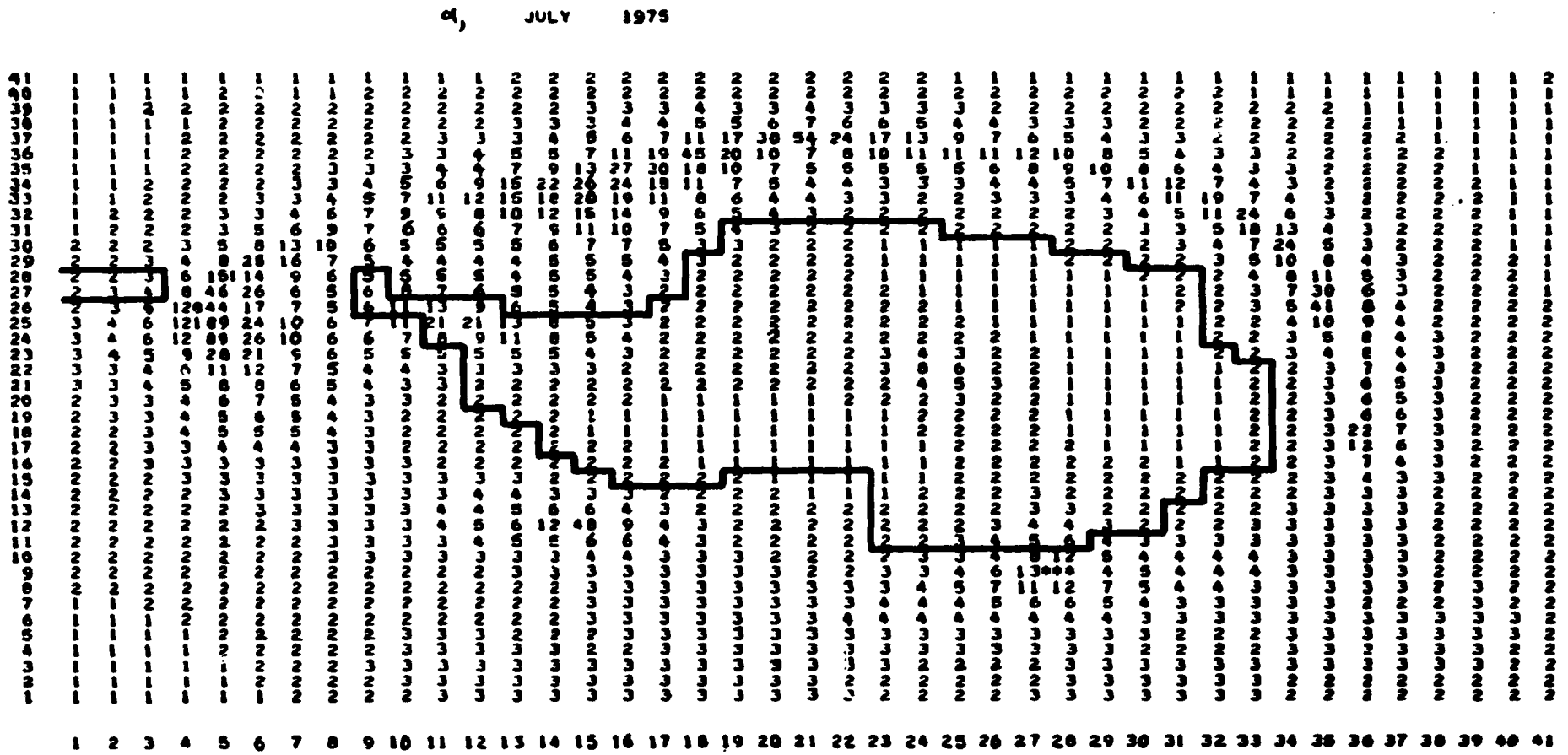

Figure 44. Ratio α over the south polar grid for July 1975.

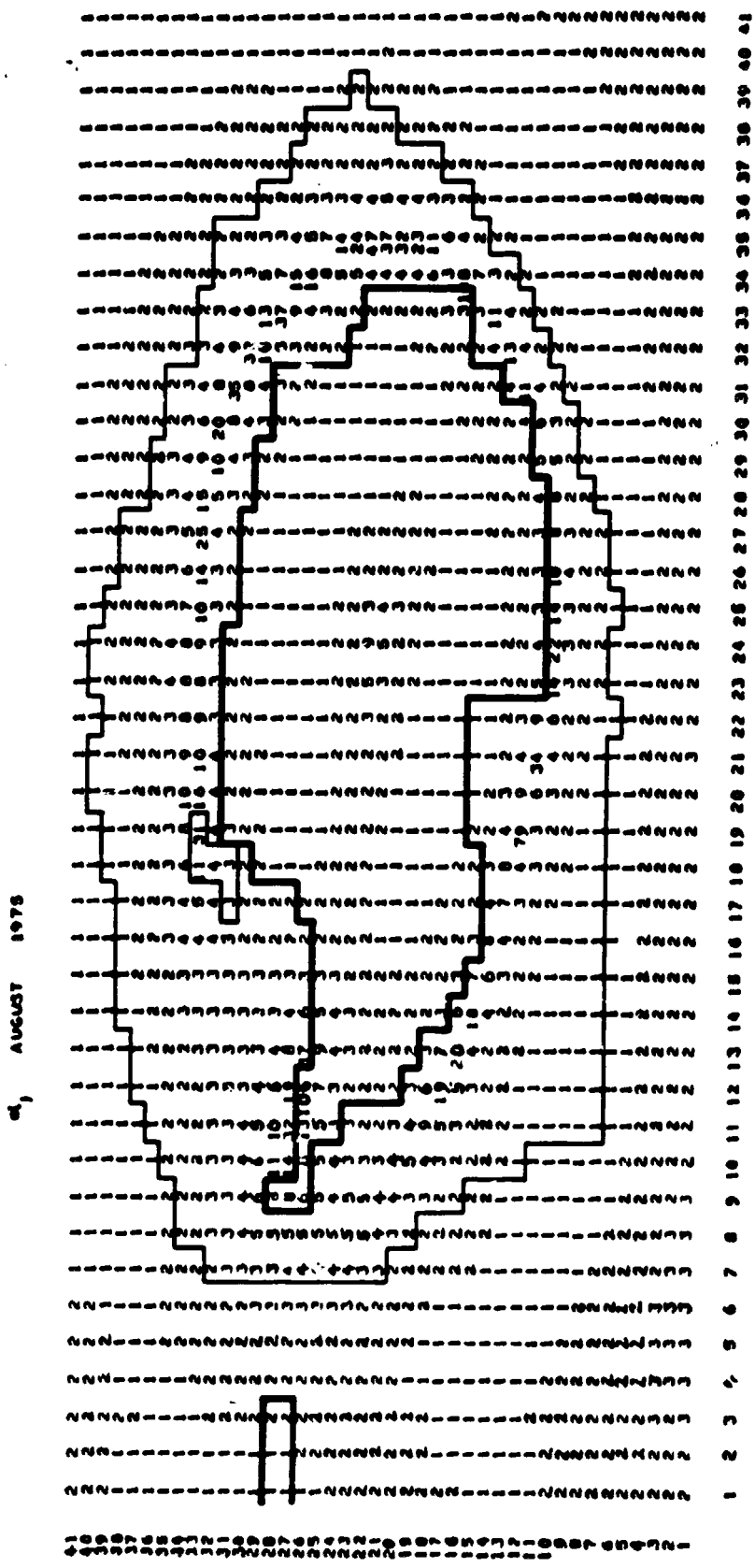

Figure 45. Ratio α over the south polar grid for August 1975.

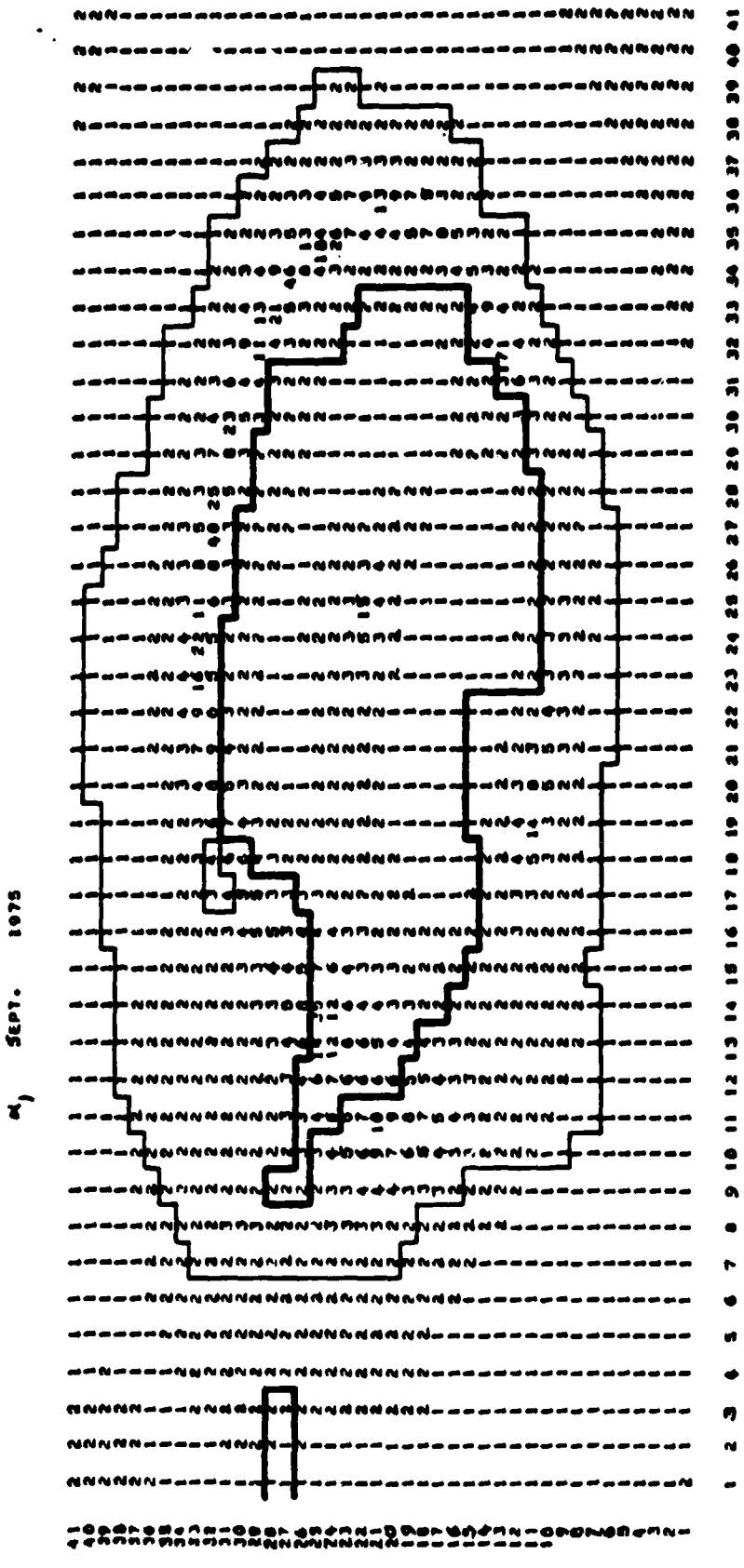

Figure 46. Ratio α over the south polar grid for September 1975.

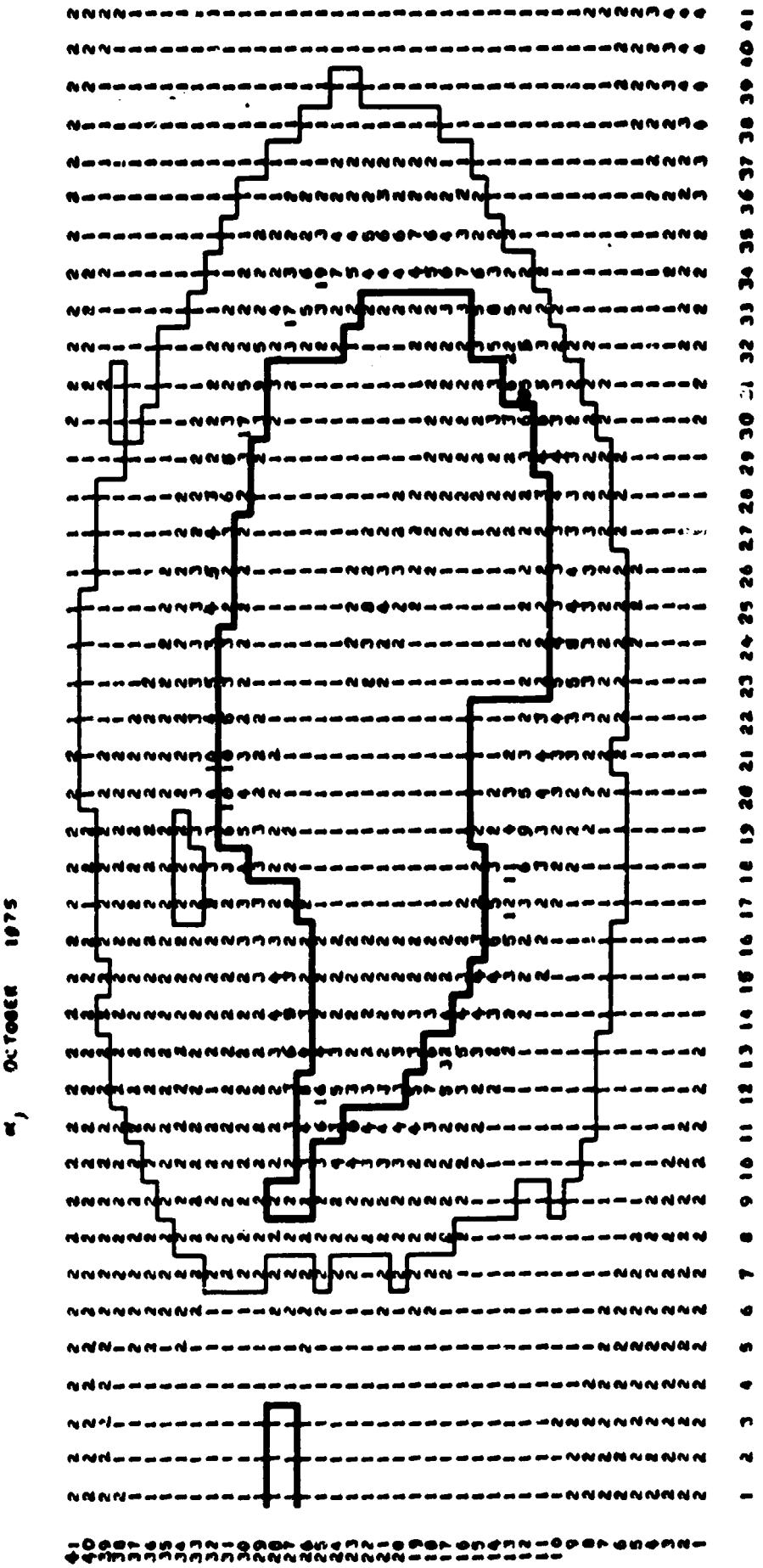

Figure 47. Ratio α over the south polar grid for October 1975.

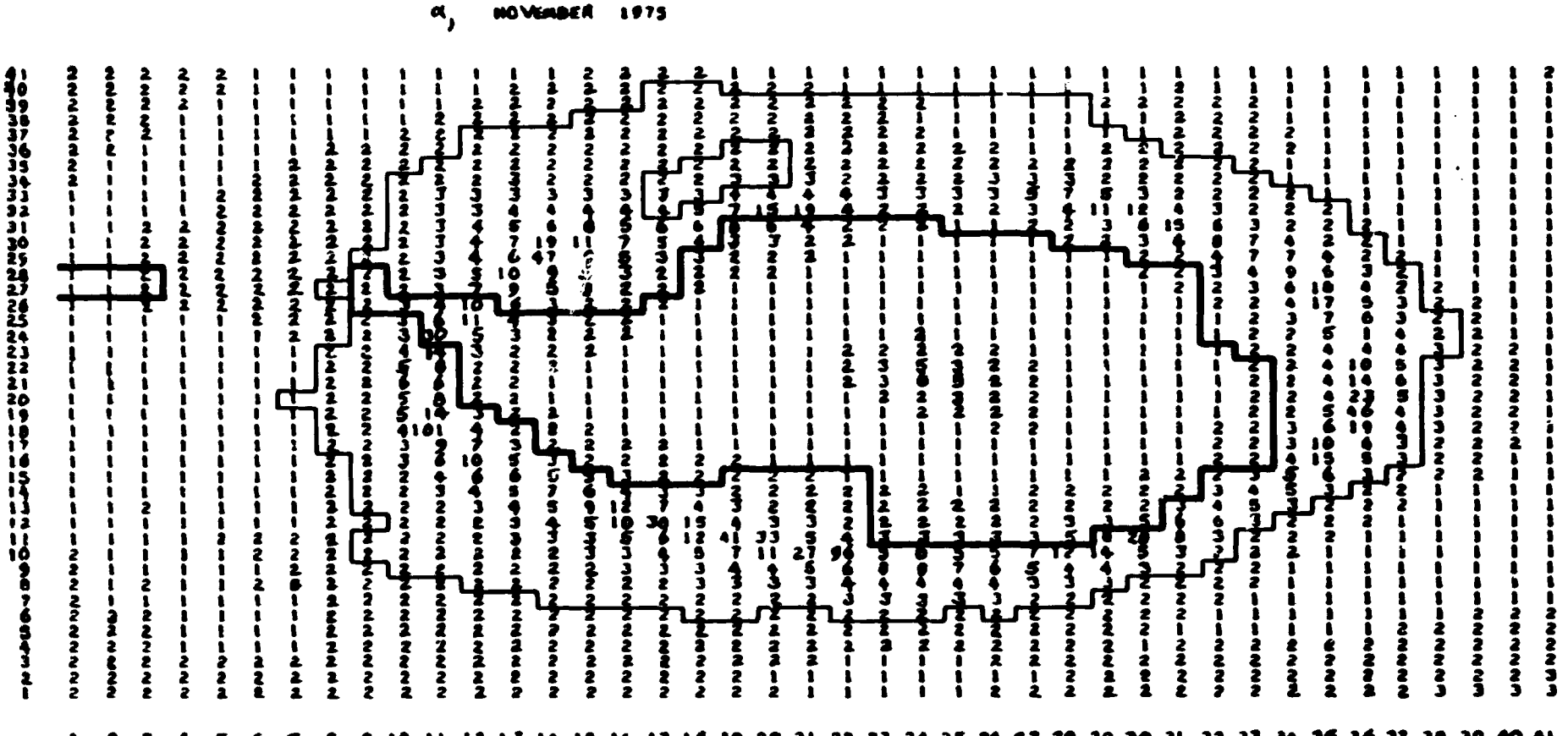

Figure 48. Ratio α over the south polar grid for November 1975.

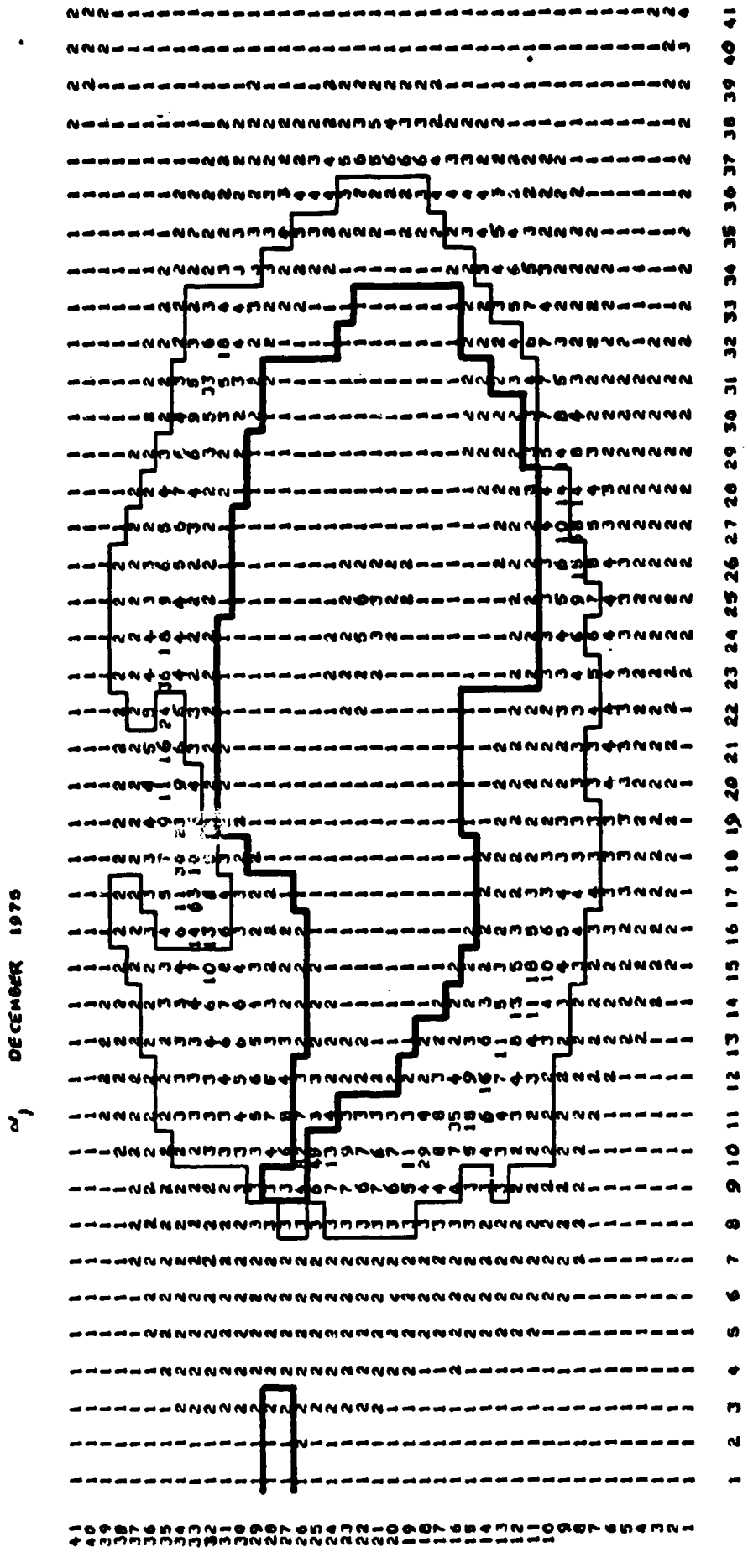

Figure 49. Ratio α over the south polar grid for December 1975.

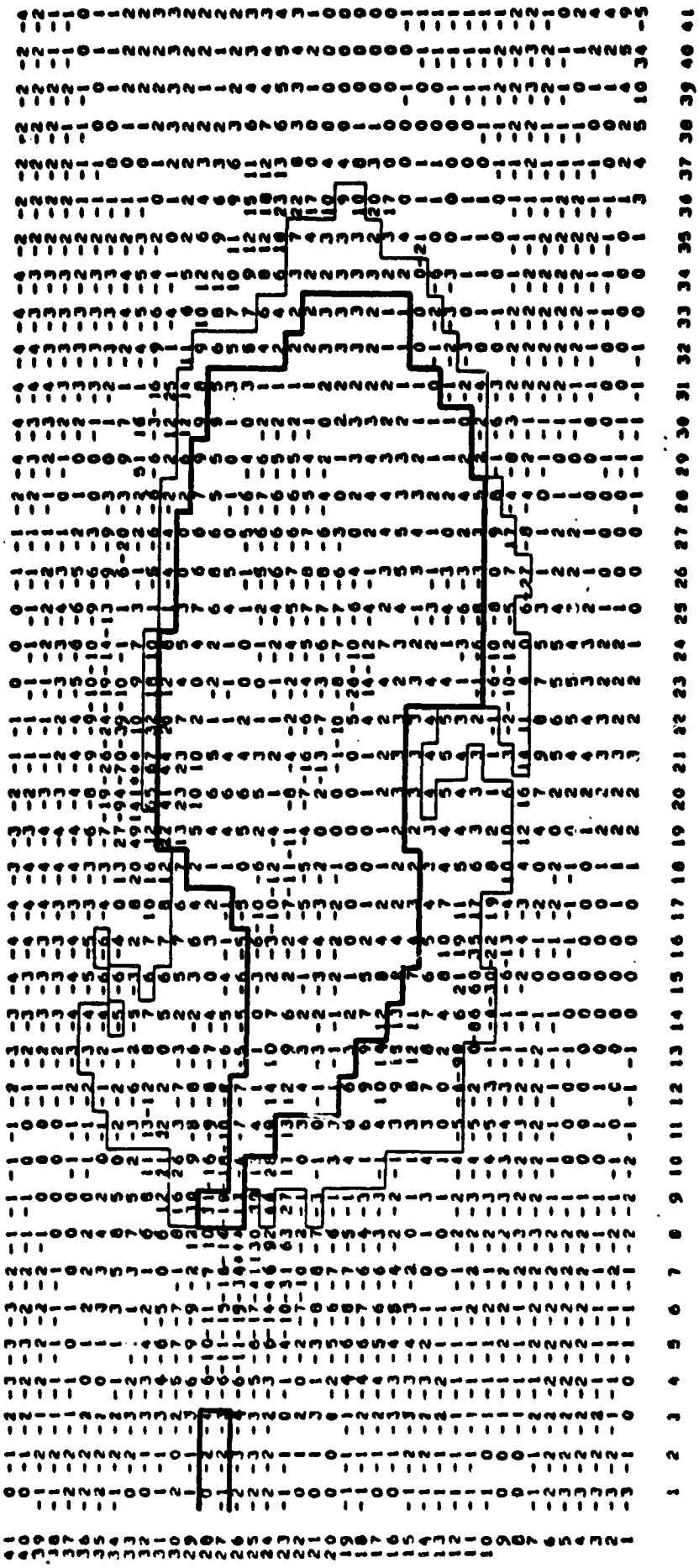

Figure 50. Turning angle A over the south polar grid for January 1974.

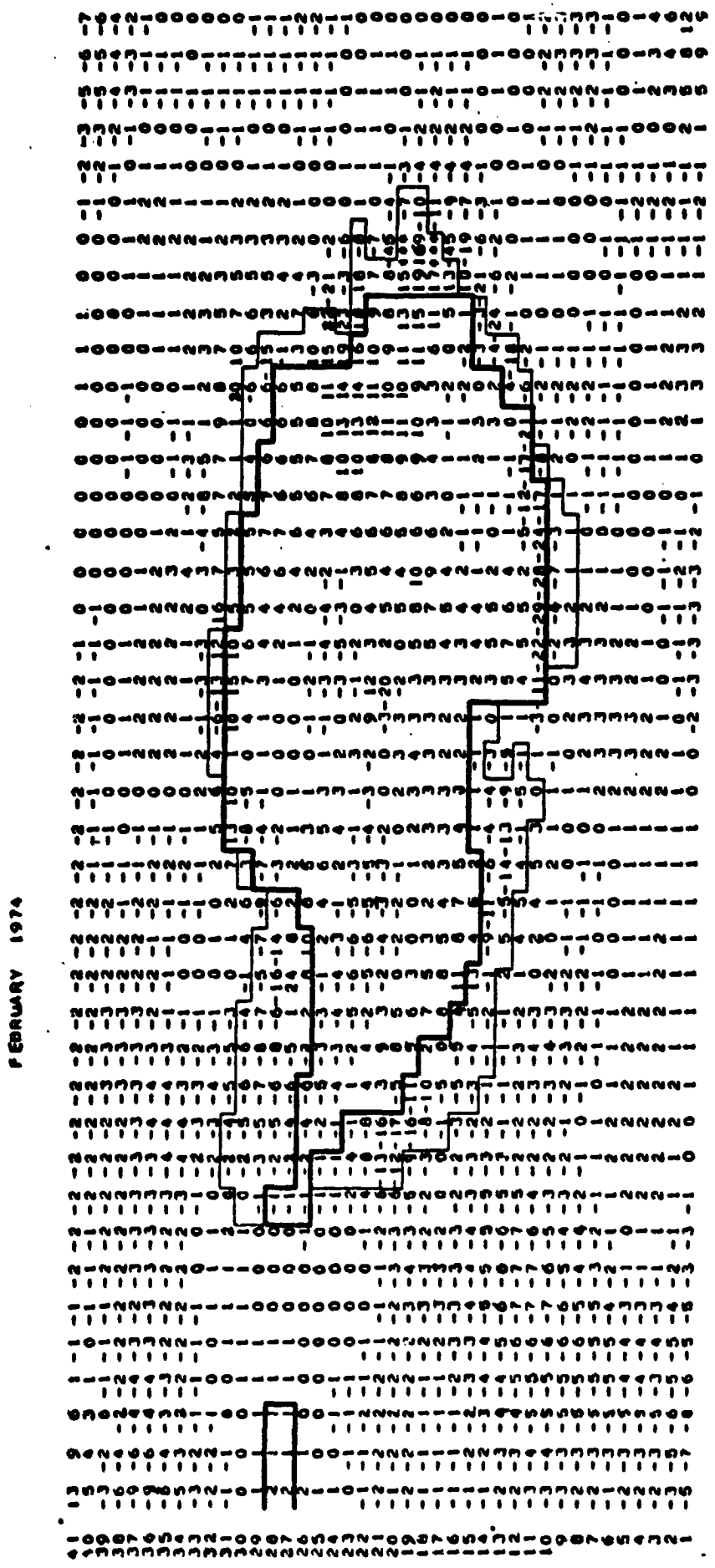

Figure 51. Turning angle A over the south polar grid for February 1974.

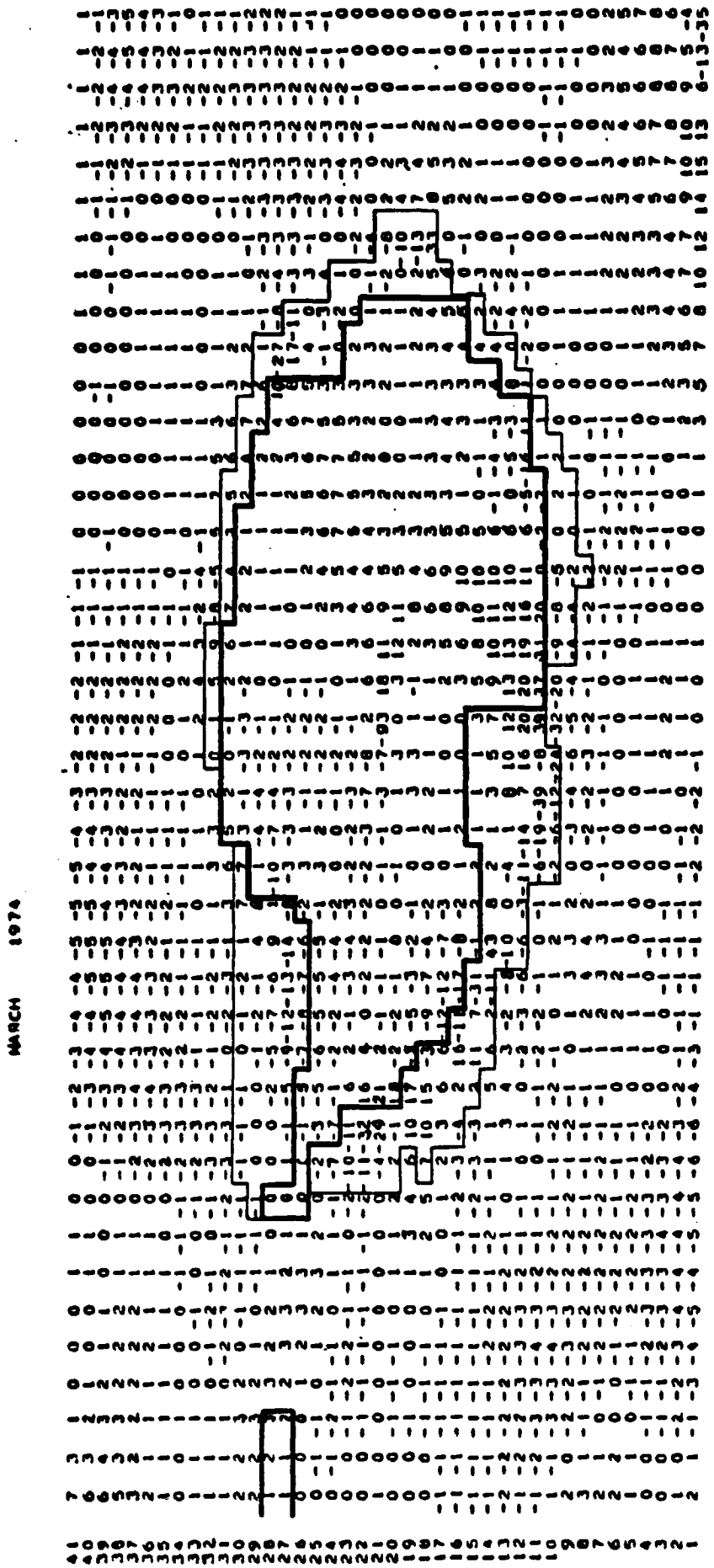

Figure 52. Turning angle A over the south polar grid for March 1974.

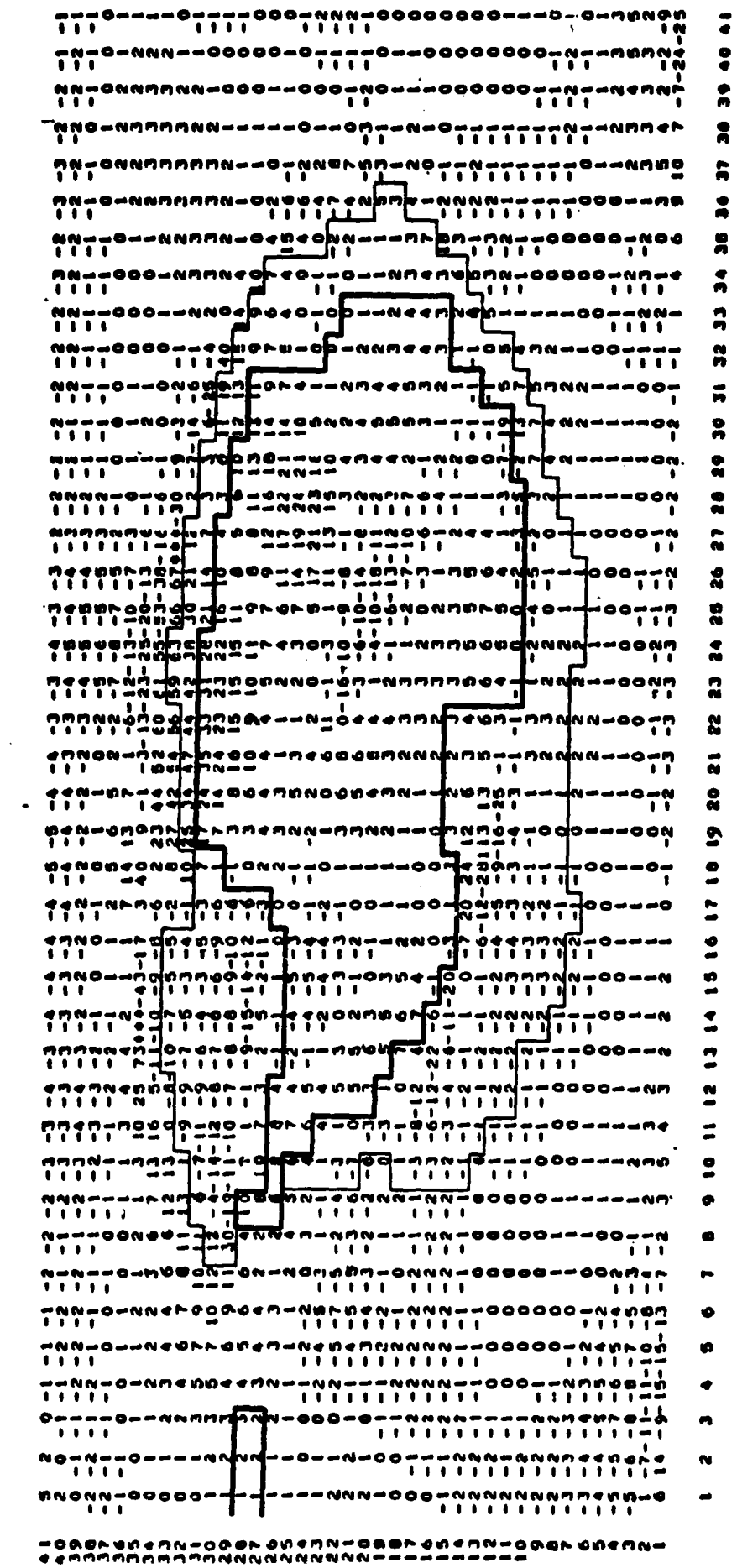

Figure 53. Turning angle A over the south polar grid for April 1974.

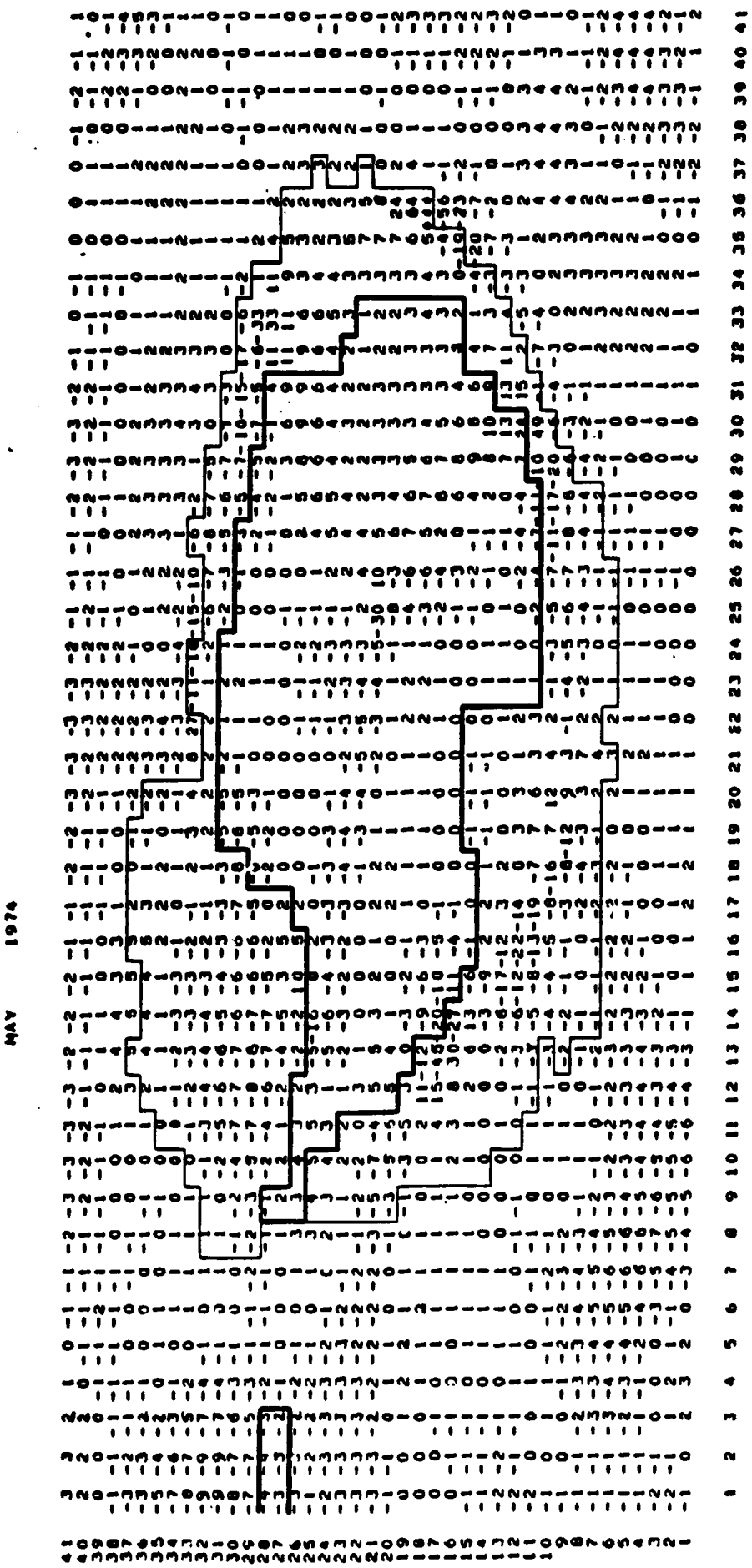

Figure 54. Turning angle A over the south polar grid for May 1974.

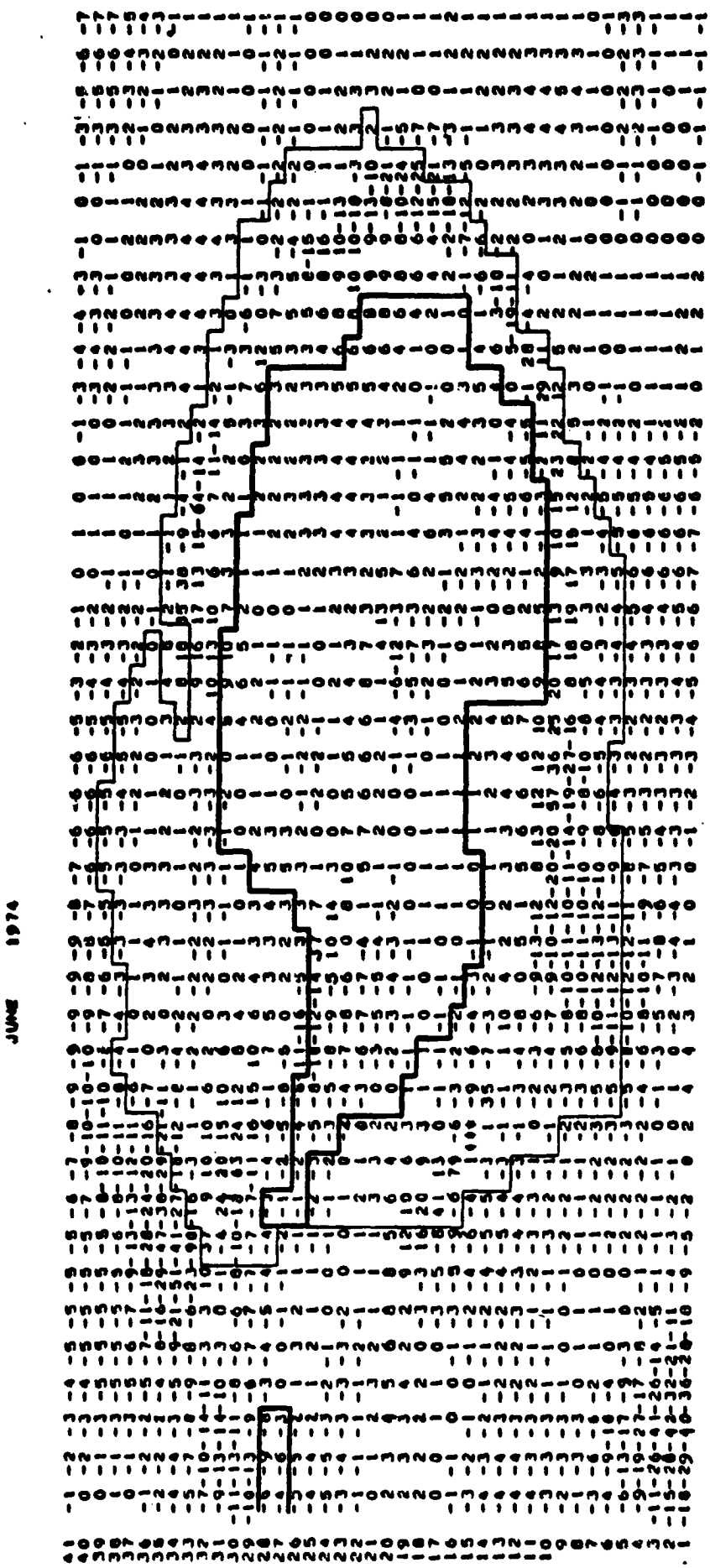

Figure 55. Turning angle A over the south polar grid for June 1974.

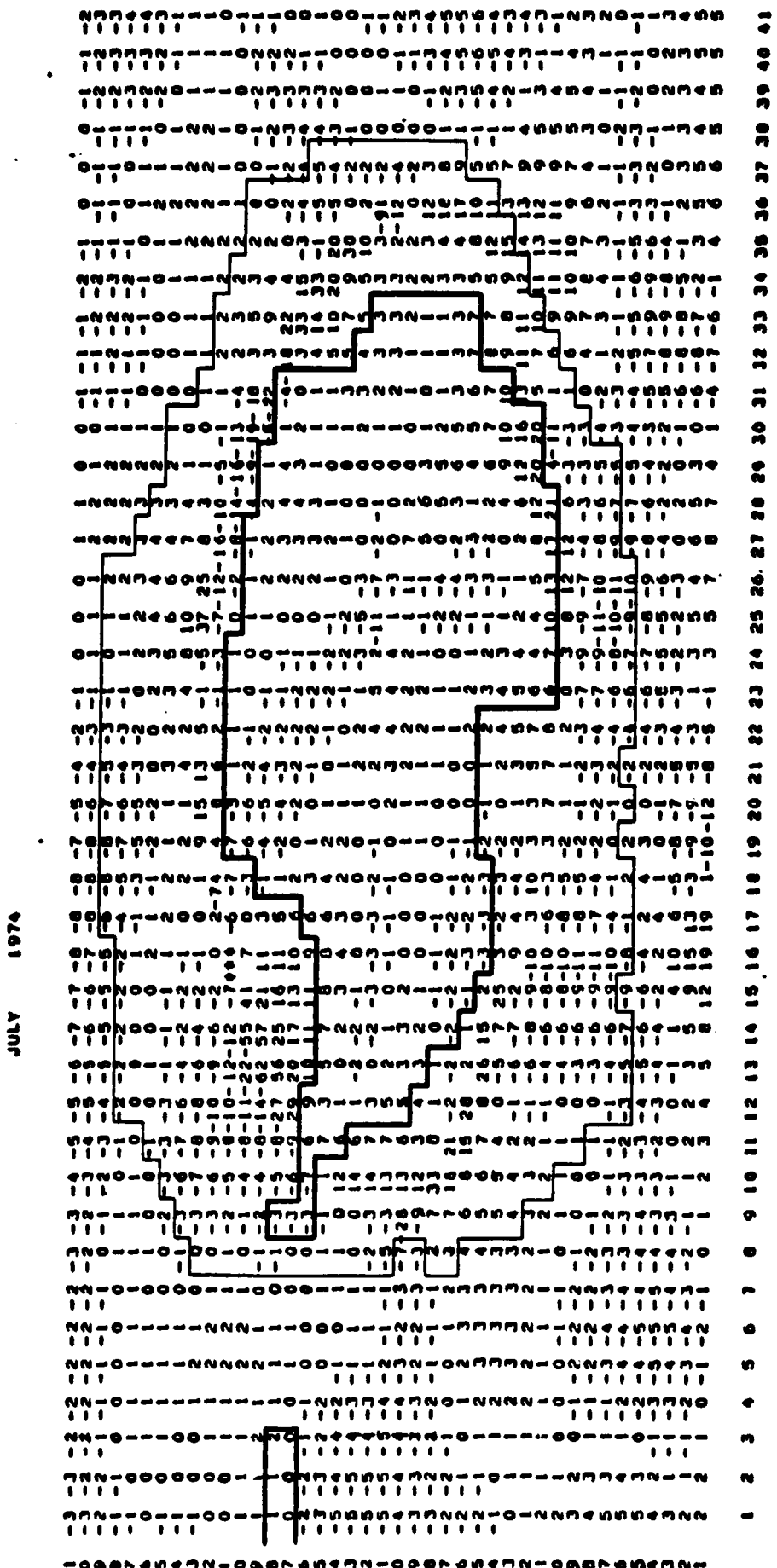

Figure 56. Turning angle A over the south polar grid for July 1974.

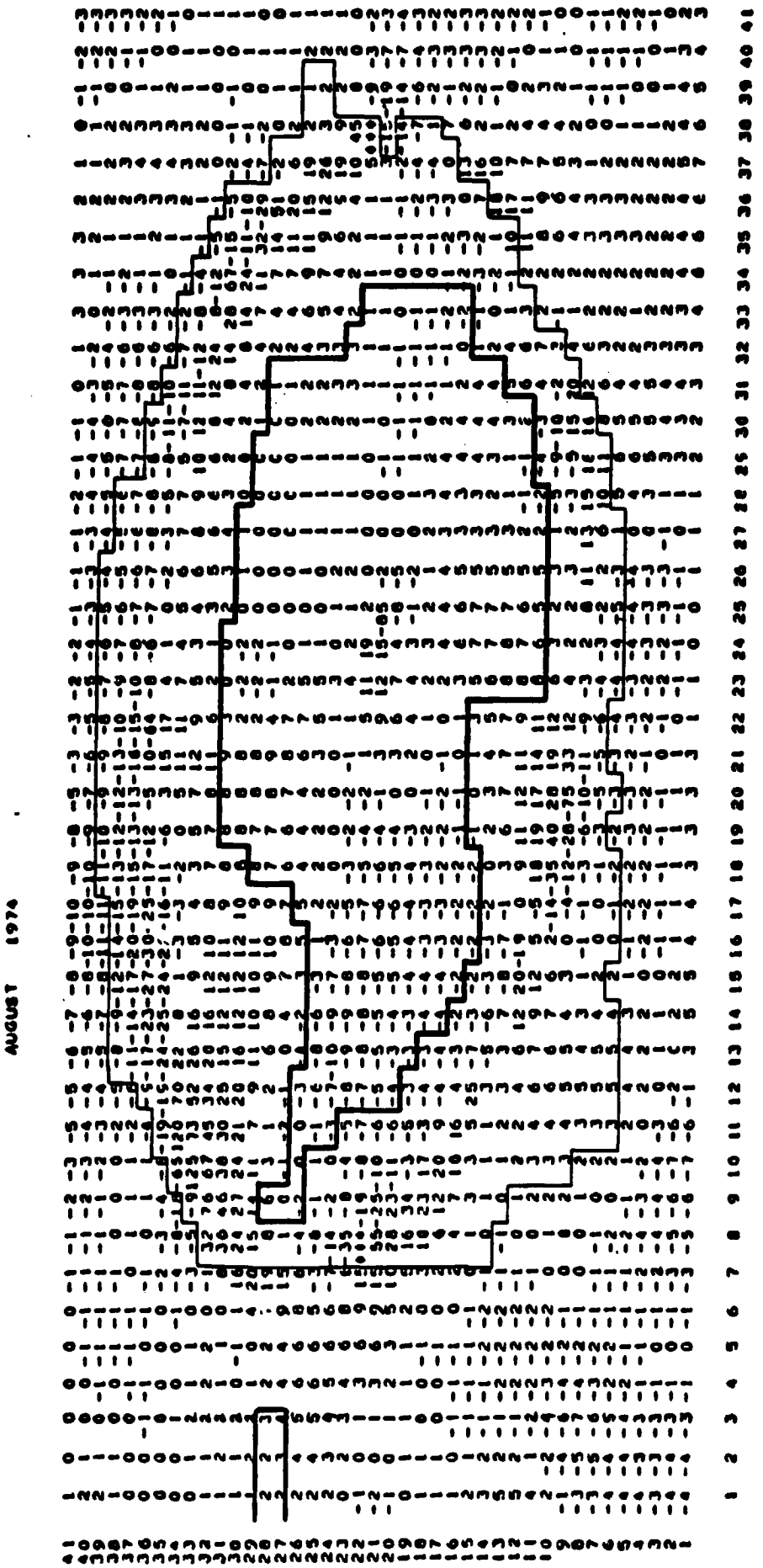

Figure 57. Turning angle A over the south polar grid for August 1974.

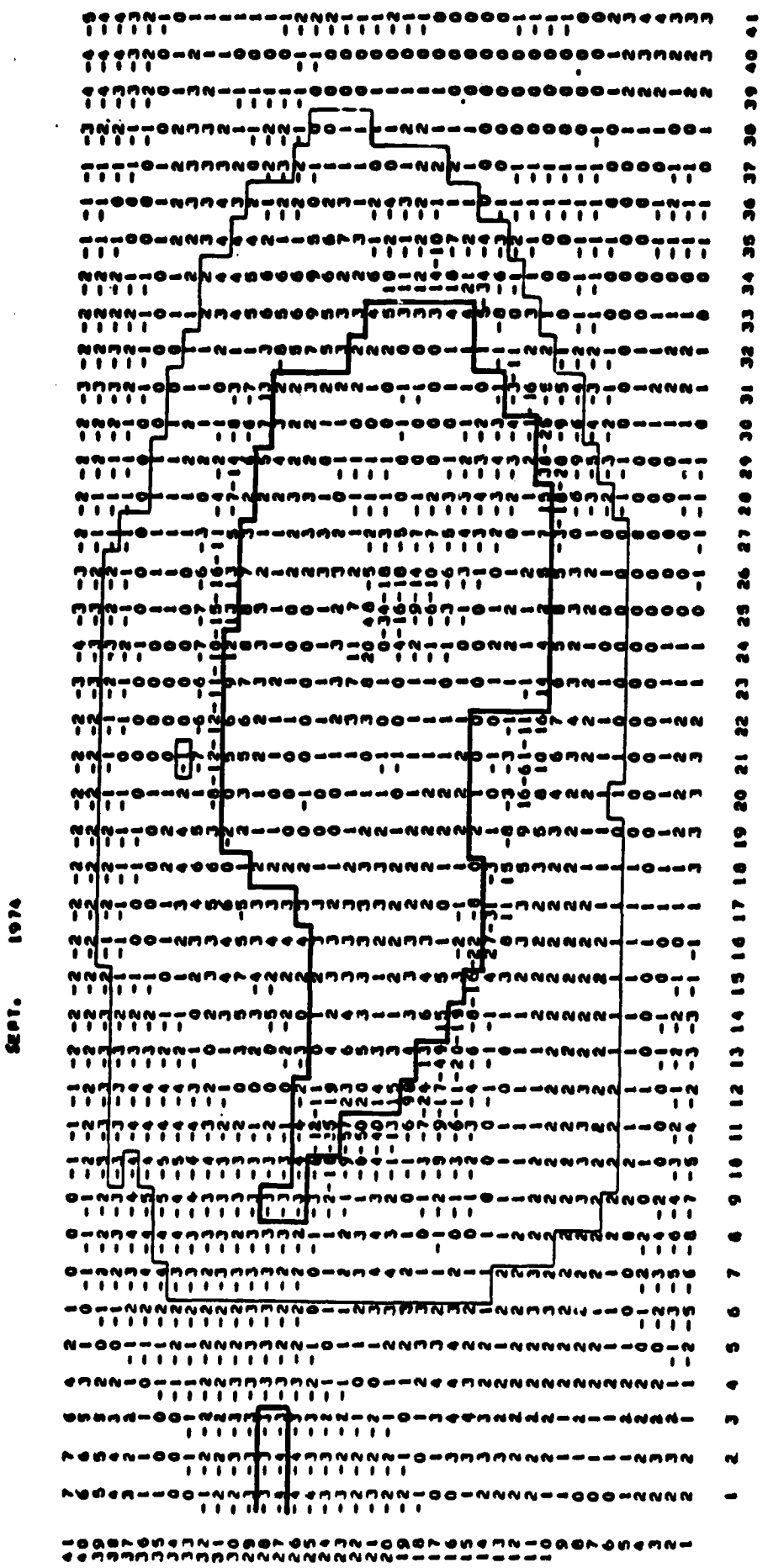

Figure 58. Turning angle A over the south polar grid for September 1974.

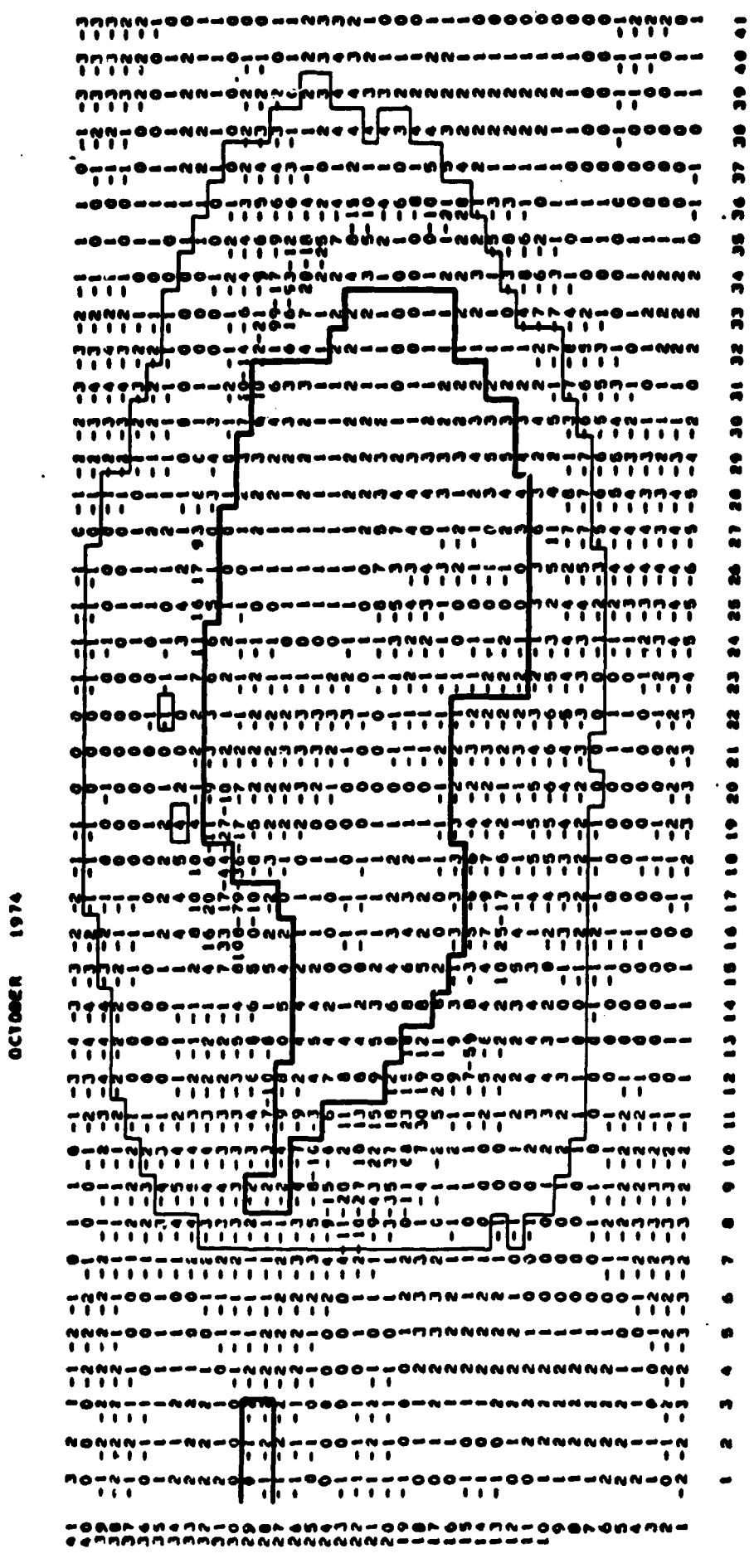

Figure 59. Turning angle A over the south polar grid for October 1974.

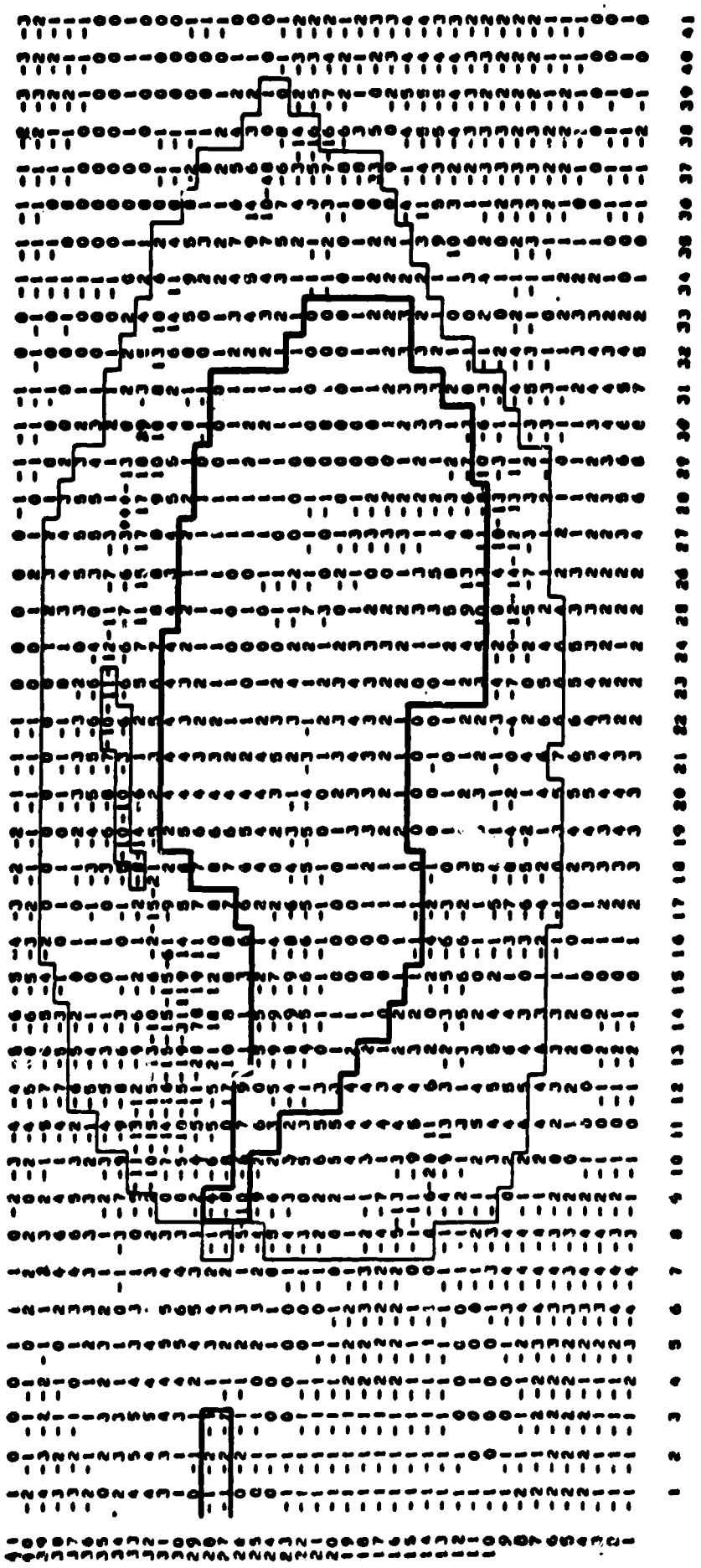

Figure 60. Turning angle A over the south polar grid for November 1974.

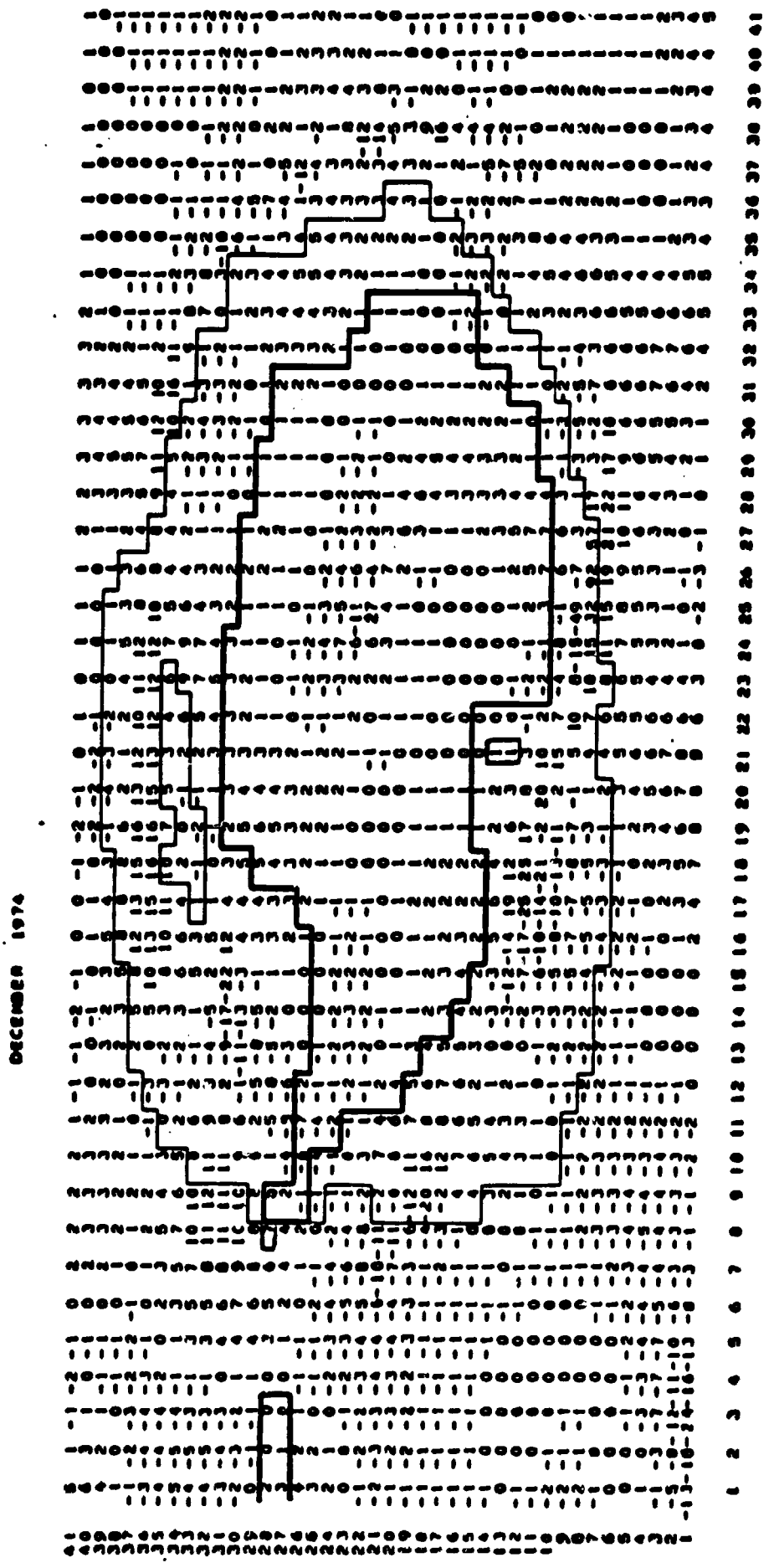

Figure 61. Turning angle A over the south polar grid for December 1974.

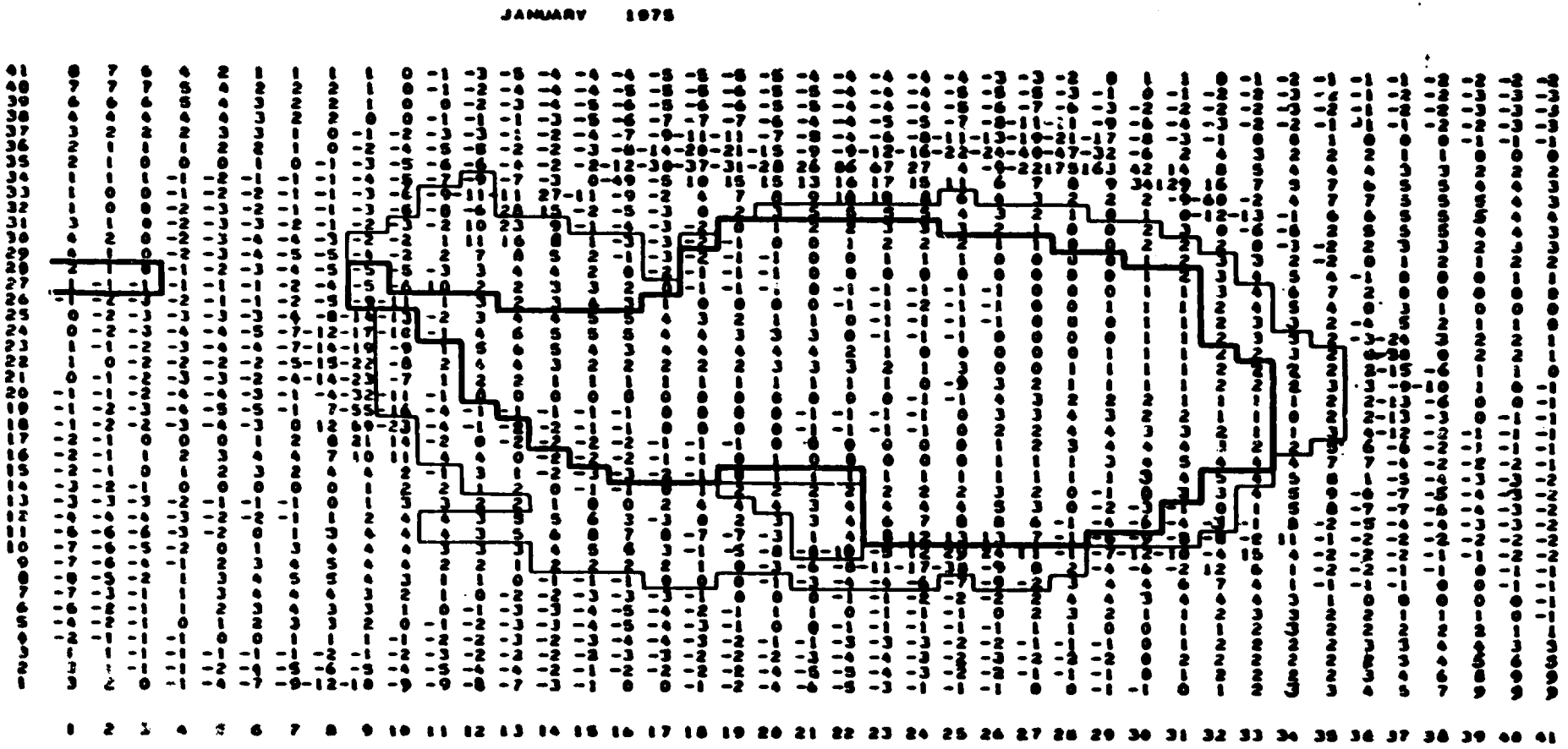

Figure 62. Turning angle A over the south polar grid for January 1975.

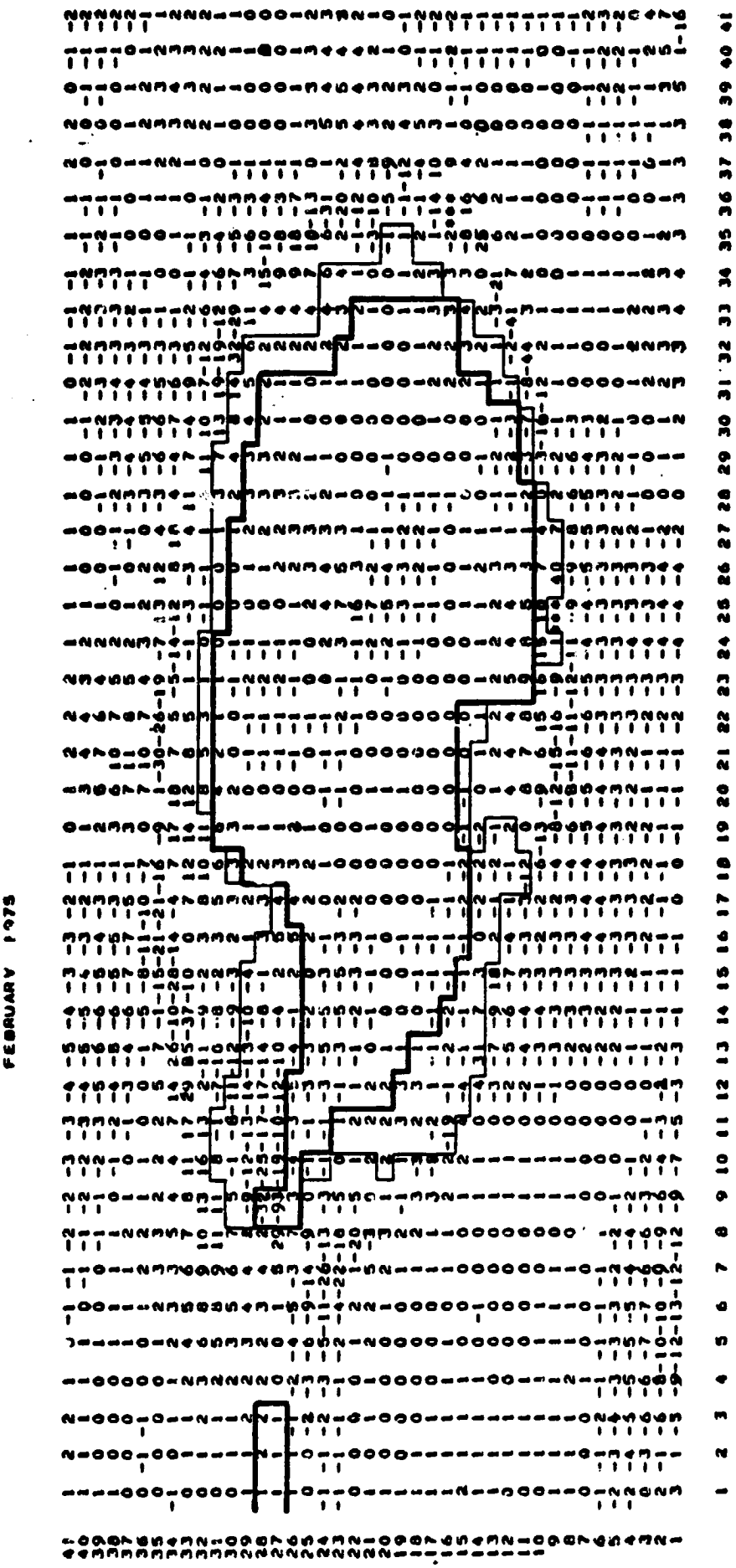

Figure 63. Turning angle A over the south polar grid for February 1975.

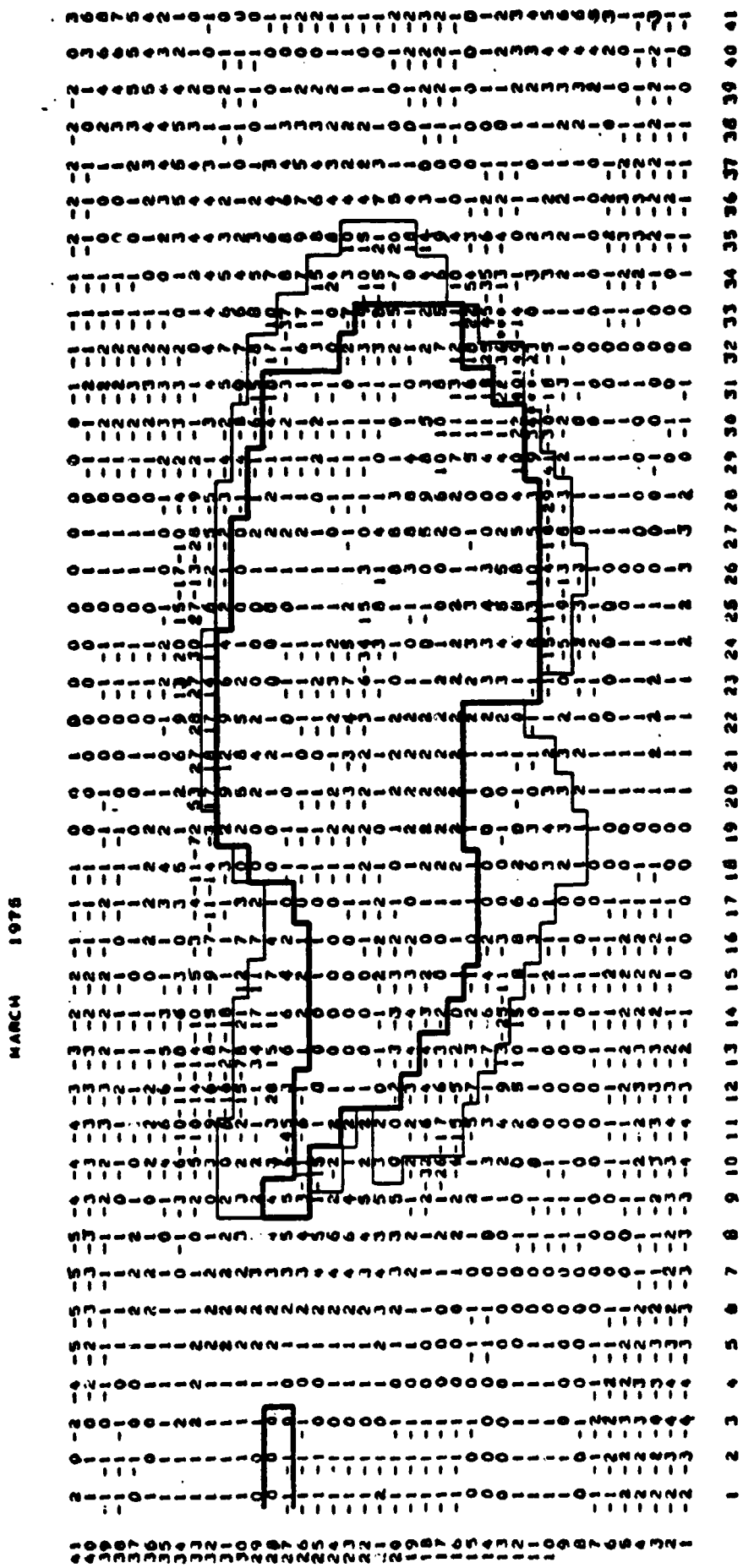

Figure 64. Turning angle A over the south polar grid for March 1975.

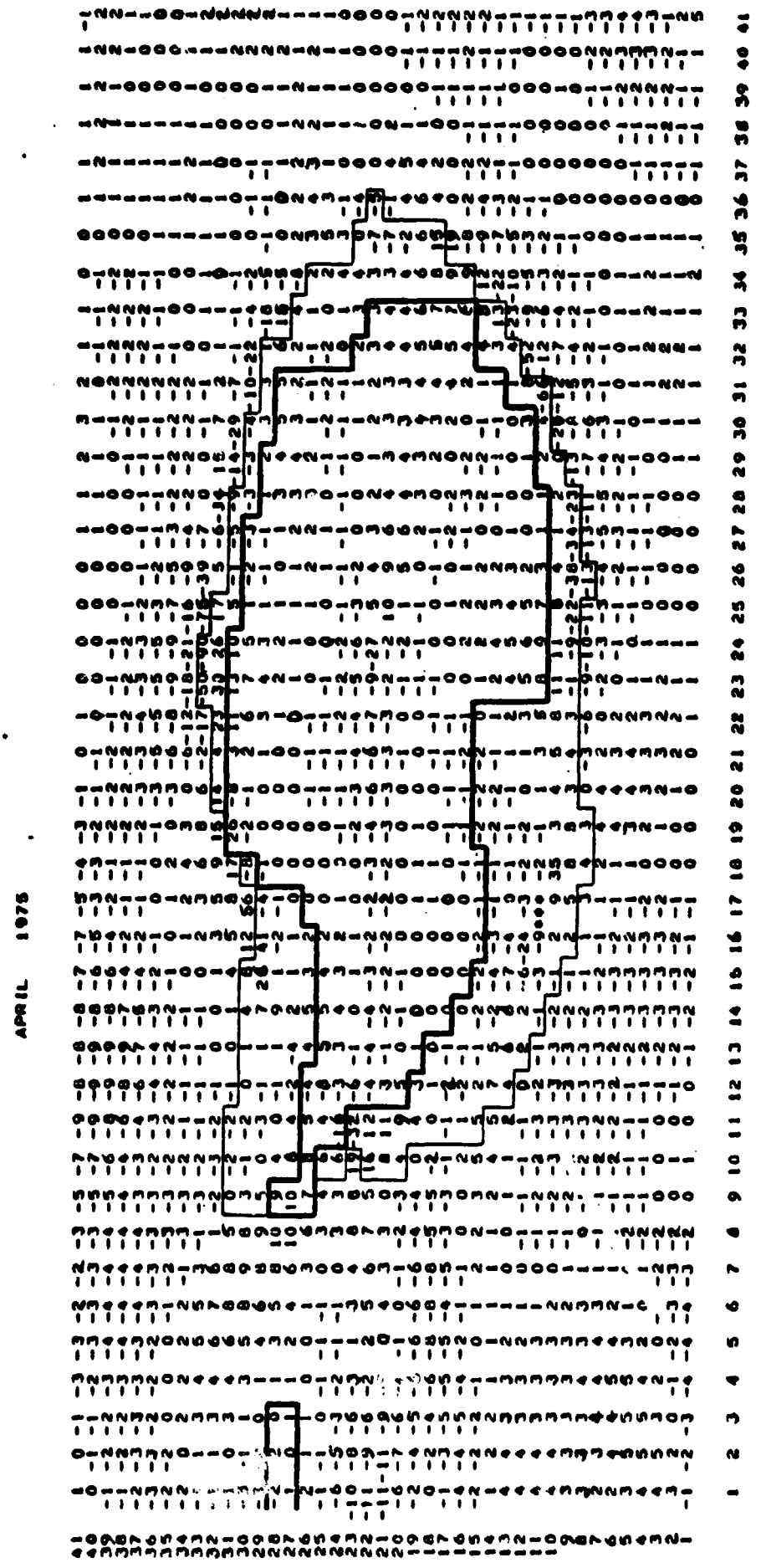

Figure 65. Turning angle A over the south polar grid for April 1975.

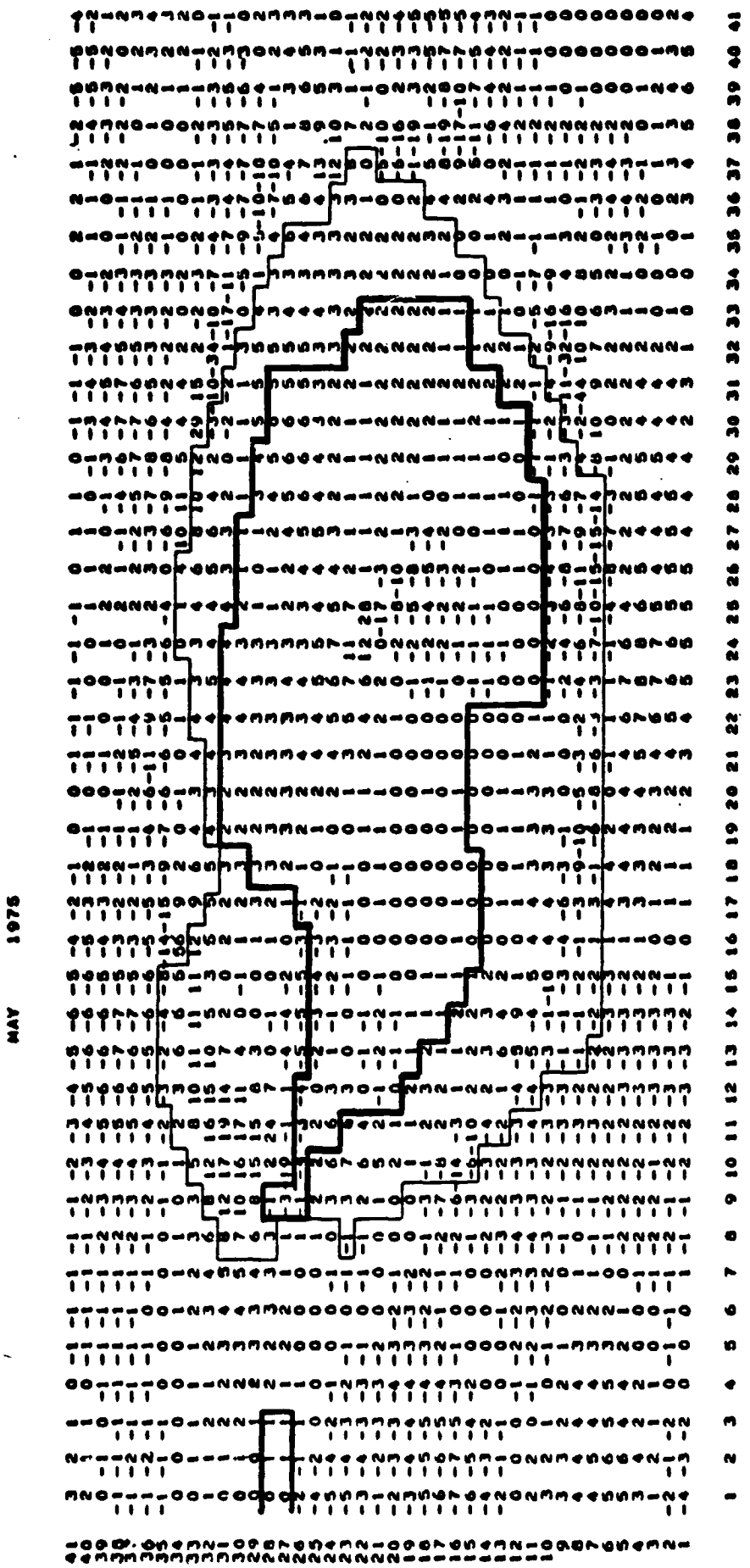

Figure 66. Turning angle A over the south polar grid for May 1975.

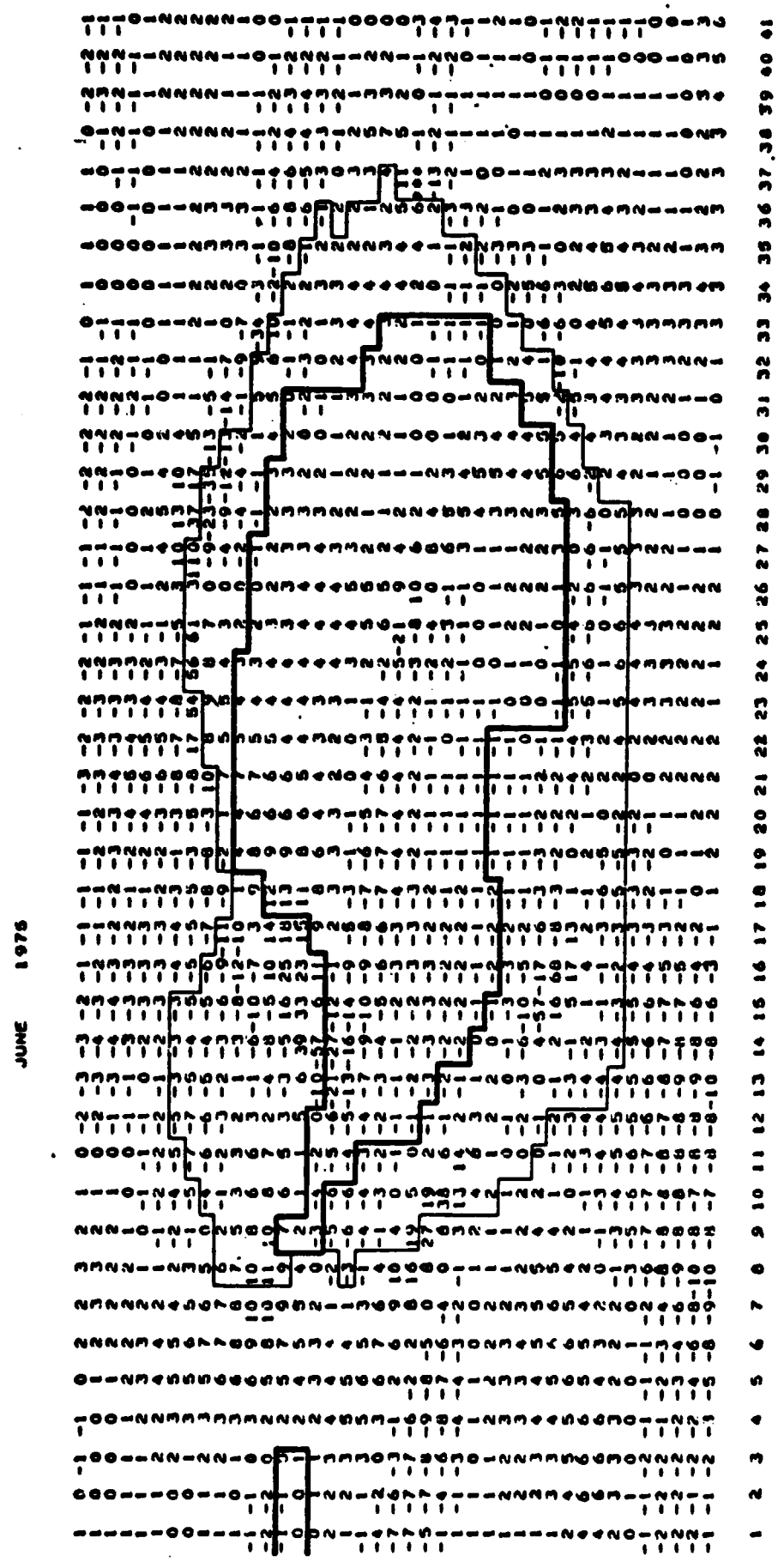

Figure 67. Turning angle A over the south polar grid for June 1975.

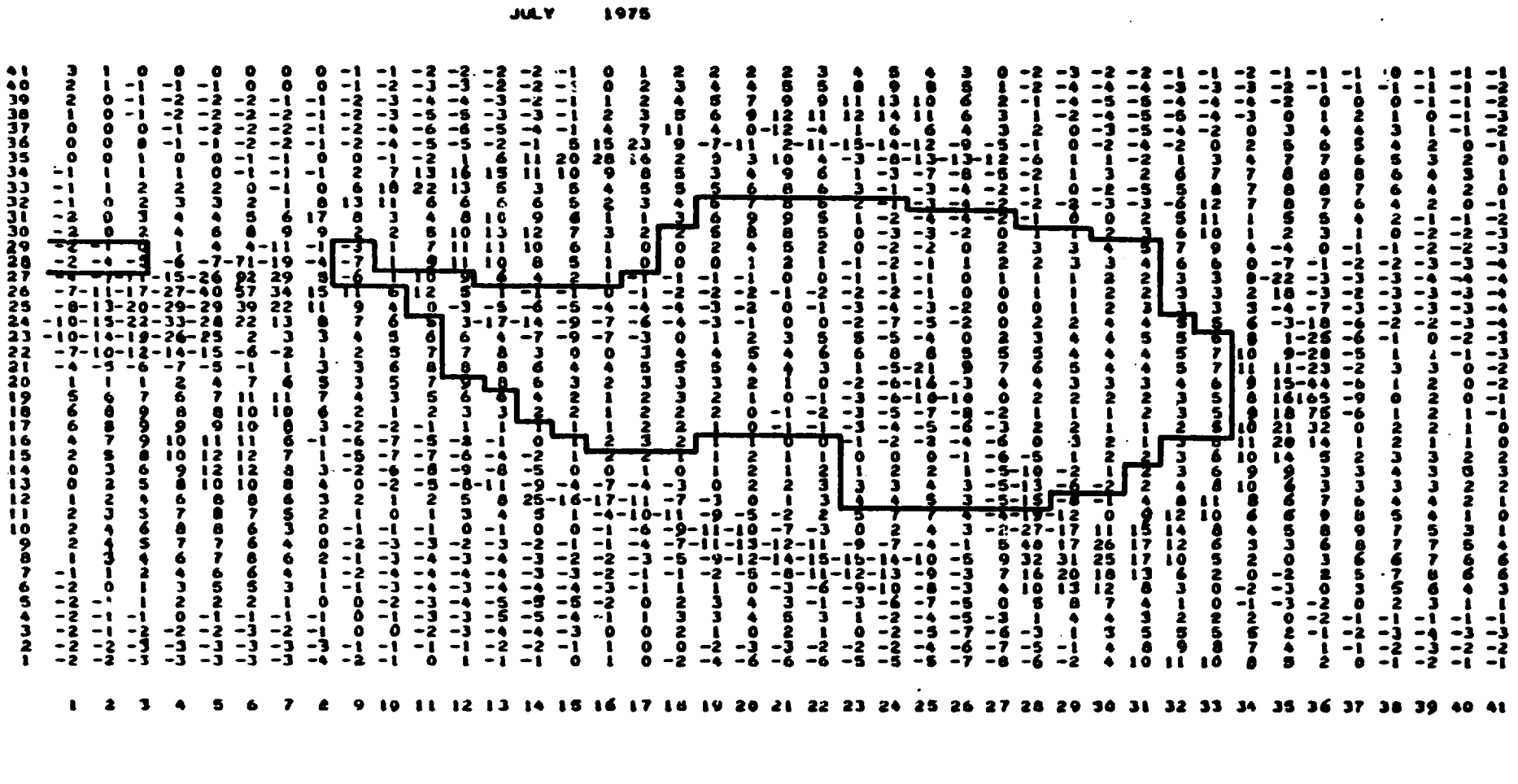

Figure 68. Turning angle A over the south polar grid for July 1975.

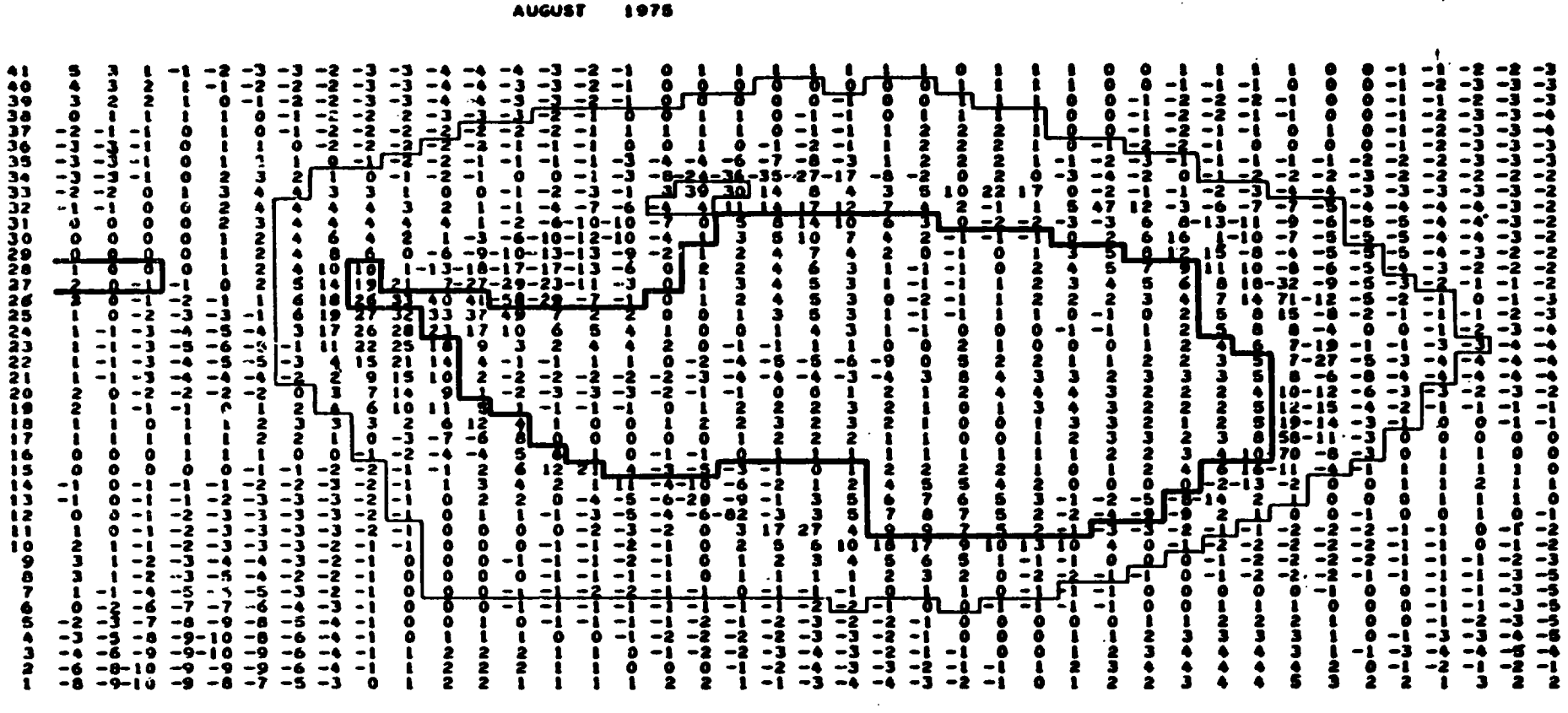

Figure 69. Turning angle A over the south polar grid for August 1975.

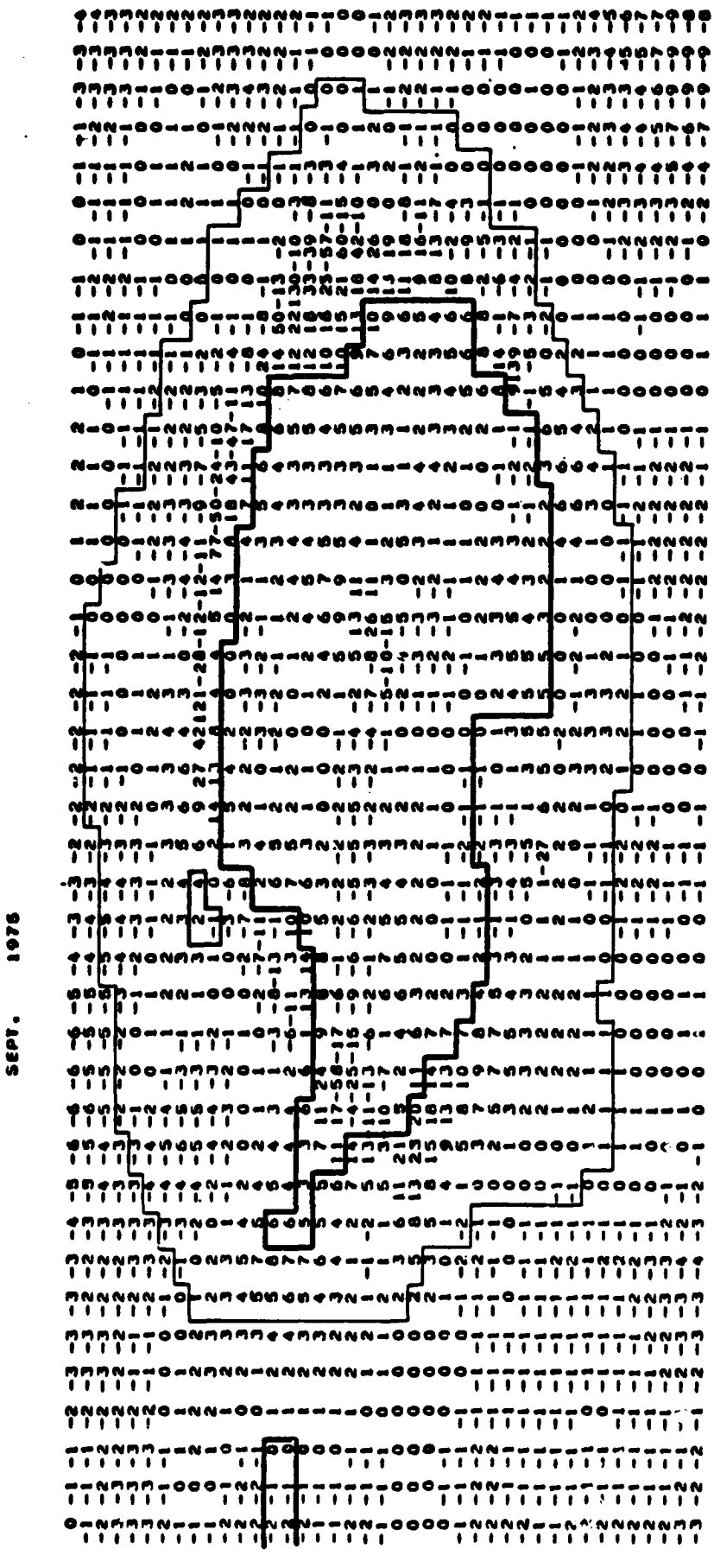

Figure 70. Turning angle A over the south polar grid for September 1975.

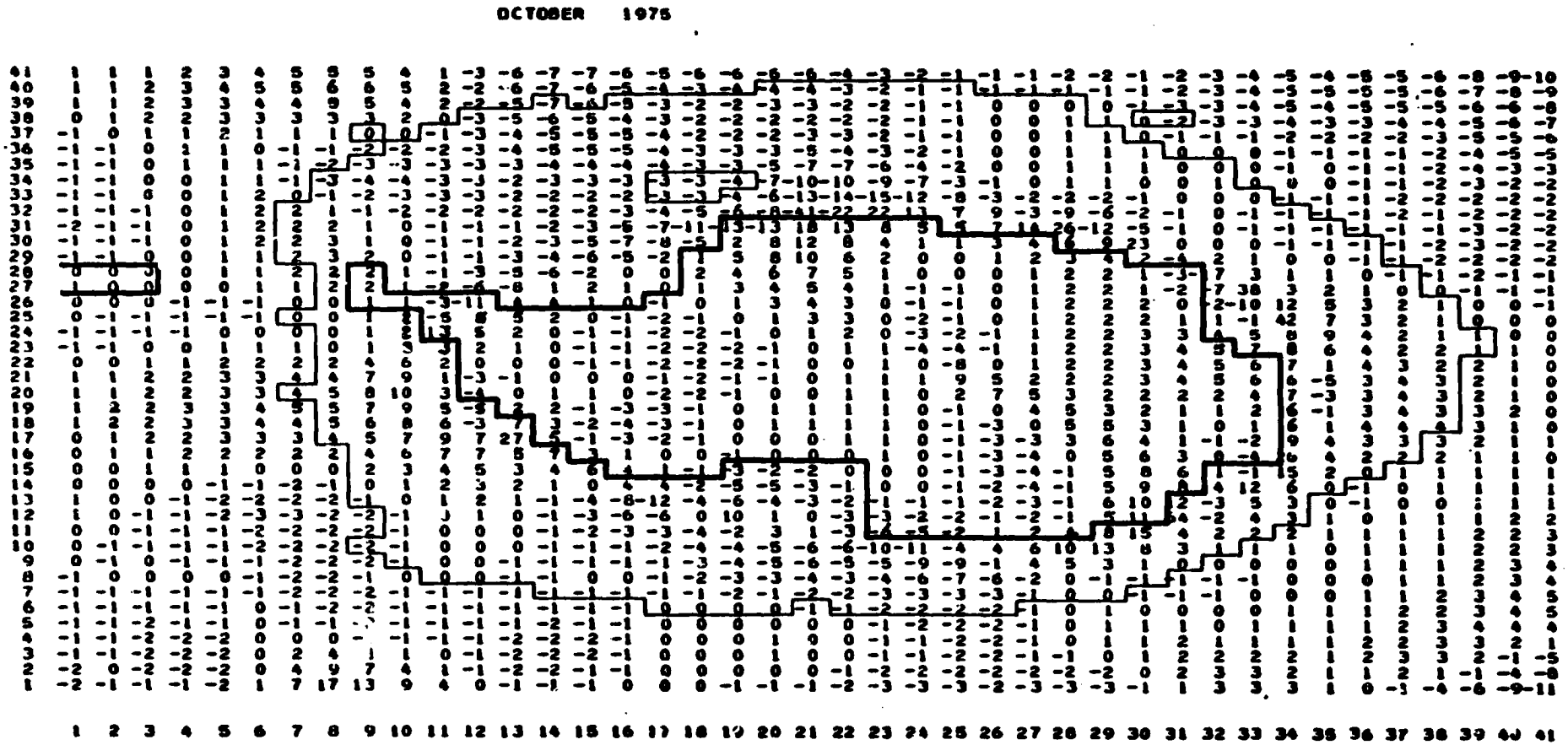

Figure 71. Turning angle A over the south polar grid for October 1975.

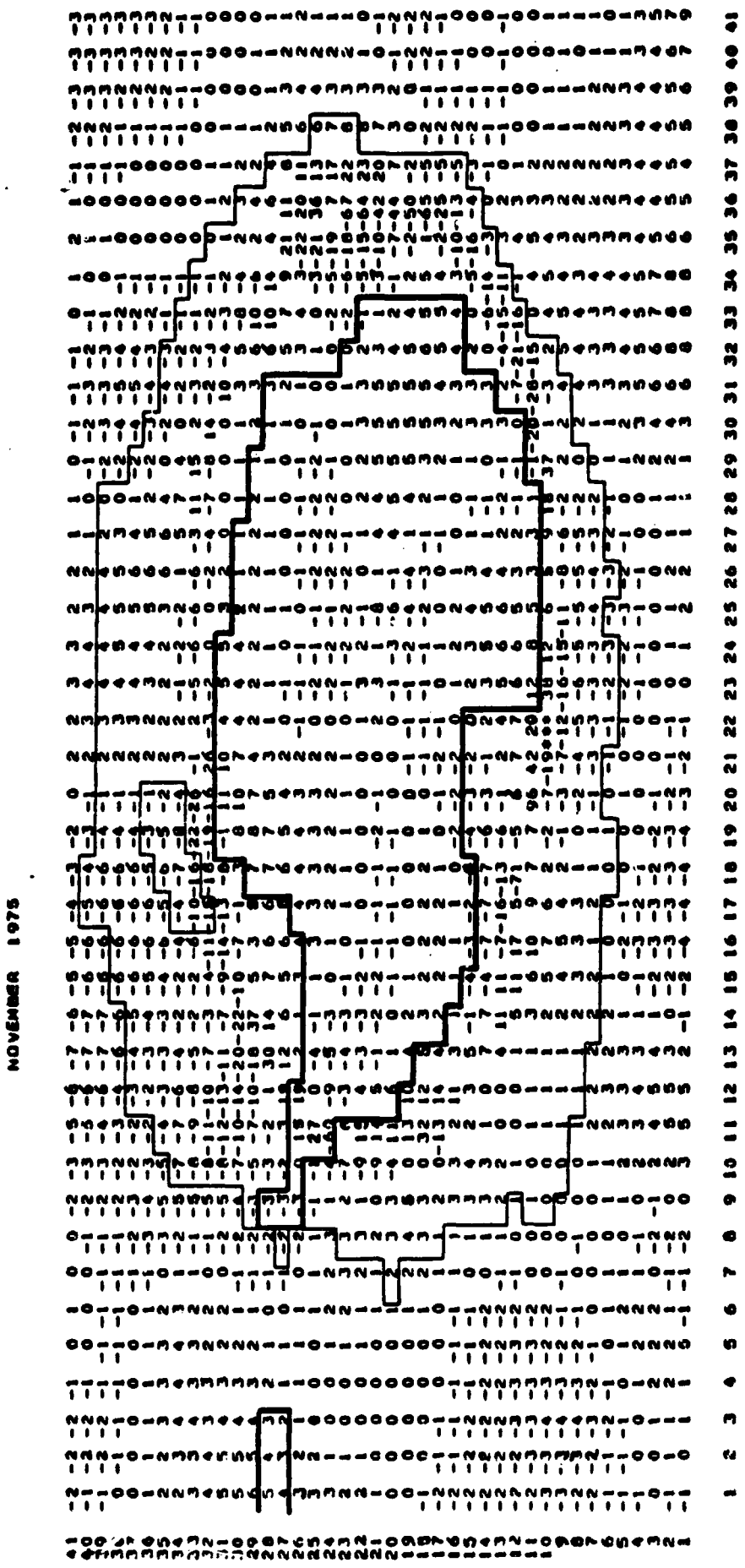

Figure 72. Turning angle A over the south polar grid for November 1975.

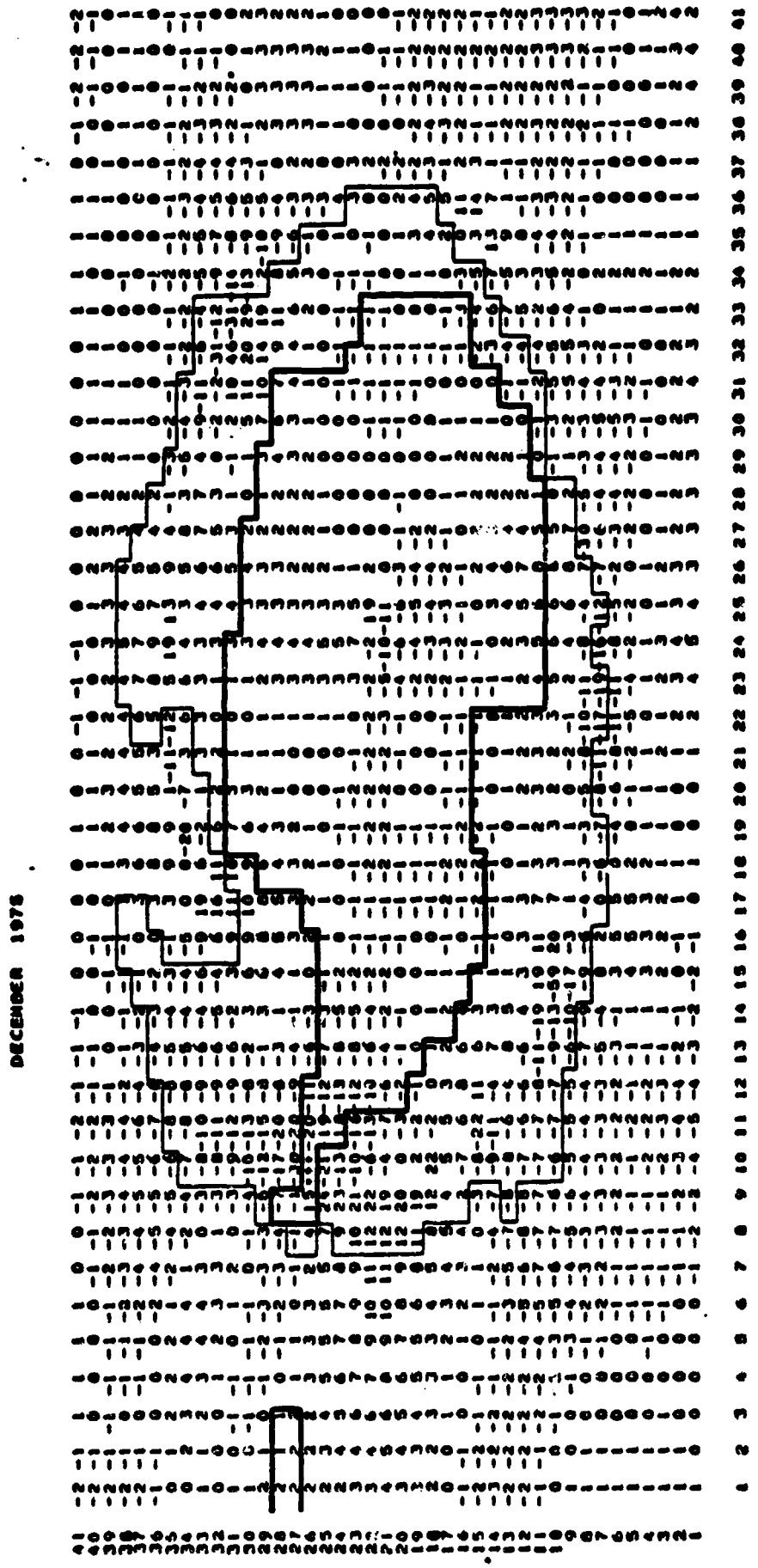

Figure 73. Turning angle A over the south polar grid for December 1975.